

October 2017



Project Report No. PR579

A 'breeder's tool kit' to improve Hagberg Falling Number for the economic and environmental sustainability of UK wheat

Cristobal Uauy¹, Nicholas Bird¹, Oluwaseyi Shorinola¹, James Simmonds¹, Jacob Lage², Peter Jack³, Chris Burt³, Tina Henriksson⁴ and Simon Berry⁵

¹John Innes Centre, Norwich Research Park, Norwich, NR4 7UH

²KWS UK Ltd. 56 Church Street, Thriplow, Royston, Hertfordshire. SG8 7RE

³RAGT Seeds Ltd. Grange Road, Ickleton, Saffron Walden, CB10 1TA

⁴Lantmannen Seeds 268 81 Svalöv, Sweden

⁵Limagrain UK, Station Road, Docking, Kings Lynn, Norfolk PE31 8LS

This is the final report of a 48 month project (2009-3659) which started in November 2010. The work was funded by BBSRC and a contract for £120,000 from AHDB Cereals & Oilseeds.

While the Agriculture and Horticulture Development Board seeks to ensure that the information contained within this document is accurate at the time of printing, no warranty is given in respect thereof and, to the maximum extent permitted by law, the Agriculture and Horticulture Development Board accepts no liability for loss, damage or injury howsoever caused (including that caused by negligence) or suffered directly or indirectly in relation to information and opinions contained in or omitted from this document.

Reference herein to trade names and proprietary products without stating that they are protected does not imply that they may be regarded as unprotected and thus free for general use. No endorsement of named products is intended, nor is any criticism implied of other alternative, but unnamed, products.

AHDB Cereals & Oilseeds is a part of the Agriculture and Horticulture Development Board (AHDB).

CONTENTS

Introduction	1
Summary	2
Financial Benefits	5
Action Points.....	5
General disclaimer.....	7
Introduction.....	7
Materials and methods	13
Results and Discussion	22
General Discussion.....	92
Conclusions	94
Knowledge and Technology Transfer	95
Glossary.....	98
References	100

Abstract

Hagberg Falling Number (HFN) is one of the principal standards against which the UK wheat crop is routinely assessed for bread-making quality. Low HFN for wheat grown for the bread-making market can present a serious problem, through reducing grower's margins and increasing costs in the processing industries. The most effective and sustainable option for achieving consistent HFN for bread-making specifications and export premiums is through appropriate varietal selection. Considerable progress has been made in understanding the genetic systems involved in HFN, primarily through an AHDB/BBSRC-funded LINK project (HGCA Report No. 480). There existed an opportunity to turn this knowledge into a 'breeder's tool kit', based on advanced molecular tools. The ultimate aim was the development of new wheat varieties with increased and more stable HFN under variable weather conditions.

We have cloned a major gene affecting pre-harvest sprouting in UK wheat (4A QTL) and developed a high-throughput perfect SNP marker which allows breeders to tag the functional polymorphism which confers resistance to pre-harvest sprouting. We screened UK germplasm based on this SNP marker and have identified different versions of the chromosome region (haplotypes). This information is now being implemented by breeding partners to deliver varieties with enhanced sprouting resistance to UK growers.

We have prioritised two additional genes which confer resistance to sprouting (1A) and pre-maturity amylase, PMA (7B). We show that these genes do not affect yield and provide an increase in HFN of 25 and 32 s, respectively. Importantly, these genes have distinct mechanisms of action, which suggests that combining them could lead to average increases in HFN of over 50 s and also could provide alternative resistance mechanism that could be triggered independently depending on weather events for the particular year. Both genes have been mapped to relatively small genetic intervals and breeder friendly markers and transferred to industrial partners to enable rapid targeted deployment into UK elite varieties.

We have developed a new tool (PolyMarker) to improve the speed of transfer of SNP from fixed platforms (e.g. iSelect 90k chip) into functional assays that can be routinely implemented in a high-throughput manner in breeders' molecular laboratories. This accelerates the rate in which new genomic information can be deployed for the benefit of UK growers. This tool is open source and is being used to generate markers for many additional traits within the breeding community. This project, alongside advances by others in the field, has now made marker-assisted selection for high HFN a reality in UK wheat breeding programmes.

Introduction

Headline

We have generated a breeders' tool kit for three major genes affecting Hagberg Falling Number (HFN) in UK wheat. This project, alongside advances in the field, has now made marker-assisted selection for high HFN a reality in UK wheat breeding programmes.

Background

The aim of this programme was to generate knowledge and tools to help develop new wheat varieties with increased and more stable HFN under variable weather conditions. This project built upon the results from a previous AHDB-Defra-LINK investment (HGCA Project No. 480) and sought to translate the knowledge generated from the initial discovery phase into a practical 'breeder's tool kit'. To achieve this we further characterized the largest and most stable regions of the wheat genome (known as QTL) which were proposed to affect HFN under UK environments. This included understanding the mode of action of each QTL, understanding any negative side-effects on yield and agronomic traits associated with the QTL, generating genomic information for each QTL, and defining them to sufficiently small regions in the wheat genome to allow marker-assisted selection by breeders. Ultimately, we aimed to produce the knowledge and the tools to allow breeders to purposely combine and deploy the genes responsible for different modes of resistance to HFN using the latest genomics and molecular marker technology.

The outcomes of this project will be realised by the UK breeding industry through the adoption of the information generated for these different QTL and by using the toolkit to deploy the genes into different UK varieties. The development of diagnostic genetic markers will greatly facilitate this task. Over the past five years we have worked closely with our breeding partners to ensure that this knowledge has been rapidly transferred into breeding programmes. This will help ensure that the outcomes of the project are reflected in the AHDB Recommended List as quickly as possible.

Summary

- We have identified a major gene affecting pre-harvest sprouting in UK wheat (Figure 1a). We translated this knowledge into a breeders' toolkit by developing a high-throughput perfect SNP marker which allows breeders to tag the mutation which confers resistance to pre-harvest sprouting (Figure 2a). This information is now being implemented by UK breeders to deliver varieties with enhanced sprouting resistance to UK industry.
- We have further prioritised two additional genes which confer improvements in HFN values in UK wheat. Both genes were confirmed and showed stable effects across multiple trials across years and locations. We show that these genes do not affect yield in a series of trials which is a critical consideration when evaluating their deployment into elite varieties. Across experiments these genes provide an increase in HFN of 25 and 32 s, respectively (Fig 1b). Importantly, these genes have distinct modes of action. This suggests that combining both genes could lead to average increases in HFN of over 50 s in UK wheat. Similarly, combining both genes provides complementary resistance mechanism that could be relevant depending on weather events for the particular year and location where the variety of grown. Both genes have been mapped to relatively small genetic intervals and breeder friendly markers have been developed and transferred to industrial partners. This will enable rapid targeted deployment into UK elite varieties.

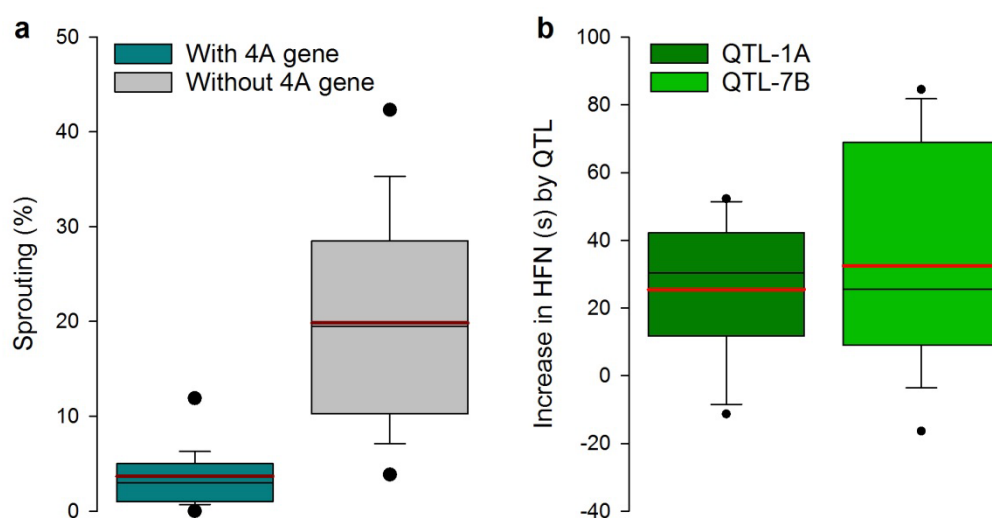


Figure 1: Summary of gene effects. **(a)** The 4A gene (teal) leads to decreases in sprouting in late harvested field samples. **(b)** The 1A and 7B QTL lead to increases in HFN across multiple sites and years ($n=11$ and 18). The boundaries of the box indicate the 25th and 75th percentiles; the black line marks the median (50th); the red line marks the mean (average).

- As an example of how this information can be taken forward, we screened and categorised UK germplasm based on the causal marker for the 4A gene (called *TaMKK3*;

Figure 2a). This marker is an example of the high-throughput assays that breeders can now use to classify lines for sprouting resistance based solely on DNA sequence and reducing the amount of destructive phenotyping of new germplasm. We developed detailed pedigree trees of UK varieties (Figure 2b) and categorised them based on this gene.

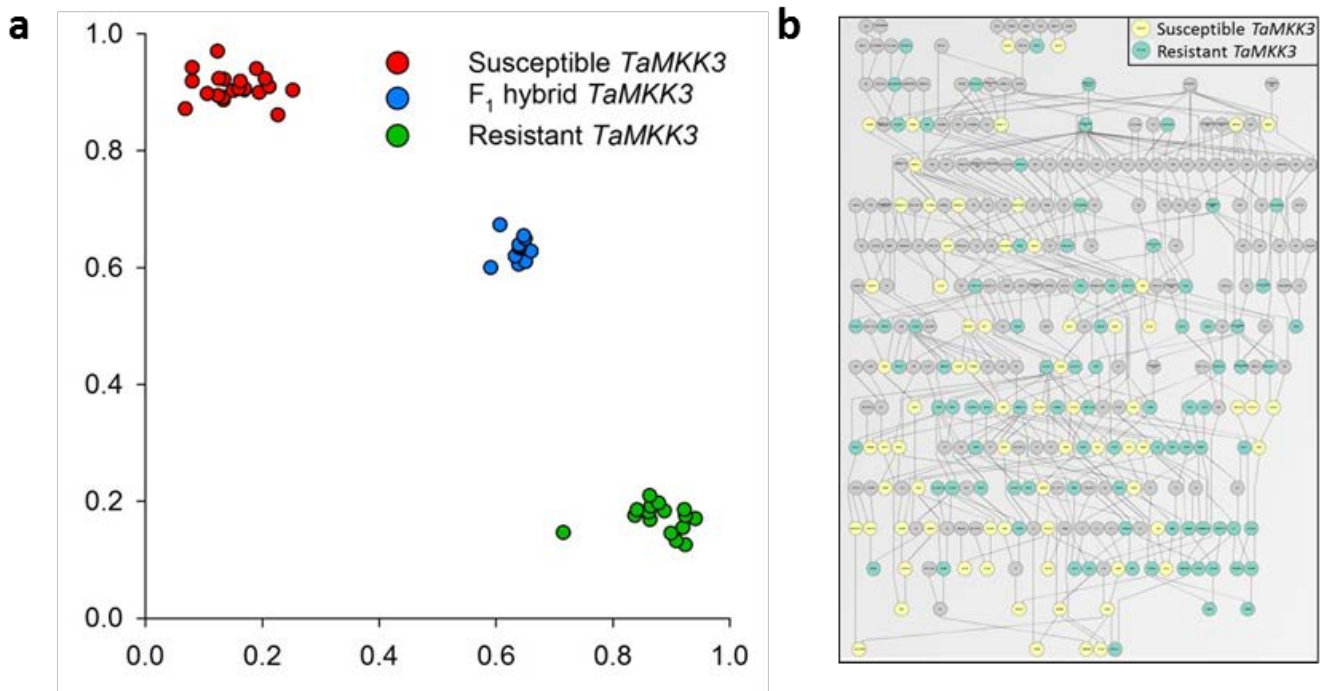


Figure 2: Allelic variation at *TaMKK3* and pedigree analysis of UK varieties (a) Genotype plot of varieties and crosses segregating for the KASP assay. (b) Pedigree of varieties with *TaMKK3* allelic status (yellow: susceptible; teal resistant).

- We also identified different versions of the wider chromosome region (called haplotypes) and categorised UK varieties based on the gene (Figure 3a, centre graph) and these wider chromosome regions (side graphs). This shows that there are three major haplotypes in UK varieties (Haplotypes 1-3-5). Examination of RL varieties showed that 85% of recent Group 1 and 2 varieties carry the resistant version of this gene (n=13), whereas only 35% of Group 3 and 4 varieties have the resistant allele (n=28; Figure 3b). This could be due to the fact that key parents of group 3 and 4 varieties (such as Claire, Robigus, and derivatives such as Nijinsky and Oakley) carry the susceptible version of this gene. This analysis now allows breeders to understand how specific genes and chromosome regions affecting HFN are being deployed in UK varieties (Figure 3c).

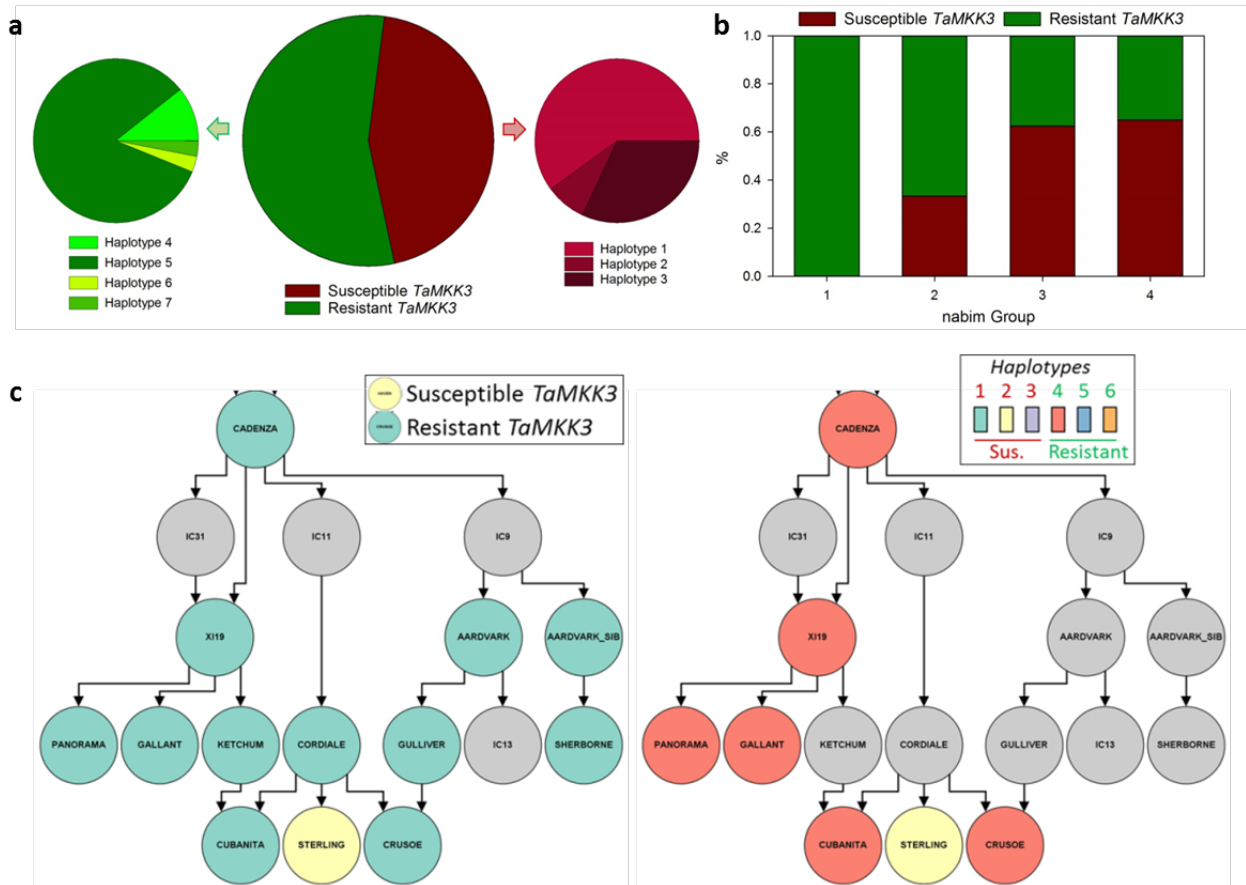


Figure 3: Allelic variation and extended haplotype analysis of the *TaMKK3* region in UK varieties (a) Centre chart shows the *TaMKK3* allele frequency and side charts show the breakdown of Haplotype groups (green: resistant; red: susceptible). (b) Frequency of two allelic variants at *TaMKK3* for 41 RL varieties classified according to their nabim Group. (c) Pedigree of Cadenza derived varieties for *TaMKK3* (left) and the chromosome haplotype (right). Group 1 and 2 varieties (Xi19, Panorama, Gallant, Cubanita, Crusoe) carry the resistance gene (teal circles) and have been selected for Haplotype 4 (red terra cotta circles).

- The 4A *TaMKK3* gene confers protection to late induction of sprouting as the gene affects the rate in which seeds lose dormancy. Hence the protective allele provides a delay in the loss of dormancy at the end of grain development. This means that seeds will not germinate in cases where late rains disrupt or delay the harvest of wheat crops. However, this protection is sufficiently short lived given that there is no effect in seed germination for commercial sowings a few months or even weeks later.
- Our results suggest that combining these three genes (1A, 4A, 7B) could provide an opportunity for robust protection against low HFN values for UK wheat. Given the way these genes work, they should provide complementary and additive resistance. Importantly, they could constitute the equivalent to an insurance against different weather events that could trigger low HFN values.

- We have also developed new tools and strategies to improve the speed of transfer of technologies arising in the academic sector into functional kits and assays that can be routinely implemented in breeders' laboratories. This has accelerated the rate in which new information gained from the wheat genome is being transferred to breeders and into new varieties with a direct benefit to UK growers.
- This project, alongside advances by others in the field, has now made marker-assisted selection for high HFN a reality in UK wheat breeding programmes.

Financial Benefits

The financial benefits of this project will arise by farmer adoption of wheat varieties with improved HFN stability. These benefits will be realised as breeders are able to translate the information and tools generated in this project into commercial wheat varieties for UK farmers. The direct costs of failing HFN thresholds of 250 s for Group 1 wheat is £20.81 per T which is the average premium for bread-making wheat over feed wheat between 2010 and 2016. The average risk of nabim Group 1 failing to meet the 250 s HFN threshold is between 1 in 4 and 1 in 5 (20-25%) but also there is extreme volatility ranging from 2% of in 2013 to 62% failing in 2012. This has important financial consequences for the sector and on-farm profitability. There are the direct costs to farmers when selling grain (£20.81 per T), but additional costs arise from the increased nitrogen fertilizations required to meet protein specifications in bread-making wheat and the loss of income given the reduced yields typically associated with group 1 wheat varieties. These extra costs are offset by the £20 per T premium for bread-making wheat, but this incentive is lost if the harvested crop falls below the HFN threshold. We have identified and characterised complementary sources for HFN resistance and developed the breeders' tool kit required for their deployment. Together, this information and tools will enable the breeding of new wheat varieties with increased and more stable HFN and reduced environmental impact, thereby reducing the costs associated with low HFN events.

Action Points

- From a growers' perspective, the main action point is to obtain varietal information from companies regarding the markers and genes which are being deployed to protect specific varieties from low HFN events. Similarly to what occurs in the RL for eyespot and orange wheat blossom midge where resistance is based on molecular marker information, the availability of a perfect marker for the 4A gene will allow this information to be available to growers upon request. This will provide growers with

additional layers of information to aid in their decision making regarding varietal choice and also timely harvest practices.

- However, caution must be exercised when interpreting this information as HFN is a much more complex problem (from a genetics point of view) compared to single gene disease resistance. HFN is determined by multiple genes which are conditioned by the environment. The knowledge of a single gene is not sufficient to predict the outcome of a given variety. As such, the information should be made available to allow growers to use this knowledge, but proper cautionary documentation is necessary to ensure that the limitations are also recognised.
- We have worked closely with the industrial partners over the course of the past 5 years to ensure that all the information that has been generated during the programme has been put into effect as soon as viably possible. We have transitioned together from low throughput and costly genetic markers into a new era of genomics. The close partnership with the breeders has ensured that the results were quickly translated into a practical set of tools and practices that could be implemented within their everyday workflows.

SCIENCE SECTION

General disclaimer

Sections of this report have previously been published in the PhD thesis of Dr. Oluwaseyi Shorinola, in a peer reviewed manuscript in the *Journal of Experimental Botany* and in an upcoming submission:

- Shorinola, O. (2015) Understanding the genetic and physiological control of pre-harvest sprouting and pre-maturity amylase in UK wheat. PhD Thesis University of East Anglia.
- Shorinola O, Bird N, Simmonds J, Berry S, Henriksson T, Jack P, Werner P, Gerjets T, Scholefield D, Balcárková B, Valárik M, Holdsworth MJ, Flintham J, Uauy C. (2016) The wheat *Phs-A1* pre-harvest sprouting resistance locus delays the rate of seed dormancy loss and maps 0.3 cM distal to the *PM19* genes in UK germplasm. *Journal of Experimental Botany*. 67 (14): 4169-4178.
- Shorinola O, Balcárková B, Holušova K, Borrill P, Distelfeld A, Valárik M, Barrero J, Uauy C. (2016) Association mapping and haplotype analysis of the major pre-harvest sprouting resistance locus *Phs-A1*, highlights a causal role of *TaMKK3* in UK and global germplasm. *in preparation*

Introduction

Wheat is the most important crop cultivated in the UK, accounting for 43 % of the total arable area on commercial holding in the last three years (DEFRA, 2015). During the 2010 to 2014 growing season, an average of 14.4 million tonnes of wheat was produced per annum in the UK (DEFRA, 2014). The UK is the 14th largest producer of wheat in the world (FAO, 2014), mainly due to its high average yield of 7.4 tonnes/ha (2010-2013).

Wheat produced in the UK is classified into four groups based on the processability and the end-use characteristic using the National Association of British and Irish Millers (nabim) classification. nabim Group 1 comprises varieties with consistent milling and baking qualities. Group 2 varieties show less milling potential but are still suitable for bread-making. Group 3 varieties are mainly used for biscuit, cakes and pastries while Group 4 varieties are grown mainly as feed for livestock.

The bread-making varieties (nabim Group 1 and 2) command a higher premium than the biscuit and feed wheat varieties. For instance, the 2015 prices of bread wheat was an average 20 % higher than feed wheat (AHDB, 2015b). However, the yield of bread-making varieties is often lower than those of biscuit and feed wheat varieties. In addition, farmers spend more

money to meet the high quality requirements (protein content, specific weight and HFN value) of bread-making varieties. Some of these costs can include higher fertiliser input and/or early harvesting and artificial drying of grains to avoid sprouting damage. These measures are not environmental sustainable (Pretty et al., 2005) and do not always guarantee the production of quality grains. As a result, bread-making wheat varieties can sometimes end up being sold as feed wheat for less than their premium price. To avert this risk, there has been a decline in recent times in the cultivation of some bread-making varieties (particularly the Group 2), while the cultivation of feed wheat varieties, which are high yielding and less cost intensive, has increased (Figure 1).

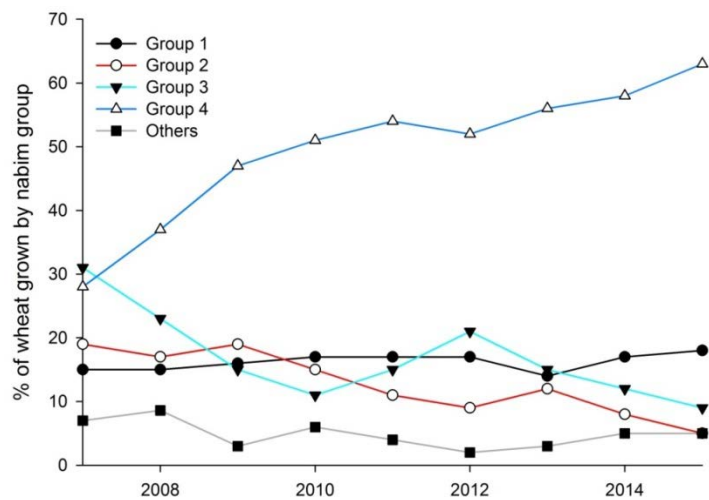


Figure 1: Percentage of wheat grown in the UK from 2007 to 2015 by NABIM group. The ‘Others’ categories refers to wheat varieties grown in the UK that are not classified by the nabim system (AHDB, 2015)

The problem of low Hagberg Falling Number (HFN) caused by the incidences of Pre-harvest sprouting (PHS) and Pre-maturity amylase (PMA) is one of the factors responsible for this decline in the cultivation of bread-making wheat varieties in the UK. The relatively wet UK weather conditions can sometimes predispose cultivated wheat to the problem of PHS and PMA. With an average summer rainfall of 85 mm (from 2000 – 2014, Met Office, 2015) during the critical stages of grain development and maturation (May-August), the UK wheat fields can be an ideal environment for PHS and PMA. However, the extent of the challenges posed by these traits varies from year to year and also from one region to the other in the UK. In 2004, 2007 and 2012, more than 50 % of the nabim Group 1 wheat varieties failed to meet the 250 sec HFN threshold for bread-making quality (Figure 2). This was particularly due to the highly conducive environmental conditions (rainfall) for the induction of PHS and PMA in these years. In contrast, in 2006 and 2013, no wheat was rejected due to this problem. On average, over the last 14 years, more than 25 % of bread-making nabim Group 1 wheat

varieties did not meet the acceptable HFN threshold (AHDB, 2014). Farmers are as such forced to sell such grains as feeds. This has consequences not only on farm profitability but also on global food security. Thus, PHS and PMA constitute a major economic threat to wheat production in the UK.

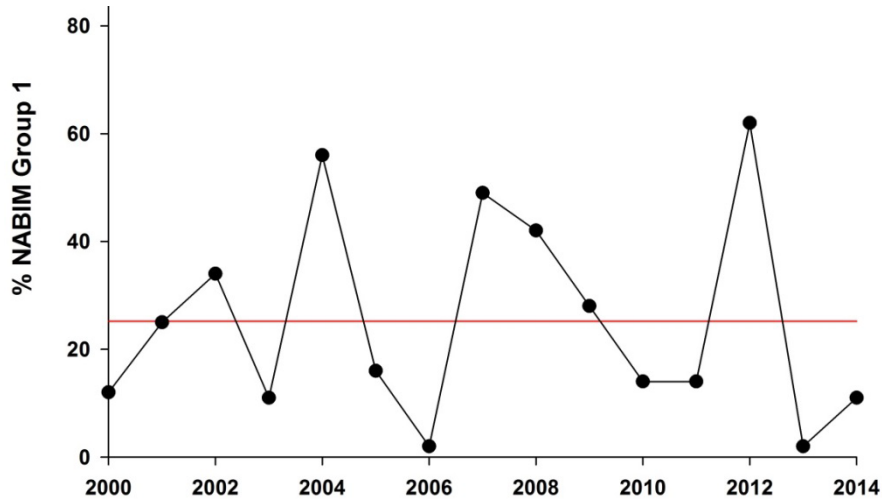


Figure 2: Incidences of low HFN in the UK. Percentages of nabim Group 1 varieties with HFN less than 250 sec from 2000 to 2014. The red line indicates mean percentage across the 15 year period.

Given the significant threats posed by PHS and PMA to UK wheat production, there have been significant research efforts aimed at stabilizing the HFN of UK bread-making wheat varieties. These have been mainly through identifying and breeding for genetic resistance against PHS and PMA. An example of this is a Defra-LINK project titled ‘An Integrated Approach to Stabilising HFN in Wheat: Screens, Genes & Understanding’. One of the outputs of this project was the identification of the genetic architecture of PHS and PMA resistance using 11 doubled haploid (DH) populations originating from 16 elite UK wheat varieties (Flintham et al 2011). The PHS and PMA resistances in these DH lines were assessed through a simulated sprouting test and a HFN test in field trials conducted in 2005 - 2008. The sprouting test done involved the use of overhead irrigation to induce sprouting in field grown materials. The HFN test, on the other hand, is a viscometric test that indirectly measures amylase activity in flour slurries and is suitable for detecting PMA, but can also detect the production of amylase that accompanies sprouting.

The field trial data, along with genetic linkage maps of the populations, enabled the identification of quantitative trait loci (QTL) for PHS and PMA resistance on almost all of the chromosomes of wheat (Figure 3). This implies an abundance of genetic variation that could

be harnessed for PHS and PMA resistance breeding in the UK. However, many of these QTL were only detected once, possibly due to strong environmental influence on the control of such QTL. However, other QTL were detected in more than one trial, and some showed consistent effects in all the trials. PHS QTL that were identified in more than one trial include QTL on wheat chromosomes 1A, 2D, 3A (two loci), 3B, 3D, 4A (2 loci), 4D, 5D (2 loci) and 7B. QTL for PMA resistances identified in at least two trials were located on chromosomes 1B, 4D, 5D, 6A and 7B (Flintham et al 2011).

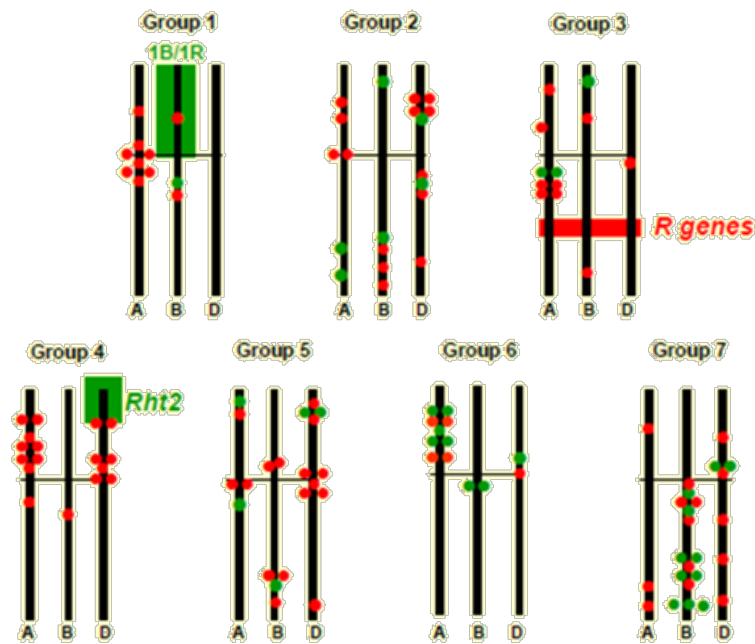


Figure 3: Distribution of PHS and PMA QTL identified in the first HFN DEFRA LINK project (Flintham et al 2011). Small circles represent PHS (red) or PMA (green) QTL in the different populations used for the study, therefore clustered dots may represent co-localising QTL. Green and red boxes represent location of major chromosome location known to have effects on PMA and PHS respectively. Note that the *R*-genes refer to the *R-1* genes. Approximate location of the QTL selected for this present study are indicated by red (PHS QTL) or green (PMA QTL) spheres. The centromere is represented by the horizontal line across each homoeologous group.

Of these QTL, six showed stable and consistent effects over different years and environments (Table 1). The 1A, 2D, 3A (two loci) QTL showed consistent effects on sprouting in all four years of field trial. The 4AL QTL effect on sprouting was observed in only two years, but it gave the highest sprouting effect observed (53 % change in sprouting between alleles) in any of the four years. Analogously, the 7B QTL consistently showed the biggest effect in the HFN test (in 2007 and 2008), but showed less pronounced effect on sprouting across the four

years indicating that this QTL is primarily a PMA resistance QTL. A summary of the QTL effects and the associated genetic markers are shown in Table 1.

Table 1: Mean effects of prioritised QTL on PHS and PMA in UK wheat varieties.

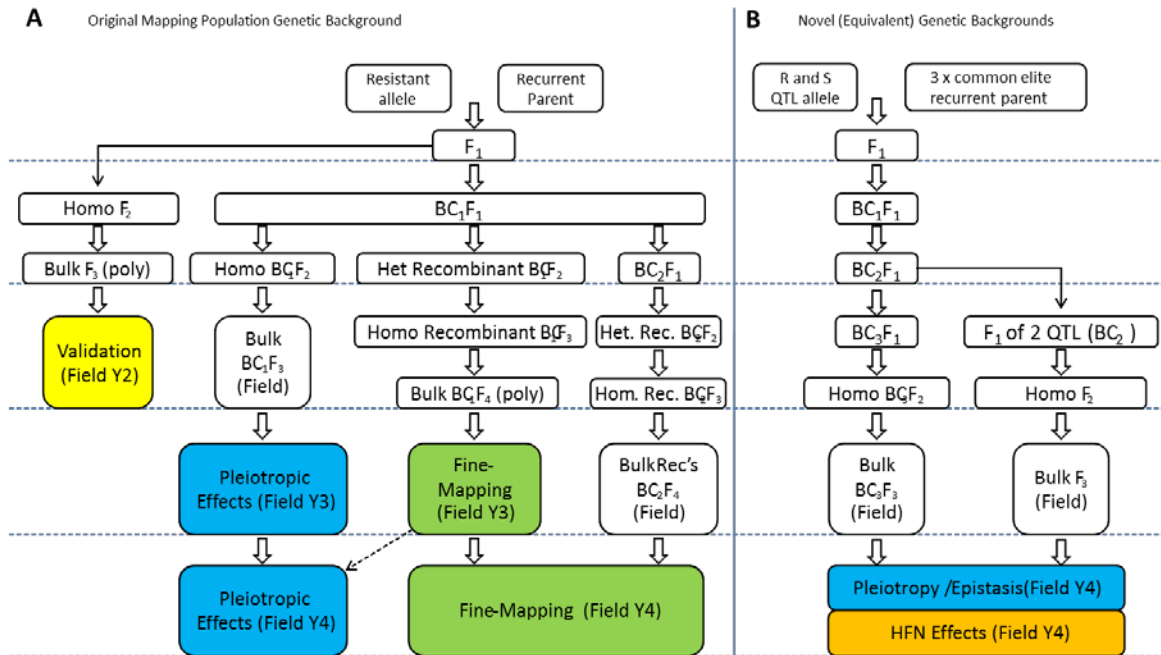
QTL	Population	Beneficial Allele	Change in Sprouting (%)				Change in HFN (%)		
			05	06	07	08	06	07	08
1A	Haven x Soleil	Soleil	26	20	26	16	19	45	31
2D	Avalon x Cadenza	Cadenza	27	25	15	33	-	54	15
3A	Avalon x Cadenza	Cadenza	29	24	19	23	-	-12	-3
3A	Savannah x Rialto	Savannah	-	-	24	-	56	45	43
4A*	Alchemy x Robigus	Alchemy	-	-	23	53	-	-	-
7B	Avalon x Cadenza	Avalon	27	4	6	24	-	107	81

Red values correspond to statistically significant effects ($P < 0.05$). Hyphen = data not available.

*The 4A QTL was also identified in an independent Option x Claire population, with Claire providing the beneficial allele.

The aim of this programme was to generate knowledge to help develop new wheat varieties with increased and more stable HFN under variable weather conditions. This project took the outputs from a previous Defra-LINK project (Flintham et al 2011) and sought to translate the knowledge generated from the initial discovery phase into a practical 'breeder's tool kit'. To achieve this we further characterized the largest and most stable QTL previously identified (Table 1), generated tightly linked markers, evaluated the effects of the QTL in different genetic backgrounds, and generated the pre-competitive germplasm required by breeders for their effective deployment into elite material. To achieve this we set out four main objectives to be achieved through a work plan outlined in Schematic 1:

- Validate and define the prioritized QTL to precise genetic intervals.
- Determine epistatic interactions between QTL and pleiotropic effects on agronomic traits.
- Perform physiological characterization of the precise germplasm to understand the mechanism of gene action.
- Perform QTL haplotype analysis using next-generation sequencing to facilitate breeder deployment.



Schematic 1: Schematic representation of the crossing streams in the (A) original mapping population genetic background and in the (B) novel genetic background as in the original proposal.

Materials and methods

Plant materials for field and physiological characterisation

We developed and used isogenic F_3 and BC_3 materials for field validation as well as for the physiological characterisation of selected QTL. BC_1 lines were used for the agronomic characterisation of the QTL effects. Prior to the development of these materials, DH lines were developed from crosses of resistant and susceptible parents listed in Table 1. Selected QTL were originally identified using these DH lines.

For each QTL, independent DH lines which carried the resistant parents alleles across the individual QTL intervals but which maximised the corresponding susceptible parent alleles in the background were crossed with their respective susceptible parents. F_1 lines produced from these crosses were either self-fertilised to produce F_2 plants or backcrossed “n” times with the susceptible parents before self-fertilisation to produce BC_nF_2 plants. At the F_2 and BC_nF_2 generations, independent F_2 and BC_nF_2 plants with the target QTL were selected using flanking markers. F_3 and BC_nF_3 plants were afterwards obtained from self-fertilisation of the selected F_2 and BC_nF_2 plants (Figure 4).

For the 4A QTL we did not have a precise genetic position at the start of the project and hence the NIL development was delayed and a different approach adopted. This is why although NILs were developed for the fine mapping (and eventual cloning of the underlying gene), we were not able to evaluate the agronomic characteristic of the QTL. Despite this, the cloning of the gene now allows breeders to run a “perfect” marker for the QTL allowing them to evaluate their years of results and be able to assign a breeding value for this specific Kompetitive Allelic Specific PCR (KASP) assay based on all their historical data. This was the desired outcome of the project and hence the inability to test the 4A QTL for agronomic effects did not adversely affect the project.

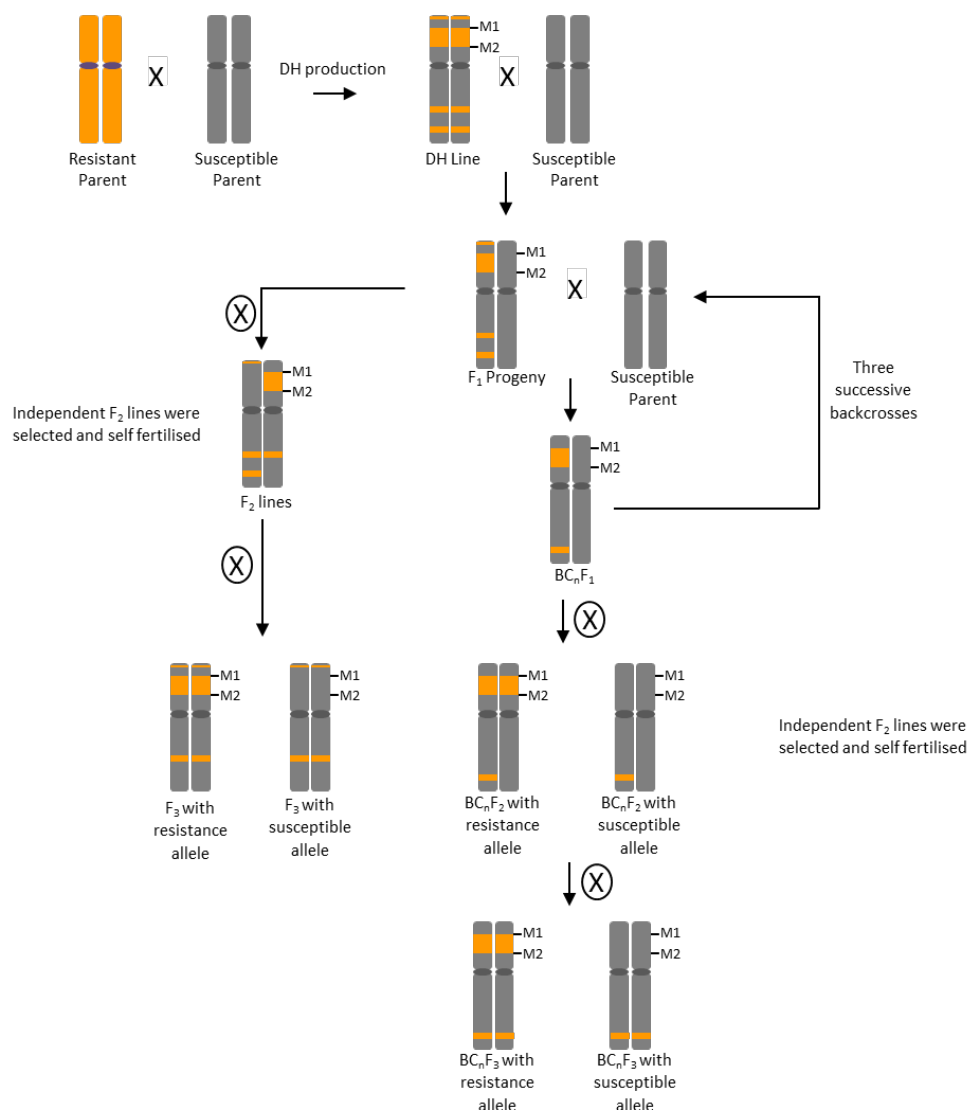


Figure 4: Development of doubled haploid (DH) lines and independent isogenic populations for individual QTL characterisation. DH lines were produced from the initial cross of resistant (orange) and susceptible (grey) parents. Selected DH lines were backcrossed recurrently with their respective susceptible parents. F₃ lines were produced by successive self-fertilisation of the progeny of the DH x susceptible parent cross, while BC_nF₃ lines were produced by successive backcrossing of the progeny to the susceptible parents. At DH, F₂ and BC_nF₂ generations, the QTL region of interest were selected with flanking markers (M1 and M2).

Plant material for fine mapping of 4A: The identification, characterisation and high-resolution fine-mapping of the 4A QTL was done in two experimental populations made from the Option x Claire and Alchemy x Robigus crosses.

Alchemy x Robigus fine-mapping population: For characterisation and fine mapping of the 4A QTL in the Alchemy x Robigus population, we developed near isogenic lines (NILs) and recombinant inbred lines (RILs). To accomplish this, five SSR markers including *barc170*, *wmc420*, *wmc707*, *wmc760* and *wmc313* were used to select DH lines homozygous for Alchemy in different, but overlapping intervals across the 4AL chromosome arm. These were independently backcrossed to the recurrent parent Robigus and advanced to the BC₃ generation by crossing heterozygous plants selected at each generation. NILs homozygous for the Alchemy introgression found in the original DH lines were selected using the SSR markers flanking the introgressions. For the development of RILs used for high resolution fine-mapping, BC₃F₂ lines heterozygous for the 4A QTL interval (*barc170-wmc420*) were self-pollinated and BC₃F₃ lines with recombination events within the interval were selected. These were advanced to the BC₃F₄ generation by self-pollination to obtain homozygous RILs.

Option x Claire fine-mapping population: We developed F₄ RILs from the Option x Claire cross. This was accomplished by crossing a DH line (OC69), homozygous for Option across the QTL interval, to Claire. Following self-fertilisation of F₁ progeny, 2400 F₂ plants were screened and 85 F₂ recombinant lines with recombination events between markers *barc170*, *wms894* and *xhbe03* were recovered. Thirty of these lines were randomly selected, self-fertilised and lines with homozygous recombinant haplotype were extracted from the F₃ population. In addition, lines with Claire or Option non-recombinant haplotype were also selected as controls. However, only 27 of these were initially phenotyped and advanced to the F₄ generation for further phenotyping.

For the other QTL a similar approach was used to extract homozygous recombinant lines across each QTL region. The specific flanking markers used for each target QTL are outlined in the results sections as are the number of recovered homozygous recombinant lines for each QTL.

Growth conditions

The various germplasm used in this project were grown either in the Controlled Environment Room (CER), Glass houses (GH) or in field sites across the UK. Materials grown in the CER or GH were first sown in 96 well trays with soil specification detailed in Borrill et al. (2015b). In brief: 15 % horticultural grit and 85 % fine peat; containing 2.7 kg m⁻³ Osmocote (3 - 4 months longevity), 0.5 kg m⁻³ wetting agent H2Gro (Everris), 4 kg m⁻³ Maglime (Francis Flower) and 1 kg m⁻³ PG Mix fertilizer (www.yara.co.uk). They were then vernalised at 6°C for 8 weeks. During vernalisation, leaf sample were harvested for DNA extraction from all the plants of each line, and this was used to genotyping with SSR or KASP markers located across the target QTL for each line. After vernalisation, plants were transplanted into 1 L pots which contained 40 % medium grade peat, 40 % sterilized soil, 20 % horticultural grit; containing 1.3 kg m⁻³ PG Mix 14-16-18 (www.yara.co.uk), 1 kg m⁻³ Osmocote Exact Mini, 0.5 kg m⁻³ wetting agent H2Gro, 3 kg m⁻³ Maglime and 300 g m⁻³ Exemptor (Bayer). The potted plants were afterwards grown in the CER or GH under the conditions detailed below.

- *CER conditions*: Plants were grown in the CER under long day conditions: 16 h light (250 - 400 mmol) at 20°C and 8 h darkness at 15°C and at 70 % humidity. For the characterisation of the effect of grain development temperature on the QTL effects, some plants of each NIL were transferred from between 1-7 days after anthesis into a different CER with 16 h light (250–400 mmol) and 8 h darkness at 13°C.
- *GH*: Plants were grown in the glass house under long day conditions: 16 h light (above 300 mmol) at a constant temperature (18 °C) and 8 h darkness at 15 °C. A relative humidity of 70 % was maintained.
- *Field Trials*: Plant materials were sown across the UK and Sweden in field trials between 2010 and 2014. In addition to the field site at the John Innes Centre (JIC), Norwich UK (52.69°N, 1.22°E), we also used field sites of our breeding partners. These included RAGT Seeds LTD (RAGT), Saffron Walden, UK (52.06°N, 0.14°E); KWS UK (KWS), Thriplow (52.09°N, 0.10°E), Limagrain (LG), Woolpit, UK (52.22°N, 0.8°E), and Lantmannen, Svalof Sweden (55.90°N, 13.11°E) . All sites were used for the field validation experiment in a split-plot randomised complete block design with at least 3 replications and where the QTL was first randomized to the plot and then the positive and negative alleles were randomised into the “split” plot. Similar design was used for the agronomic characterisation experiments where assessment of the QTL effect was prioritised using the split-plot design.

Phenotyping

A series of agronomic traits were measured on field grown materials and a subset was measured in CER and GH grown samples. These included

- *Days to ear emergence*: number of days for half of the plants to show emergence of at least half portion of the ear (spike) from the enclosure of the leaf sheath.
- *Height*: measured after physiological maturity and was an estimate of the average height of plant in each plot.
- *Grain morphometric measurements*: Thousand gran weight (TGW), area, width and length were obtained using the Marvin seed analyser (GTA Sensorik GmbH).
- *Yield*: total plot yield was measured and adjusted by moisture content.
- *Hagberg Falling Number*: Harvest-ripe spikes were harvested from the field and threshed to obtain seeds. About 10 - 15 g of seeds from each sample was ground in a cyclone laboratory mill (UDY Corporation). The flour produced from each sample was allowed to equilibrate to constant moisture content at 30°C. The moisture content of the flour was determined by drying a representative sub-sample in a 65°C incubator and obtaining the weight before and after drying. Based on the moisture content of the flour, an amount of flour equivalent to 7 g of 14 % moisture content was used. The HFN value of the flour was measured with a Falling Number 1900 machine (Perten Instrument, Sweden). To do this, the flour was mixed with 25 mL of water in a viscometer tube, and this was shaken vigorously to homogenise the suspension. The tube, with a Falling number stirrer inserted, was placed in a hot water bath of the Falling Number machine. After an automatic stirring for 60 sec, the stirrer was released from its top position. The time it took for stirring (60 sec) and for the stirrer to fall to the bottom of the tube under gravity was recorded as the HFN value. More information can be obtained from www.perten.com/Products/Falling-Number/The-Falling-Number-Method.
- *Germination index (GI) assays*: At four stages of grain maturation and after ripening including physiological maturity, harvest maturity (7 days after physiological maturity), as well as 14 and 28 days after harvest maturity, ears were harvested and gently threshed to obtain grains from the central portion of the ear. For plants grown under constant 13 °C in GI experiment 3, harvest maturity was reached 12 days after physiological maturity. Twenty grains were placed with the crease facing down in 90 mm petri dishes containing two layers of Sartorius filter paper and were incubated in 5 mL of sterile water for seven days. After each day of incubation, germinated seeds (with ruptured seed coat) were counted and removed from the plate. The number of

germinated seeds per day was used to calculate a weighted GI score using the formula described by Walker-Simmons (1987) with a slight modification: $GI = ((7 \times n_1) + (6 \times n_2) + (5 \times n_3) + (4 \times n_4) + (3 \times n_5) + (2 \times n_6) + (1 \times n_7)) / (7 \times (N - M))$. Where n_1, n_2, \dots, n_7 are the number of germinated grains on the first, second, and n th days until the 7th day, respectively; N is the total number of grains per plate and M is the number of mouldy grains after the 7 days of incubation. Specifically for the fine mapping of the 4A QTL, three GI experiments were conducted in the Alchemy x Robigus population. In GI experiment-1 plants were grown in the glasshouse under long day conditions with 16 h light (300 mmol) at 18 °C, 8 h darkness at 15 °C and at relative humidity of 70 %. In GI experiment-2 plants were grown in CER under long day conditions with 16 h light (250 – 400 mmol) at 20 °C, 8 h darkness at 15 °C and at 70 % relative humidity. GI experiment 3 was designed to test if the 4A QTL was still effective when grains are developed at low temperature. In this experiment, plants were transferred from between 1 and 7 days after anthesis into a CER and maintained at constant day and night temperature of 13 °C.

- *Sprouting*: Spikes from each line, harvested from similar time post anthesis, were allowed to after-ripening at room temperature. During this period of after-ripening, the germination status of the parents were monitored weekly via the GI test. When GI difference was observed between the parental samples, after-ripened spikes (two – three spikes from each plant) were arranged on metallic racks. The spikes were then misted for 5 - 7 days in a sprouting chamber containing a humidifier and a revolving platform. Misted spikes were dried and gently threshed together to collect the seeds. The seeds were examined for the symptoms of sprouting (breakage of the seed coat near the embryo), and the number of sprouted seeds in each biological replication was used to calculate the percentage of sprouting. This was then used to calculate weighted percentage sprouting averages and standard error of the mean. Specifically, for the 4A fine mapping, five sprouting experiments were conducted in the Alchemy x Robigus (sprouting experiment 1 and 5) and the Option x Claire (sprouting experiment 2, 3, and 4) populations. In sprouting experiment-1, 3 and 5, plants were grown in the glasshouse under long day conditions with 16 h light (300 mmol) at 18 °C, 8 h darkness at 15 °C and at relative humidity of 70 %. In sprouting experiment-4, plants were grown in CER under long day conditions with 16 h light (250 – 400 mmol) at 20 °C, 8 h darkness at 15 °C and at 70 % relative humidity. Plant materials for sprouting experiment-2 were grown in the field at KWS (Thriplow, UK; 52.1°N, 0.1°E) as single rows in 1 m² plots using in a randomised complete block design with two replications per line.

- *α-Amylase activity*: This was determined using the Ceralpha α -amylase assay kit (Megazyme). Samples of 0.25 g of grains were ground in mortar and pestle with Liquid nitrogen. Amylase extract was obtained by addition of 1.5 mL of Ceralpha Extraction Buffer and incubated at room temperature for 40 mins. Following centrifugation, the activity of amylase was assayed according to the manufacturer manual. The Ceralpha procedure is based on the endo-acting activity of α -amylase to hydrolyse a non-reducing-end blocked p-nitrophenyl maltoheptaoside in the presence of excess amylogucosidase and α -glucosidase. Following hydrolysis, the p-nitrophenyl maltosaccharide fragments are made accessible to the activity of amylogucosidase and α -glucosidase and these produce free glucose and p-nitrophenol. The addition of Trizma base solution stops the reaction and produces a colour change. The absorbance of the product is measured at 400 nM, and this corresponds to the level of α -amylase in the original sample.

SNP and SSR genotyping

DNA extraction was done in a 96-well plate format according to the protocol developed by Pallotta et al. (2003). For single nucleotide polymorphism (SNP) discovery we genotyped the BC₃ NIL pairs with the iSelect 90k wheat SNP chip. DNA samples from the sibling BC₃ NILs differing across each target QTL were sent to Bristol University where they were ran on the SNP array. We used the published POPSEQ genetic map as a first approximation of map position and implemented a two-step strategy (described in the results section) to further define the SNPs across our target intervals. We also performed a similar analysis using the 820k wheat SNP chip when this became available in 2014. All marker information was made available to breeders to facilitate rapid implementation of the markers into their breeding programmes.

In the early stages of the project we ran SSR markers, especially for the development of the 4A isogenic lines. For this target QTL we used five SSR markers (*wmc420*, *barc170*, *wmc707*, *wmc760* and *wmc313*) to develop the Alchemy x Robigus NILs and *wms894* and *xhbe03* to genotype Option x Claire RILs. The primers sequences were obtained from the GrainGenes database (<http://wheat.pw.usda.gov/GG3>), except for *wms894* which was obtained from RAGT Seed, UK. SSRs were labelled with the FAM, VIC, NED or PET fluorescent dye (Applied Biosystems) for the multiplexing of assays. PCR were performed with the Qiagen Hotstart Master Mix (Qiagen, Cat No: 203443) and in volume of 6.25 μ L containing 3.125 μ L of Hotstart mix, 0.625 μ L of primer mix and 2.5 μ L of DNA. Thermal cycling conditions was as follow: Hotstart at 95 °C for 15 min, 35 cycles of 95 °C for 1 min; 50 - 60 °C (depending on

annealing temperature of primers) for 1 min, 72 °C for 1 min and a final extension step of 72 °C for 10 mins. PCR amplicons were afterwards run on an Applied Biosystems 3730 DNA Analyzer using GeneScan 500 LIZ (Thermo Fisher Scientific; Cat. No:4322682) as size standard. Genotype data were analysed on the GeneScan® Analysis Software (Applied Biosystems).

SNP markers were developed from the wheat sequence was used to design the iSelect and Axiom SNP arrays. We developed a bespoke pipeline to rapidly generate KASP assays (Ramirez-Gonzalez et al., 2015). This technology was chosen given its use by breeders hence allowing a quick adoption of the project's outcomes into the breeding programmes. In some cases, we also developed SNP markers from wheat sequences orthologous to *Brachypodium* genes based on synteny. KASP assays were performed in 384-well plate format in a 5.07 µL volume containing 2.5 µL of DNA, 2.5 µL of KASP master mix (LGC, UK) and 0.07 µL of primer mix. PCR was performed on an Eppendorf Mastercycler pro 384 using the following protocol: Hotstart at 95°C for 5 min, ten touchdown cycles (95°C for 20 s; touchdown 65°C, -1°C per cycle, 25 s) followed by 30 - 40 cycles of amplification (95°C for 10 s; 57°C for 1 min). No extension step is necessary as KASP amplicons are smaller than 100 bp. Plates were read using the Tecan SAFIRE Fluorescent Scanner and genotype data was viewed graphically with the KlusterCaller™ software (LGC, UK).

4A physical map construction

Twenty-four bacteria clones containing Bacterial Artificial Chromosome (BAC) that constitute the Minimum Tilling Path (MTP) of the three main BAC clusters (cluster 16421, 285 and 7335) found in the 4AL PHS QTL region were obtained from Prof. Jaroslav Dolezel's lab at the Centre for Plant Structural and Functional Genomic, Institute of Experimental Botany (IEB), Czech Republic. BACs were extracted from the bacteria clones using the Qiagen Plasmid Midi Kit (Qiagen, Cat. No. 12143) following the manufacturer's protocol. High-quality BAC DNA were supplied to The Earlham Institute (previously TGAC, Norwich, UK) for sequencing. TGAC prepared the NGS library with an average library insert sizes of 360, 460 and 440 bps for cluster 16421, 285 and 7335 respectively. BACs were multiplexed for sequencing on Illumina Miseq lanes and overlapping 250 bp paired-end reads were obtained for each BAC. The paired-end reads obtained from Illumina sequencing were assembled using the CLC Bio genomic software (www.clcbio.com). Before assembly, reads were first filtered to remove contaminant sequences by mapping to the pIndigoBAC-5 vector and the *Escherichia coli* genome. *De novo* assembly of reads that do not map to these contaminant reference sequences was then done. Parameters for *de novo* assembly included: Word size (64 bp);

Bubble size (250 bp); Mismatch cost (2); Insertion cost (3); Deletion cost (3); Length fraction (90%); Similarity fraction (95%).

Transposable element sequences in the assembled BAC contigs and the Barley BAC scaffolds were searched for by BLAST analysis of the assembly contig sequences against the Triticeae Repeat Database (TREP) accessible at wheat.pw.usda.gov/ITMI/Repeats. Repeat sequences identified were annotated and masked to distinguish them from non-repeat sequence. Gene models in repeat-masked BAC sequence were searched for by BLAST analysis of the BAC sequence against a custom database containing wheat gene models described by Krasileva et al. (2013) and by BLASTX analysis on NCBI (blast.ncbi.nlm.nih.gov/Blast). Gene models were also obtained by ab-initio gene prediction with FGENESH (Solovyev et al., 2006). Only FGENESH gene model with protein sequence support from NCBI or Ensembl Plant database (plants.ensembl.org) were used. Gene models with greater than 90 % protein or nucleotide sequence identity and more than 75 % sequence coverage to already annotated genes on the NCBI or Ensembl databases were considered as high confidence genes. While gene models that do not meet these criteria were considered as low confidence gene. The annotation of Barley BAC scaffolds was done by BLAST analysis of the scaffold sequences against the high confidence gene model (IBGSC, 2012) database of the barley genome hosted at IPK Barley BLAST Server (webblast.ipk-gatersleben.de/barley/viroblast).

Statistical analyses

Statistical significance was calculated using either one-way or two-way analyses of variance (ANOVA). Tukey's Honestly Significant Difference tests and Dunnett's tests (using parental varieties as controls) were performed for multiple comparisons between NIL, RILs and parents. Data which did not meet the ANOVA assumption of homogeneity of variance was arcsin transformed and confirmed to meet the assumptions before being used for the ANOVA analysis. Statistical analyses were performed in Genstat (version15.2.0.8821), Microsoft Excel and Minitab (Version, 17.2.1).

Results and Discussion

1. Validate and define the prioritized QTL to precise genetic intervals.

Objective 1.1: Validate six QTL for PHS/HFN segregating in elite UK germplasm

Doubled Haploid: We first validated the QTL by selecting five pairs of doubled haploid (DH) lines which differed in genotype across the QTL interval but had the most equivalent genotype across background markers. These DH pairs were characterised by all partners in the 2010-2011 field season under natural induction with two sampling points (early and late HFN measurements). As mentioned in the methods section, the 4A QTL was treated differently as we did not have a precise map position to allow this evaluation.

Across experiments the DH pairs for the 1A, 3A SxR and 7B QTL were significant ($P < 0.001$) across locations improving HFN scores compared to the alternative allele in both early and late harvests (Figure 5-7). For the 2D QTL a positive effect was also observed at KWS, but the overall effect was not statistically significant across locations (Figure 6). The 3A AxC QTL showed a significant negative effect between the DH pairs at RAGT and Svalof. Overall, no interactions were seen for early and late HFN measurements.

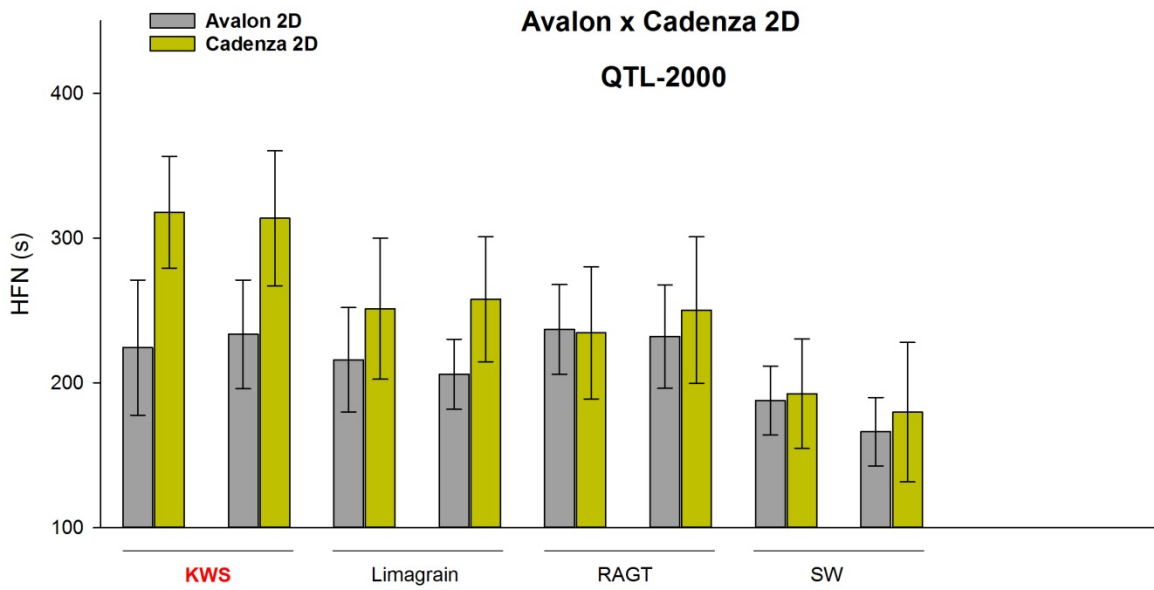
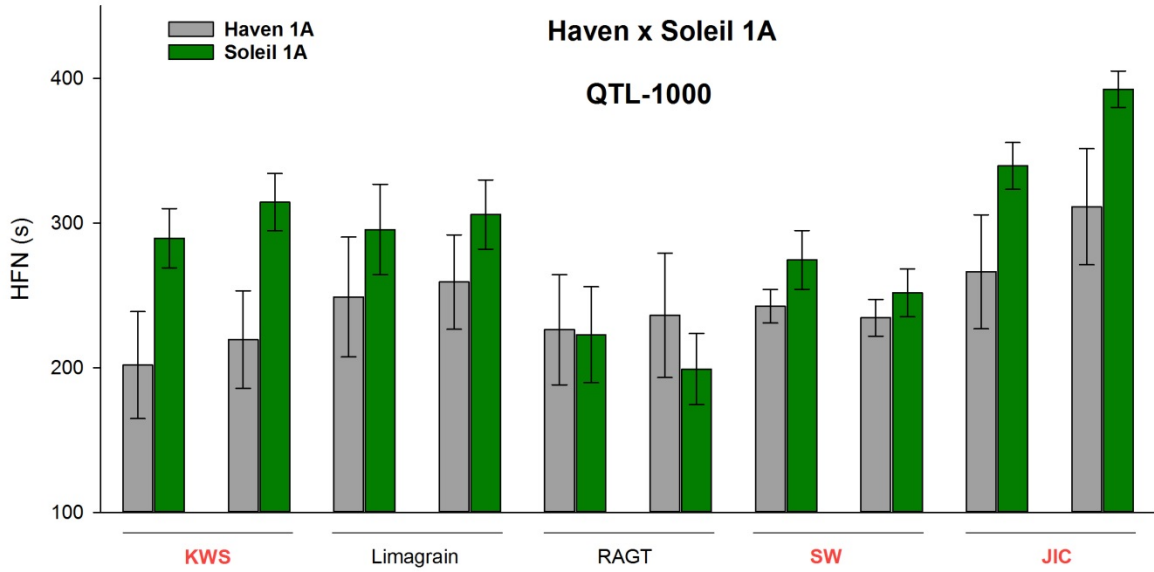


Figure 5: Differences in Hagberg Falling Number (HFN in seconds) for sets of DH lines which differ for the parental allele across the Haven x Soleil 1A (top) and Avalon x Cadenza 2D (bottom) QTL regions. Results are an average of between three and ten replications per time point. The two sets of bars correspond to an early (harvest ripeness) and late (2 weeks later) harvest time points. Significant effects are indicated by the red bold font in the X axis.

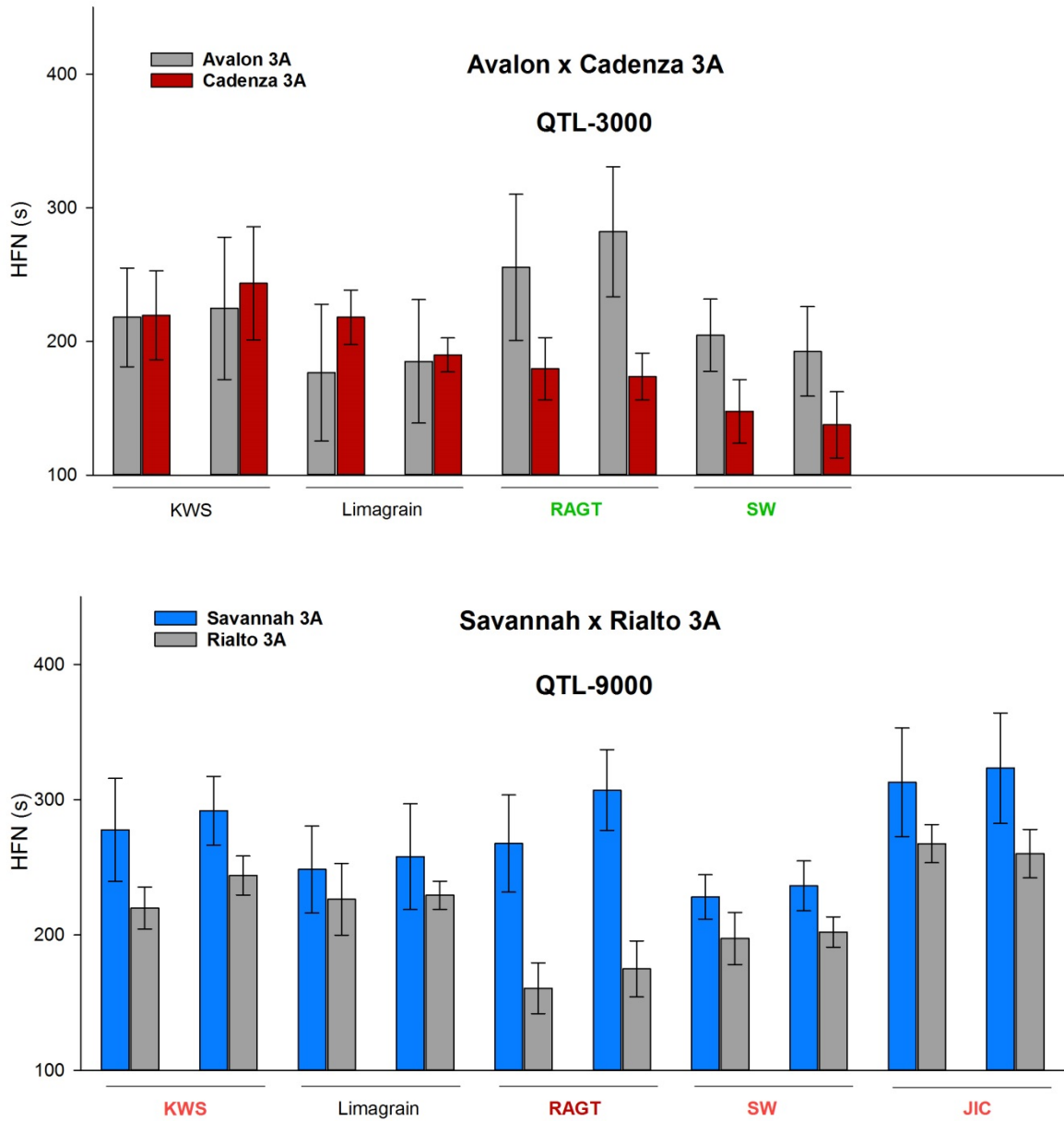


Figure 6: Differences in Hagberg Falling Number (HFN in seconds) for sets of DH lines which differ for the parental allele across the Avalon x Cadenza 3A (top) and Savannah x Rialto 3A (bottom) QTL regions. Results are an average of between three and ten replications per time point. The two sets of bars correspond to an early (harvest ripeness) and late (2 weeks later) harvest time points. Significant positive effects are indicated by the red bold font in the X axis, where significant negative effects are indicated in green bold font (Avalon x Cadenza 3A).

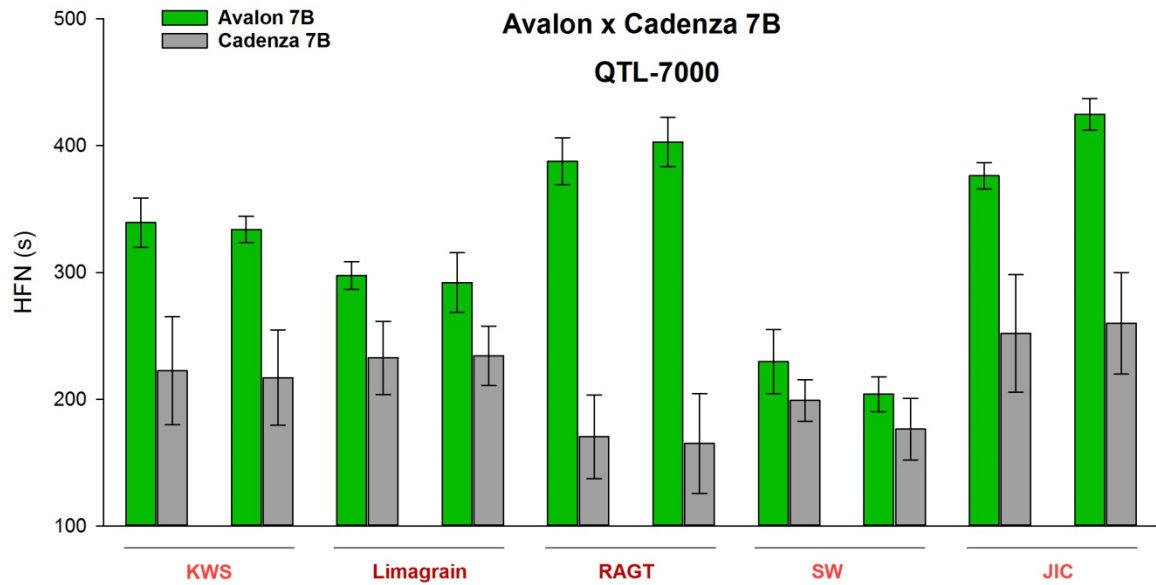


Figure 7: Differences in Hagberg Falling Number (HFN in seconds) for sets of DH lines which differ for the parental allele across the Avalon x Cadenza 7B QTL region. Results are an average of between three and ten replications per time point. The two sets of bars correspond to an early (harvest ripeness) and late (2 weeks later) harvest time points. Significant effects in the expected orientation are indicated by the red bold font in the X axis.

F₃ validation: The QTL chosen for characterisation in this study were identified in DH populations but have not been validated in independent genetic materials. In addition, DH populations do not allow for the independent study of individual QTL effects because such DH populations may have additional small effect QTL segregating. Therefore, to validate the QTL effects in independent genetic material, we used independent F₃ lines with contrasting resistant and susceptible alleles of each QTL. F₃ lines were developed for the 1A, 2D, 3A SxR, and 7B QTL and no F₃ lines were available for the 3A AxC and 4A QTL. Field trials were conducted at four different locations in the UK including: the John Innes Centre (JIC), RAGT Seeds (RAGT), Limagrain UK (LG) and KWS UK (KWS).

Resistance effects were observed for all the QTL in at least one experimental location, except for the 3A SxR QTL. These effects were, for the most part, consistent across all locations (Figures 8-9). The 1A QTL showed highly significant HFN effects at the JIC and KWS field sites. Lines with the resistance allele maintained close to two-fold higher HFN scores to those of susceptible F₃ lines. Although a similar effect was observed at the RAGT site, the difference between alleles was not significant. No difference was observed at Limagrain, most likely due to the higher HFN values for all the QTL at this location compared to the other locations. The 2D F₃ lines showed relatively higher HFN value compared to the 1A line, however, a statistically significant positive effect was observed for the 2D QTL at the KWS and JIC field sites (Figure 8). The 7B QTL showed the strongest effect conferring significant protection across the multiple environments with differences of over 100 s in most locations. Interestingly, the 3A SxR effect was not identified despite the relatively low HFN values in three locations, suggesting that conditions were inductive for low HFN and a putative resistance effect from the QTL. Given the results in other experiments outlined in the report, in consultation we decided to not pursue the fine-mapping of this QTL through additional recombinants. As for the DH lines, both an early (harvest maturity) and a late (2 weeks after-ripening) harvest were performed for the F₃ lines in the breeder's trials.

General agronomic traits were also scored to get an initial estimation of possible pleiotropic effects of the QTL. Overall, there were no consistent effects for flowering or height apart from a very strong effect of the 2D resistant allele which increased height by approximately 13 cm. This is consistent with a linkage in phase between the resistant QTL and the *Rht8* gene on this chromosome arm (Gasparini et al 2012).

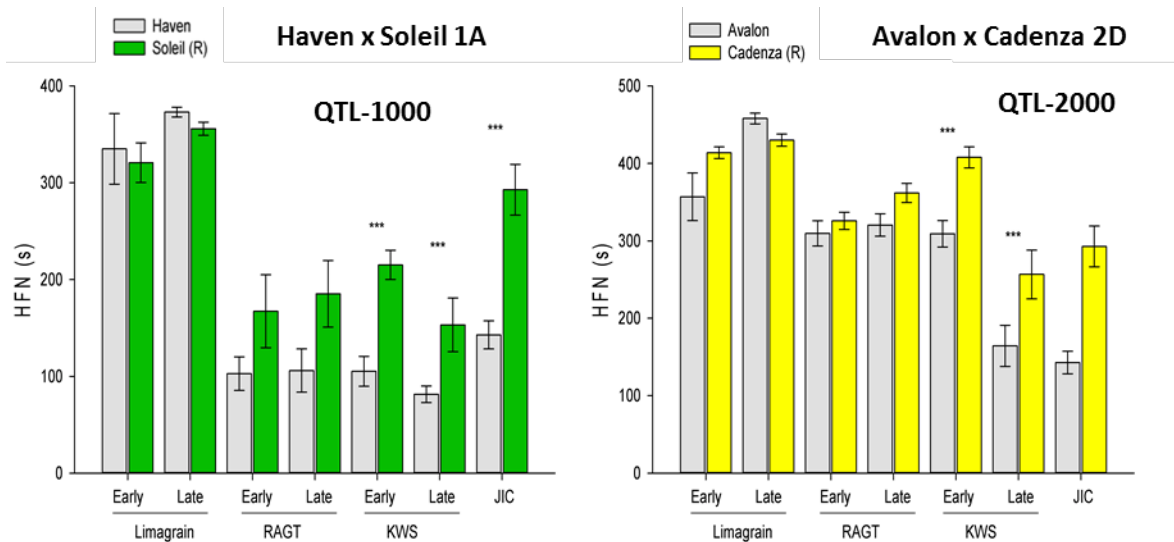


Figure 8: Multi-location validation of QTL in F_3 lines. The HFN score of the resistant (coloured) and susceptible (grey) 1A and 2D QTLs grown at the John Innes Centre (JIC), RAGT, Limagrain and KWS field site. Error bars represent standard error of mean of at least 3 replications. Significant differences at $P < 0.001$ (***) are indicated.

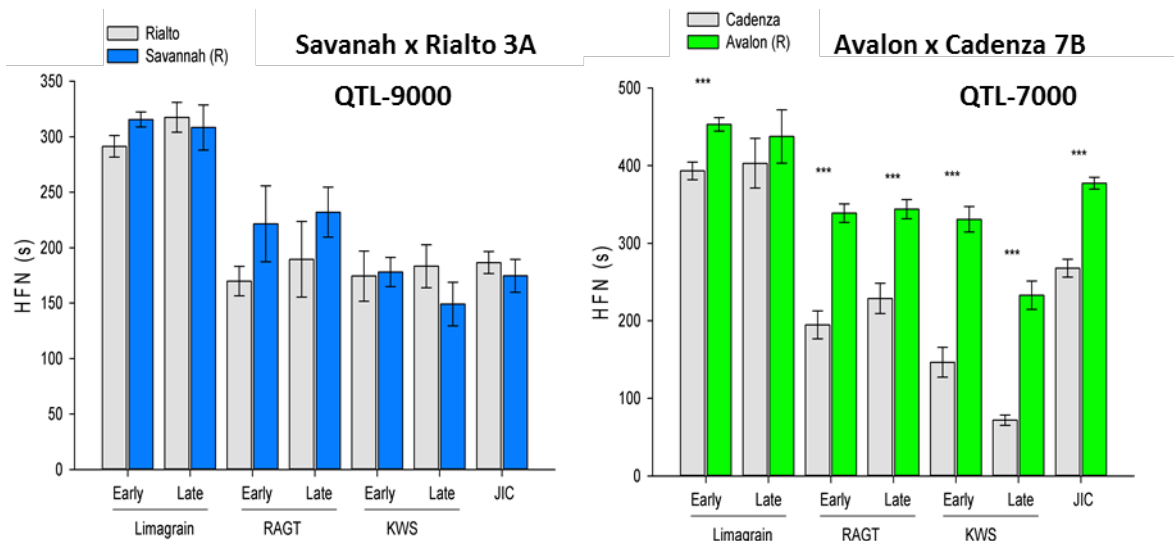


Figure 9: Multi-location validation of QTL in F_3 lines. The HFN score of the resistant (coloured) and susceptible (grey) 3A SxR and 7B QTLs grown at the John Innes Centre (JIC), RAGT, Limagrain and KWS field site. Error bars represent standard error of mean of at least 3 replications. Significant differences at $P < 0.001$ (***) are indicated.

Objective 1.2: Increase marker density across all QTL intervals

To facilitate targeted polymorphism discovery precisely within the target QTL region, we obtained pre-publication access to the iSelect SNP array, later published in Wang et al (2014). We used this to genotype independent resistant and susceptible BC₃ NIL pairs for each QTL along with their respective parents. Using this approach between 8 and 13 % of the 90,000 iSelect SNPs were found to be polymorphic between parental pairs (Table 2). These numbers represent a whole genome SNP distribution between the parental pairs, many of which are not located within the QTL region of interest. To enrich for polymorphisms within the respective QTL regions, a SNP filtering approach that took into account the background homogeneity of the NILs except at the target QTL interval was employed. Two criteria were used to search for SNPs that map within the QTL region. First, SNPs must be monomorphic *within* each allele group and, second, SNPs must be polymorphic *between* allele groups (Figure 10).

Table 2: Number of polymorphic SNPs between parents and NILs for each target QTL.

QTL	Population	QTL	SNPs between Parents (%)	SNPs between allele groups	SNPs mapped to QTL chromosome arm	SNP on QTL chromosome arm (%)
QTL-1000	Haven x Soleil	1A	6,764 (8 %)	353	195	55.2
QTL-2000	Avalon x Cadenza	2D	11,235 (13 %)	163	20	12.3
QTL-3000	Avalon x Cadenza	3A	11,235 (13 %)	221	77	34.8
QTL-9000	Rialto x Savannah	3A	8,670 (10 %)	181	159	87.8
QTL-4000	Alchemy x Robigus	4A	8,598 (10 %)	352	46	13.1
QTL-7000	Avalon x Cadenza	7B	11,235 (13 %)	131	82	62.6

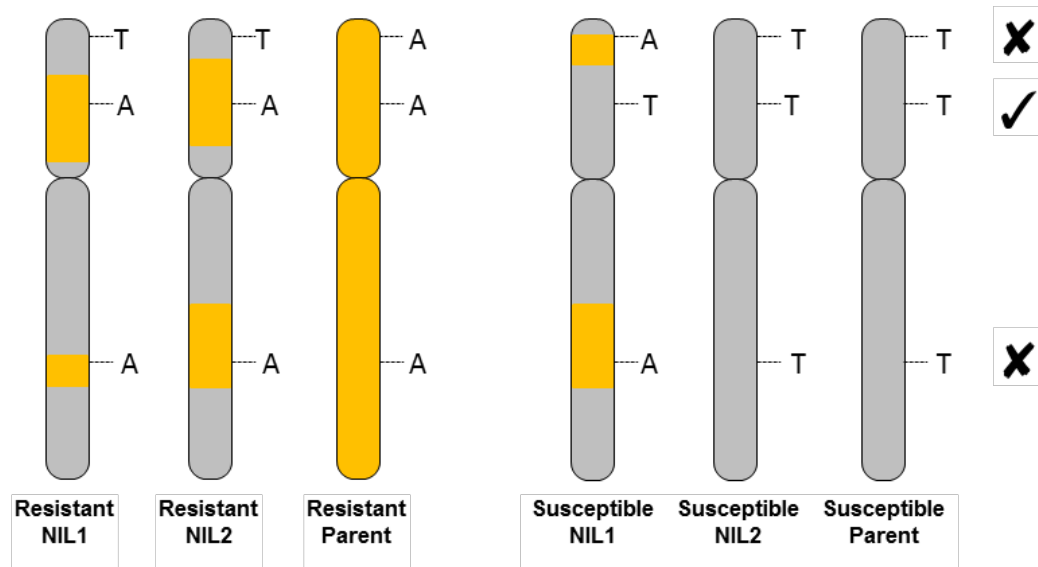


Figure 10: Targeted SNP discovery within QTL regions. Following the genotyping of isogenic materials and parents, only SNPs which were monomorphic *within* allele group, but polymorphic between allele groups were selected (check mark). SNPs that did not meet these criteria were not carried forward (x mark)

Using these criteria, between 131 and 353 polymorphic SNPs were found between the NIL pairs for each QTL. The SNPs were assigned a putative chromosome arm location based on the best BLASTN hit of the sequence surrounding the SNP against the IWGSC CSS chromosome arm sequences (Meyer et al 2014). Unsurprisingly, for most of the QTL, a large proportion of the SNPs map *in-silico* to the chromosome arm harbouring the targeted QTL region (Figure 11 and Table 2). For instance, for the 1A, 3A SxR and 7B NIL pairs, between 55 and 88 % of the SNP mapped to the corresponding chromosome arms (Figure 11). This represents an average of 29-fold enrichment compared to the 2.4% that would have been expected if the SNPs were uniformly distributed across the entire wheat chromosome arms.

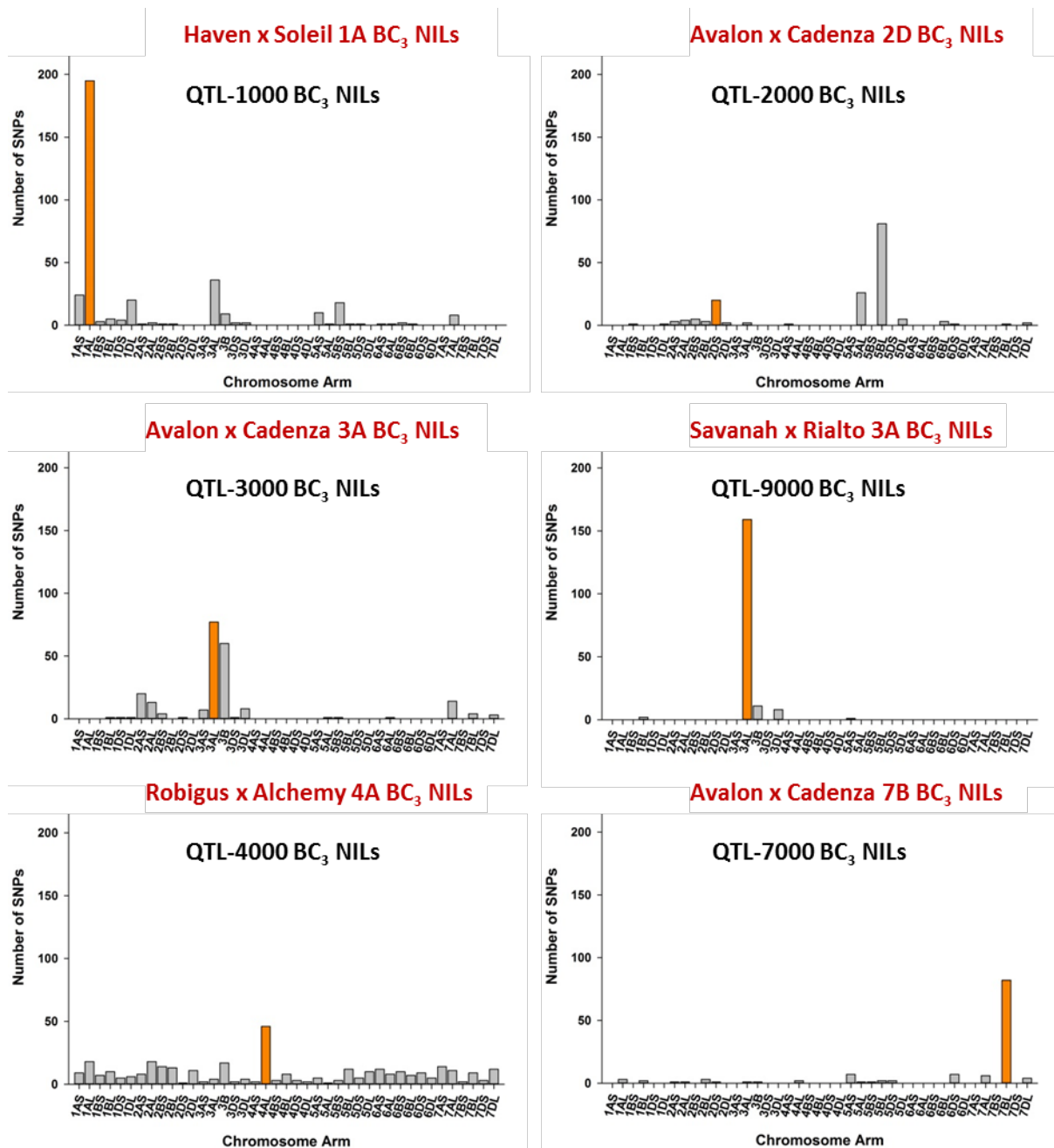


Figure 11: The distribution of polymorphic SNPs across the wheat genome. The locations of polymorphic SNPs between resistant and susceptible allele groups for 1A, 2D, 3A AxC, 3A SxR, 4A and 7B QTL are plotted across all chromosome arms. The chromosome arm where each QTL is located is represented by the orange bar while other chromosomes are in grey.

Similar to the other QTL described above, a significant proportion (35 %) of the polymorphic SNPs found between the 3A AxC QTL NILs mapped to the 3AL chromosome arm (Figure 11). This percentage is less than was observed for the 1A, 3A SxR and 7B QTL regions, however this is most likely do to some SNPs being wrongly assigned to the homoeologous

3B chromosome. For the 4A isogenic material, the 4AL chromosome arm harboured the highest percentage of the polymorphic SNP but the other chromosomes arms also showed a significant amount of variation between NIL pairs. This is most likely due to the fact that the contrasting NIL pairs used for the 4AL QTL were developed from two independent DH lines which differ in their sizes of the resistant parent (Alchemy) introgression.

We obtained one unexpected result. The NIL pairs for the 2D QTL have more variations mapping to the 5BL and 5AL chromosome arms than to the 2DL region (Figure 11). This suggests that the 2D NIL selection also included segments of group 5 chromosomes. After several quality control checks we believe this to be a *bona fide* translocation in the parental variety. With the increase in SNP density this same translocation has also been identified by other groups. The translocation affects the recombination and genetic maps developed for this QTL. This is also the most likely explanation for the reduced number of recombinant plants across the interval compared to other regions (Figure 13).

The SNPs identified through this strategy were then used to further define the QTL intervals. However, the SNPs are part of a 90k array which is too expensive to run in a commercial breeding operation for many individual samples. We therefore developed a bespoke pipeline (PolyMarker) for KASPar marker development to aid in this conversion of a SNP into a functional assay (Ramirez-Gonzalez et al 2015). This tool was made available online (<http://polymarker.tgac.ac.uk/>) and has been widely adopted in academic and industrial sectors. Given the issues surrounding the classification of SNPs to specific chromosomes, we took SNPs which satisfied the criteria outlined in Figure 10 and which were mapped *in silico* to the homoeologous group chromosome. So for example, we took SNPs which mapped to 3A, 3B and 3D for the 3A SxR QTL. We were able to design KASP assays for the majority of the SNPs identified across the QTL regions and these were used to fine map the QTL (Table 3). All relevant SNP assays were quickly transferred to industrial partners who also use the KASP genotyping system.

Table 3: SNP markers developed with PolyMarker across the target QTL regions. SNP markers were selected based on non-homoeologous SNPs and KASP assays prioritised based on genome specificity (specific or semi-specific).

QTL	Population	QTL	Correct group	non-homoeologous	specific	semi-specific
QTL-1000	Haven x Soleil	1A	158	97	26	38
QTL-3000	Avalon x Cadenza	3A	506	346	62	66
QTL-9000	Rialto x Savannah	3A	203	123	39	25
QTL-4000	Alchemy x Robigus	4A	83	58	5	5
QTL-7000	Avalon x Cadenza	7B	285	165	22	26

Fine mapping 1A QTL:

To further define the 1A QTL we developed BC₂ homozygous recombinant lines during the NIL production. We identified lines which carried heterozygous recombination event using KASP markers M2 and M19. These BC₂F₂ plants were self-pollinated and the next generation was screened with the same markers to identify homozygous recombinants across the QTL interval. In total we recovered and bulked seed for 44 homozygous recombinant lines.

Subsets of these lines were distributed to breeders for field trials in 2014 and 2015. Not all lines were sown in all locations given limited seed stocks and the need to sow during a narrow time window in 2014. However, most recombinants were sown in at least 3 independent locations and evaluated for HFN and other traits at an early and late harvest, similar to the phenotyping carried out for the NILs.

We also used the homozygous recombinant lines to map additional markers across the QTL interval and delimit the recombination events. Based on the wheat POPSEQ genetic map and the SNPs identified in the NILs using the iSelect array, we mapped 19 markers across the region to produce a high density genetic map of the 1A QTL (Figure 12).

To map the QTL as a discrete qualitative trait we used the HFN scores from 2014 and 2015 to assign each homozygous recombinant line to a parental class. To account for the uneven replication and the expected variation across experiments, we assigned individuals based on a weighted score from the multiple field tests. We were able to assign 17 homozygous recombinant lines to the susceptible category (Haven), 20 lines to the resistant category (Soleil) and 7 lines were intermediate and we did not assign them to any specific class.

Using this classification we mapped the QTL to a 4 cM interval flanked by markers M16 and M17. This is consistent with the original QTL whose peak coincided with M17 (Figure 12). Some recombinant lines were not consistent in their classification (e.g. HFN1019 and HFN1017), but this is expected from a quantitative phenotype. Based on the iSelect SNP data we have identified an additional 27 polymorphic markers between the flanking M16 and M17 markers. These have been provided to the breeding partners for further validation and use in breeding.

	M1	M2	M3	M4	M5	M6	M7	M8	M9	M10	M11	M12	M13	M14	M15	M16	1A-gene	M17	M18	M19
HFN 1041	-	B	B	B	B	B	B	B	-	A	-	A	A	A	A	-	262.3	-	B	A
HFN 1027	A	B	B	B	B	B	A	A	-	-	-	B	-	-	-	-	271.7	-	B	A
HFN 1026	B	A	A	A	A	A	A	-	-	-	B	B	-	-	-	-	285.1	-	B	-
HFN 1060	B	B	B	A	A	B	A	A	-	-	A	A	A	A	-	-	275.3	A	B	-
HFN 1029	B	B	-	-	-	A	B	B	A	A	-	A	-	-	A	-	168.9	B	B	B
HFN 1049	A	A	B	-	B	A	B	-	A	-	-	A	A	A	-	-	302.8	B	A	B
HFN 1012	B	B	B	B	B	B	B	B	A	A	A	A	A	A	A	A	232.6	-	B	A
HFN 1035	A	A	A	A	A	A	-	A	A	A	A	A	A	A	A	A	236.7	-	B	B
HFN 1028	B	B	B	B	-	B	B	B	A	A	A	A	A	A	A	A	193.6	A	A	A
HFN 1050	B	B	B	A	A	A	A	A	-	-	A	A	A	A	-	A	210.1	A	-	B
HFN 1020	-	B	B	B	B	B	B	B	A	A	-	A	A	A	A	A	243.9	A	A	A
HFN 1014	B	B	B	B	B	B	B	B	A	A	A	A	A	A	A	A	248.8	A	A	A
HFN 1019	-	B	B	B	B	B	B	B	A	A	A	A	A	A	A	A	270.7	A	A	A
HFN 1007	B	B	B	B	B	B	B	B	A	A	A	A	A	A	A	A	301.1	A	A	-
HFN 1001	-	A	-	B	-	A	A	-	B	-	B	B	B	B	B	A	204.9	B	A	-
HFN 1033	B	B	B	B	B	B	B	B	A	A	A	-	-	-	A	A	206.7	B	B	A
HFN 1015	A	A	A	A	A	A	-	A	A	A	A	A	A	A	A	A	231.6	B	B	B
HFN 1043	B	B	-	-	-	-	B	B	-	A	A	A	A	A	A	A	232.1	B	-	B
HFN 1040	A	A	A	A	A	A	-	A	-	A	A	A	A	A	A	A	234.7	B	B	B
HFN 1006	B	B	B	B	B	B	B	B	A	A	A	A	A	A	A	A	249	B	B	-
HFN 1036	A	A	A	A	A	A	A	-	A	A	A	A	A	A	A	A	254.8	B	-	-
HFN 1025	A	B	B	B	B	B	A	-	B	-	-	-	-	-	-	A	269.1	B	A	A
HFN 1031	A	B	-	-	-	-	B	B	A	A	A	A	A	A	A	A	287.4	B	B	A
HFN 1010	-	-	A	-	-	A	-	A	A	A	A	A	A	A	A	A	290.7	B	B	B
HFN 1008	B	B	B	B	B	B	B	B	A	A	A	A	A	A	A	A	290.7	B	B	A
HFN 1016	-	A	A	-	-	-	A	-	A	A	A	A	A	A	A	A	297.3	B	B	A
HFN 1044	-	B	-	-	A	-	B	B	-	-	B	B	A	A	A	A	302.7	B	-	B
HFN 1023	A	B	-	-	A	-	B	B	-	B	B	B	A	A	A	A	309.2	B	A	A
HFN 1021	B	B	B	B	B	B	B	B	A	A	-	A	A	A	A	A	332.1	B	-	A
HFN 1034	A	A	A	A	A	A	A	-	B	B	B	B	B	B	B	B	248.7	-	A	B
HFN 1009	B	B	B	B	B	B	B	B	B	B	B	B	B	B	B	B	284.8	-	B	-
HFN 1022	B	B	-	-	-	-	B	B	B	B	B	B	B	B	B	B	194	A	A	A
HFN 1047	A	B	-	B	B	B	-	-	A	A	-	-	B	B	B	B	195.9	A	A	A
HFN 1039	B	B	B	B	B	B	B	B	B	B	B	B	B	B	B	B	208.4	A	A	-
HFN 1030	B	B	B	B	B	B	B	B	B	B	B	B	B	B	B	B	208.7	A	A	-
HFN 1037	B	B	B	B	B	B	B	B	B	B	B	B	B	B	B	B	219	A	A	-
HFN 1018	-	A	B	B	B	B	B	B	B	-	B	B	B	B	B	B	233	A	A	A
HFN 1046	A	B	B	B	B	B	A	-	-	A	A	-	-	B	B	B	258.7	A	A	A
HFN 1013	B	B	B	B	B	B	B	B	B	B	B	B	B	B	B	B	273.1	A	A	A
HFN 1024	A	B	-	B	B	B	A	-	-	A	A	-	-	B	B	B	274.9	A	A	A
HFN 1011	B	B	B	B	B	B	B	B	B	B	B	B	B	B	B	B	289.6	A	A	-
HFN 1032	B	B	B	B	B	B	B	B	B	B	B	B	B	B	B	B	358.7	A	A	A
HFN 1017	A	A	A	A	A	A	-	A	B	B	B	B	B	B	B	B	231.5	B	B	B
HFN 1038	A	A	B	A	A	A	A	-	B	B	B	B	B	B	B	B	281.8	B	B	B

Figure 12: Graphical genotypes of homozygous recombinants across the 1A QTL interval. Flanking markers M2 and M19 are shown in orange and additional markers are indicated across the top of the figure. The genotype of each homozygous recombinant is shown across the row. The Haven susceptible alleles are shown in grey (A), whereas the Soleil resistant alleles are shown in green (B).

Fine mapping 2D QTL:

A similar approach as for 1A was used to fine map the 2D QTL. However, we uncovered a complex chromosome rearrangement in Cadenza 2D that became evident with the iSelect data for the NILs (Figure 11). This meant that we need to identify novel homozygous recombinant lines and that we had reduced recombination across the region. We mapped 16 genetic markers across the region to define a total of 38 homozygous recombinants in the region between flanking markers M1 and M16. These lines were phenotyped for sprouting as well as for agronomic traits, importantly height, given the close linkage between the 2D QTL and *Rht8*.

We measured sprouting in early and late harvested samples from field grown lines in 2014 and 2015. Based on these values and in the changes in sprouting between the early and late harvested samples we assigned 12 homozygous recombinant lines to the susceptible (Avalon) class, 16 to the resistant (Cadenza) class and 10 lines were inconclusive (Figure 13). We were also able to classify 33 lines as either tall or short based on three trials and in which the difference between tall and short lines was over 15 cm.

In summary, the 2D sprouting gene mapped between marker M6 and M7 and was closely linked with the height effect. We did however identify recombinant lines which did not have coinciding effects for sprouting and height (HFN2035 and HFN2037). This suggests that although tightly linked, the 2D QTL is distinct from the height effect.

	M1	M2	M3	M4	M5	M6	Height	2D-gene	M7	M8	M9	M10	M11	M12	M13	M14	M15	M16
HFN2012	A	B	B	-	B	-	-	-	-	A	A	A	B	A	A	A	A	A
HFN2018	B	B	B	-	B	-	B	b	-	B	B	B	B	A	A	A	A	A
HFN2060	B	B	B	-	B	-	B	B	-	B	B	B	B	A	A	A	B	B
HFN2150	-	B	B	A	A	-	A	A	-	A	A	-	A	A	-	-	A	A
HFN2161	-	A	A	B	A	-	A	A	-	B	B	-	A	B	-	-	A	A
HFN2163	-	A	A	A	A	-	-	a	-	B	B	-	A	A	-	-	A	A
HFN2172	-	B	B	B	A	-	A	a	-	A	A	-	A	A	-	-	A	A
HFN2194	-	A	A	B	B	-	-	a	-	B	B	-	-	A	-	-	A	A
HFN2221	-	B	B	A	A	-	A	a	-	A	A	-	A	B	-	-	A	A
HFN2008	A	A	A	-	A	A	B	b	-	B	B	B	B	B	B	B	B	B
HFN2001	B	B	B	-	B	B	B	b	-	B	B	B	B	A	A	A	A	A
HFN2013	B	B	B	-	B	B	B	B	-	B	B	B	-	A	-	A	-	B
HFN2017	B	B	B	-	B	B	B	b	-	B	B	B	B	A	A	A	A	A
HFN2054	B	B	B	-	-	B	B	b	-	-	-	B	-	A	A	B	-	-
HFN2068	B	B	B	-	B	B	B	B	-	B	B	B	B	A	A	A	B	B
HFN2021	B	B	B	A	-	A	A	-	A	-	-	A	-	B	B	B	-	-
HFN2029	B	B	B	A	-	A	A	a	-	A	-	-	A	-	B	B	B	-
HFN2034	B	B	B	A	-	A	A	-	A	-	-	A	-	B	B	B	-	-
HFN2035	B	B	B	A	-	A	A	b	A	-	-	A	-	B	B	B	-	-
HFN2037	B	B	B	A	-	A	A	b	A	-	-	A	-	B	B	B	-	-
HFN2040	B	B	B	A	-	A	A	a	A	-	-	A	-	B	B	B	-	-
HFN2041	B	B	B	A	-	A	-	a	A	-	-	A	-	B	B	B	-	-
HFN2043	B	B	B	A	B	A	A	inc	A	A	A	A	-	B	B	B	A	A
HFN2044	A	B	B	A	-	A	A	a	A	-	-	A	-	-	B	B	-	-
HFN2046	B	B	B	A	A	A	A	inc	A	A	A	A	A	B	B	-	A	A
HFN2055	-	A	A	-	-	A	-	a	A	-	-	A	-	B	B	B	-	-
HFN2057	A	A	A	-	-	A	B	b	A	-	-	-	-	A	A	A	-	-
HFN2062	A	A	A	-	-	A	A	-	A	-	-	-	-	B	B	B	-	-
HFN2070	B	B	B	-	B	A	A	inc	A	A	A	A	-	A	A	-	A	A
HFN2031	B	B	B	B	-	B	A	a	A	-	-	A	-	A	B	B	-	-
HFN2024	B	B	B	B	-	B	B	-	B	-	-	B	-	A	A	B	-	-
HFN2025	B	B	B	B	-	B	B	b	B	-	-	B	-	A	A	A	-	-
HFN2027	B	B	B	B	-	B	B	-	B	-	-	B	-	A	A	A	-	-
HFN2028	B	B	B	B	-	B	B	b	B	-	-	B	-	A	A	A	-	-
HFN2030	B	B	B	B	-	B	B	b	B	-	-	B	-	A	A	A	-	-
HFN2042	B	B	B	B	-	B	B	-	B	-	-	B	-	A	A	-	-	-
HFN2049	A	B	B	B	-	B	B	b	B	-	-	B	-	A	A	A	-	-
HFN2053	B	B	B	B	B	B	B	b	B	B	B	B	B	B	B	A	B	B

Figure 13: Graphical genotypes of homozygous recombinants across the 2D QTL interval. Flanking markers M1 and M16 are in orange and additional markers are indicated across the top of the figure. The genotype of each homozygous recombinant is shown across the row. The Avalon susceptible alleles are shown in grey (A), whereas the Cadenza resistant alleles are shown in yellow (B). The putative position of the 2D gene between M6 and M7 is based on the combined phenotype of the 38 homozygous recombinant lines. Note that two recombinant lines (HFN2035 and HFN2037; in red) do not coincide for their height and sprouting phenotypes.

Fine mapping 3A AxC QTL:

We identified 21 homozygous recombinants across the 3A AxC QTL by screening with flanking markers M1 and M18. Using the 2014 and 2015 data we were able to classify only 9 lines unequivocally as either parental class. This was due to inconsistent results in 2014 NILs and parents which decrease our confidence in the 2014 results for this particular QTL. Despite this, we mapped the 3A AxC QTL between M3 and M4 (Figure 14). As described in the NILs later on (see Figure 33) we identified a height effect closely linked to the 3A gene, but there was one line HFN3058 which broke the linkage. This suggests that selection for the height effect should allow simultaneous selection for the HFN resistance allele.

	M1	M2	M3	Height	3A-gene	M4	M5	M6	M7	M8	M9	M10	M11	M12	M13	M14	M15	M16	M17	M18
HFN3076	A	A	A	A	A	A	A	A	A	A	A	A	A	A	A	A	A	A	B	A
HFN3064	A	A	A	A	A	A	A	A	A	-	A	A	A	A	A	A	B	B	-	B
HFN3065	A	A	A	A	A	A	A	A	A	A	A	A	A	A	-	A	A	A	-	A
HFN3053	A	A	A	A	A	B	B	B	B	B	B	B	B	B	B	B	B	B	-	-
HFN3061	A	A	A	A	-	A	A	A	A	-	A	A	A	A	A	A	B	B	B	B
HFN3062	A	A	A	A	-	A	A	A	B	-	B	B	A	B	B	B	B	B	B	B
HFN3075	A	A	A	A	-	A	A	A	A	A	A	A	A	A	A	A	B	B	-	A
HFN3057	A	A	A	A		A	A	A	A	-	A	A	A	B	B	B	B	B	B	-
HFN3068	A	A	A	A		A	A	A	A	A	A	A	A	A	A	A	-	A	-	A
HFN3047	A	A	A	A		A	A	A	A	A	A	A	A	A	A	A	A	A	B	B
HFN3058	B	B	B	A	B	-	-	B	B	-	-	-	A	B	B	B	-	A	A	A
HFN3072	B	B	B	B	B	B	B	B	B	B	B	-	-	A	A	A	A	A	-	A
HFN3081	B	B	B	B	B	B	B	B	B	B	B	B	-	A	A	A	A	A	A	A
HFN3085	A	B	B	B	B	-	B	B	B	B	B	-	B	B	B	B	B	B	-	A
HFN3041	B	B	B	B	B	B	B	B	B	B	B	B	B	B	B	B	B	A	B	-
HFN3051	B	B	B	B		B	B	B	B	B	B	B	B	B	B	B	A	A	A	A
HFN3073	B	B	B	B		B	B	B	B	B	B	B	B	A	A	A	A	A	A	A
HFN3066	B	B	B	B		B	B	B	B	B	B	B	B	A	A	A	A	A	A	A
HFN3045	B	B	B	B		B	B	B	B	B	B	B	B	A	A	A	A	A	A	A
HFN3067	B	B	B	B		B	B	B	B	B	B	B	B	A	A	A	-	A	A	A
HFN3071	B	B	B	B		B	B	B	B	B	B	B	B	A	A	A	A	A	A	A

Figure 14: Graphical genotypes of homozygous recombinants across the 3A AxC QTL interval. Avalon susceptible alleles are shown in grey (A); Cadenza resistant alleles are in red (B). The putative position of the 3A gene M3 and M4 is based on the phenotype of the 9 homozygous recombinant lines. Note that recombinant lines HFN3058 (red) did not coincide between height and HFN phenotypes.

Fine mapping of 7B QTL:

Similarly to the methods outlined previously, we identified a total of 56 homozygous lines with recombination between M1 and M38. These lines were sown in the field in 2014 and 2015 and evaluated for HFN in early and late harvests. We were able to classify 23 lines as resistant (Avalon), 21 lines as susceptible (Cadenza), 8 lines were inconclusive and 4 lines were not evaluated. It is important to note that the recombinants were fixed for the susceptible Avalon haplotype across the other QTL on chromosomes 2D and 3A.

Based on this phenotype we mapped the 7B gene to the distal end of chromosome between markers M13 and M14 (Figure 15). This corresponds to an 8 cM interval which importantly defines it within a discrete region and not in the end of the chromosome. This will allow breeders to use proper flanking markers to select the gene which confers the highest increase in HFN scores from all QTL studied. Additional markers across this region are now being developed.

Objective 2: Epistatic interactions between QTL and pleiotropic effects on grain and plant characters

Resistance to PHS and PMA induction is a desirable trait that ultimately improves the bread-making quality of wheat grains. However, it is important that these are not achieved at the expense of other agronomic traits that are of high breeding value. Such traits include yield, grains morphometric parameters (size, weight and thousand grain weight) and adaptive traits like plant height, and flowering time. It is, therefore, important to examine whether the PHS and PMA QTL studied have detrimental effects on these other agronomic traits either by linkage or pleiotropy.

Objective 2.1: Define agronomic effects of each QTL on grain and plant characters

To determine the effects of the QTL on agronomic traits, BC₁ NILs carrying alternate alleles of the 2D, 3A AxC, 3A SxR and 7B QTL along with their parents (Avalon, Cadenza, Rialto and Savannah) were sown in field sites of breeding partners across the UK and Sweden (KWS, Limagrain, SW (now Lantmannen), RAGT) in 2012, 2013 and 2014. The yield, height, ear emergence and grain size parameters of these NILs were examined. Due to insufficient amount of seeds for field trials in 2012, the 1A NILs were not included in this year. Also, for the 7B QTL, only one NIL per QTL allele was used for 2012 and later increased for 2013 and 2014 (Table 4).

Table 4: Summary of near isogenic lines (NILs) used to evaluate the agronomic performance of the target QTL. Y=yes; N=no. Number of NILs indicated in right-most columns.

			Year			+ NILs	- NILs
			12	13	14		
QTL-1000	Haven x Soleil	1A	N	Y	Y	4	3
QTL-2000	Avalon x Cadenza	2D	Y	Y	Y	5	5
QTL-3000	Avalon x Cadenza	3A	Y	Y	Y	5	5
QTL-9000	Rialto x Savannah	3A	N	N	Y	5	5
QTL-7000	Avalon x Cadenza	7B	Y	Y	Y	3	3

To facilitate discussion and presentation of results across years and sites we will outline each phenotype in turn.

Yield: We did not identify any negative yield effects from the four tested QTL in 2012 across the four locations tested. In most locations, there was no significant yield difference between the resistant and susceptible NILs. The 2D and 7B QTL showed significant yield increase in one and two of the three experimental locations, respectively, associated with the resistant allele. However, overall there was no significant effect across locations for any of the QTL (Figure 16).

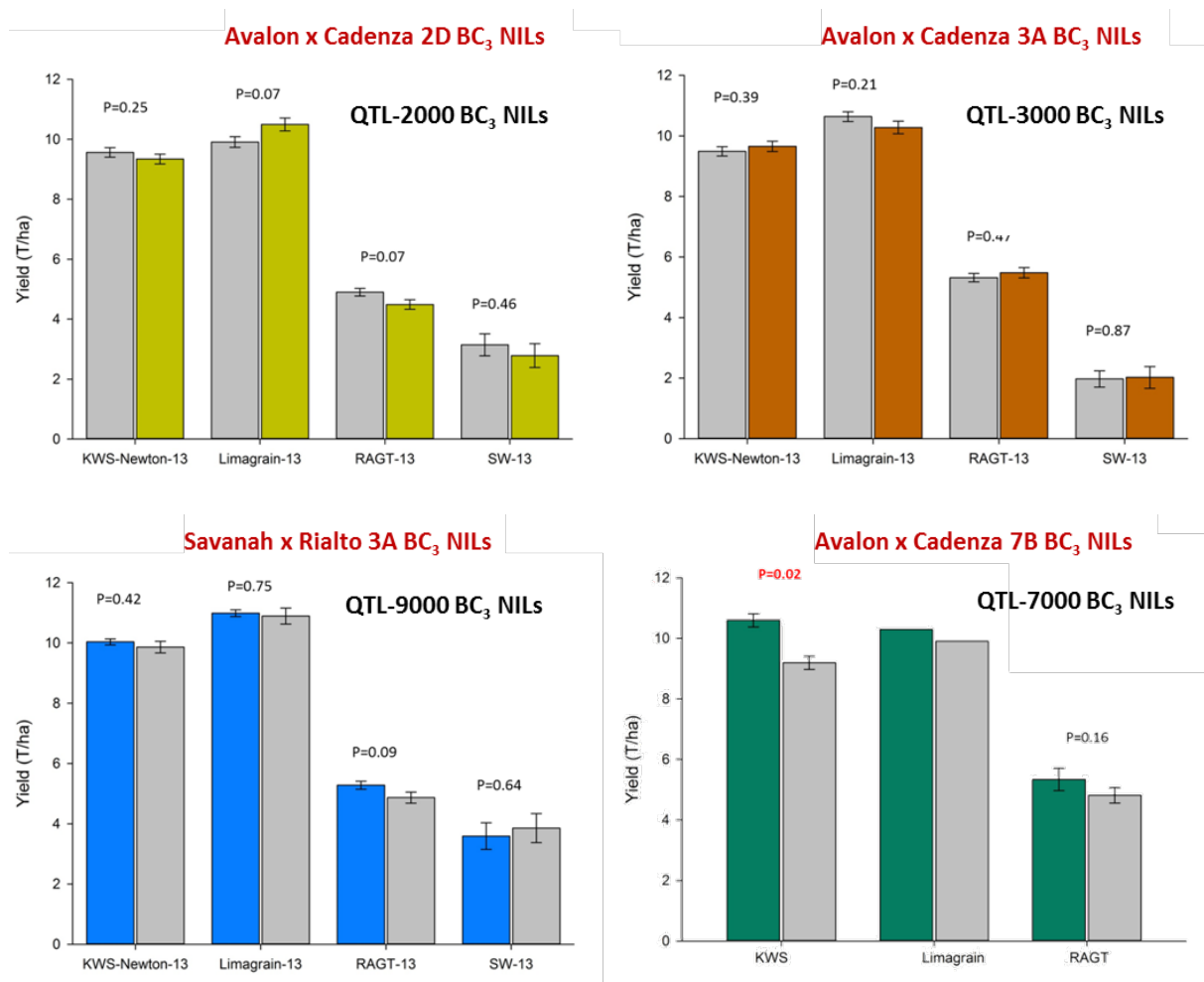


Figure 16: Yield effect of individual QTL in BC₁ NILs across four field locations in 2012-2013. NILs with the positive allele for each QTL are shown in coloured highlight whereas negative NILs are in grey. P values are indicated for each location except LG QTL-7000 which was unreplicated.

Height: We found significant effects on height for four of the five QTL tested, with the significant positive effect on height linked with the resistant QTL allele in three of these cases. The 1A positive allele had a non-significant height increase of 2.2 cm (Figure 17). Across all locations, the 2D QTL resistant NILs were taller than their susceptible counterpart by an

average height of 12.6 ± 0.9 cm and this was associated with the cadenza *Rht8* allele. Similarly, the 3A AxC resistant allele was associated with a significant 4.7 ± 0.8 cm height increase (Figure 18). In contrast, the 3A SxR resistance QTL introgression led to a reduction in height across locations. On average, resistant NILs were 4.5 cm shorter than their susceptible counterparts. A smaller effect was observed for the 7B resistance allele which increased height significantly by an average of 2.5 ± 0.6 cm. These effects were largely consistent across locations and can be seen in glasshouse grown plants (Figures 17-18).

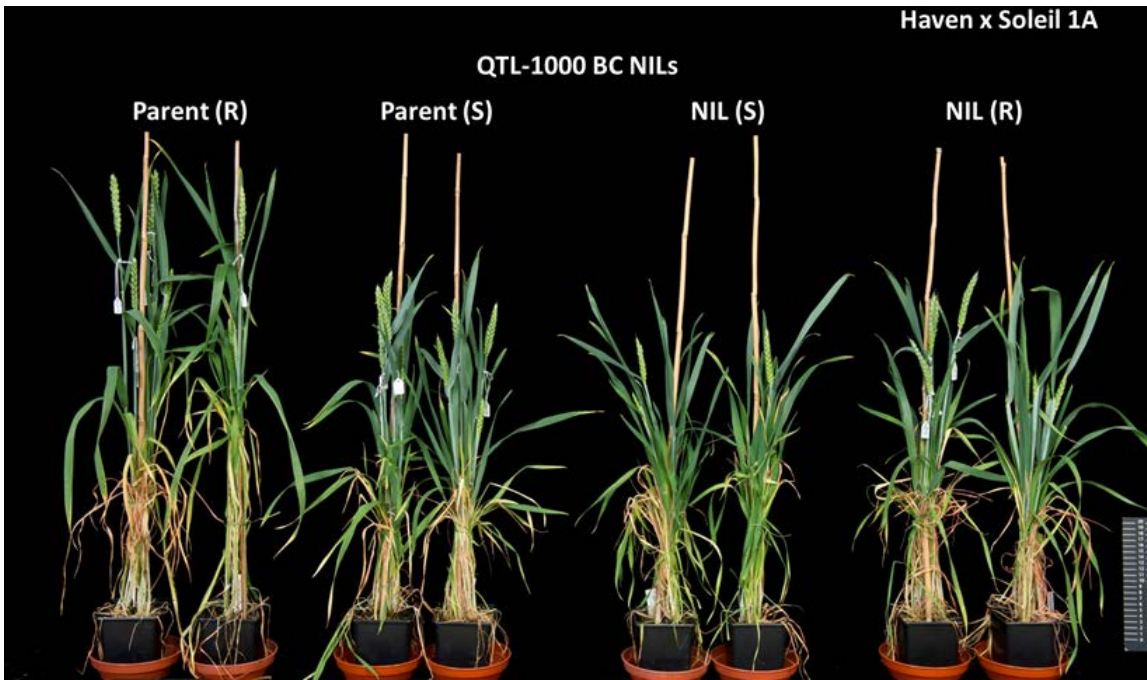


Figure 17: Representative plants of 1A parents and NILs. The non-significant 2.2 cm effect on height is seen in the resistant NIL in the right-hand side of the figure. Note that the NILs have heights comparable to the susceptible recurrent parent.

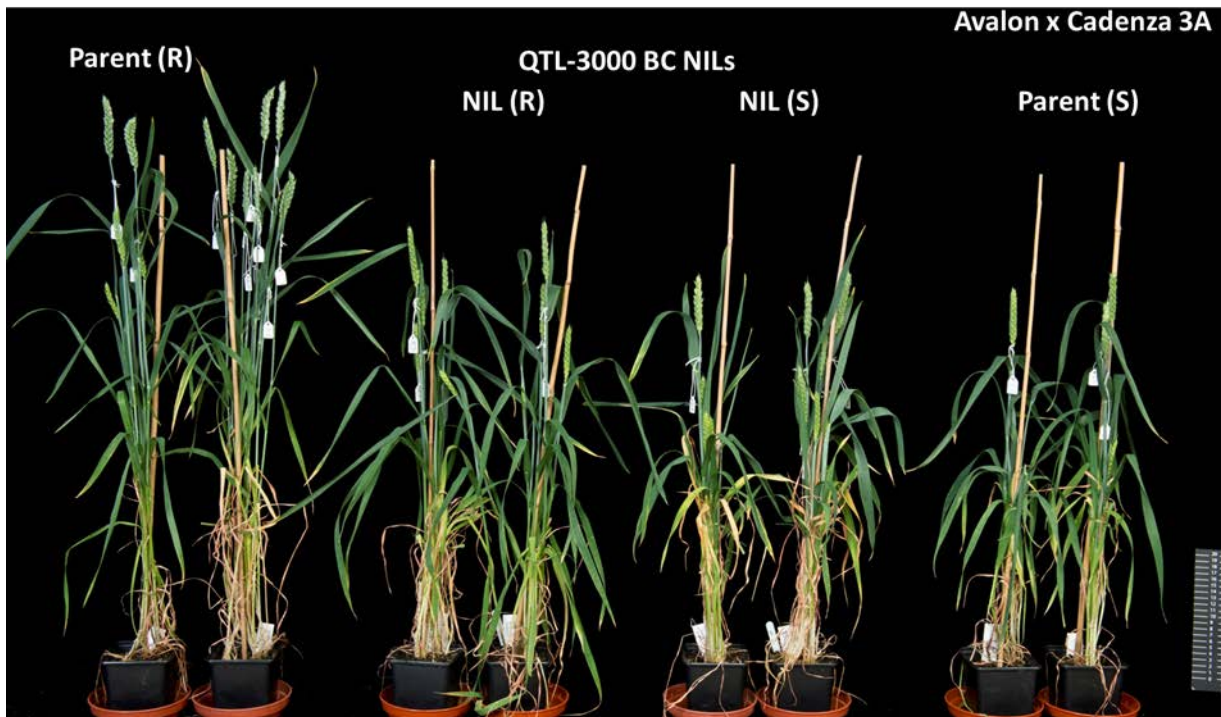


Figure 18: Representative plants of 3A AxC parents and NILs. The significant 4.7 ± 0.8 cm height increase in resistant NILs is seen in the comparison of the middle plants. These NILs used Avalon (right) as the recurrent parent.

Flowering: Days to ear emergence was used for the evaluation of the flowering time trait. Field evaluation of the NILs showed that only the 3A AxC and 3A SxR QTL showed effects on days to ear emergence, and this was consistent in all the locations tested. In the Avalon x Cadenza 3A population, the resistant NILs reached ear emergence on an average of 2.2 days later than the susceptible NILs. This was also true for the Savannah x Rialto population with the resistant allele associated with a later ear emergence phenotype of 2 days. Interestingly, the flowering delay in the 3A region was not linked in cis with the height effect described above since Savannah carries a combination of “PHS resistance + delay flowering + tall” whereas Cadenza is “PHS resistant + delay flowering + short” across the 3A region. A subtle earlier flowering was seen for the 2D resistance allele (-0.7 days) but this was not significant.

Grain parameters: The effects of the QTL on grain size and shape variation in the NILs were also examined. This was done by measuring thousand grain weight (TGW) and morphometric parameters like grain area, width and length. We found contrasting effects across years. Whereas in 2012-2013 we identified a series of significant effects from the different NILs, we did not replicate these in 2014-2015.

HFN: We measured HFN in early and late harvested materials and compared the effects across years and locations. Across locations we observed significant effects of four QTL on HFN values. The 1A QTL (n=11 experiments) provided on average a 25 ± 6 s increase in HFN compared to the susceptible NIL. Similarly the 2D QTL (n=8) conferred a 21 ± 6 s improvement in HFN. The 3A AxC effect (n=17) was more variable with an average 11 ± 8 s improvement, although in 2015 we found significant negative effects of the QTL at JIC and KWS. The 7B QTL (n=18) has the strongest effect on HFN with significant improvements of 32 ± 7 s compared to the susceptible NIL (Figure 19).

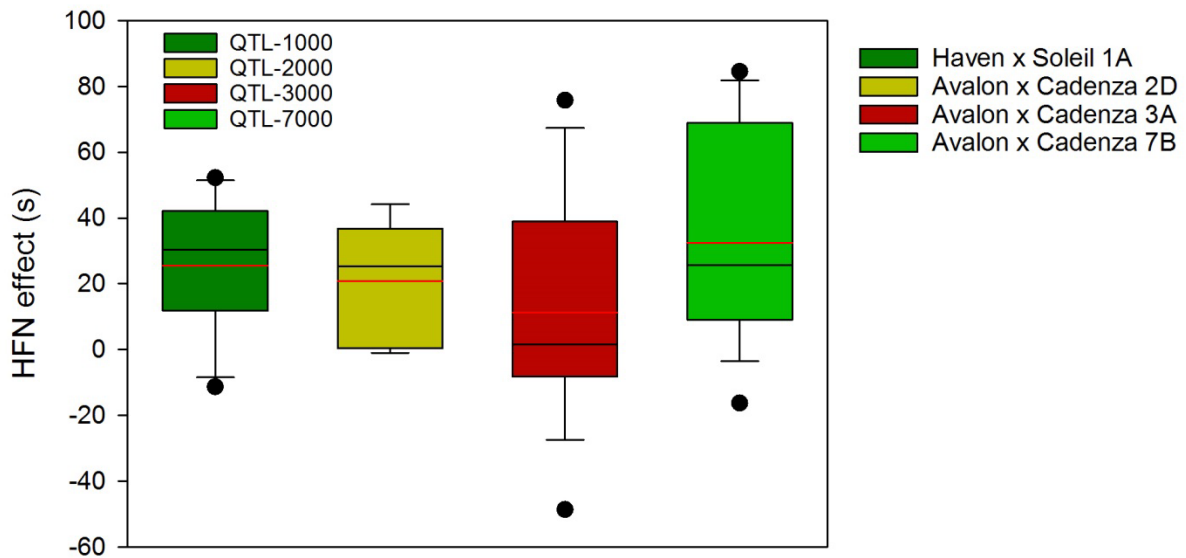


Figure 19: Average HFN effect of four QTL in NILs grown across 2012-2014 field trials. The left boundary of the box indicates the 25th percentile, the black line within the box marks the median (50th percentile), and the right boundary of the box indicates the 75th percentile. The error bars (whiskers) on either side of the box indicate the 10th and 90th percentiles. Outlier data are shown by the small black circles. The red line within the box marks the mean. From left to right N= 11, 8, 17, 18 independent experiments.

Objective 2.2 Evaluate pair-wise interactions between QTL and in novel backgrounds

We developed a series of BC₃ NILs in which we transferred the resistant and susceptible alleles into four common genetic backgrounds. Two of the recurrent parent lines were also parents of the bi-parental mapping populations and had QTL associated with them (Avalon and Cadenza). The other two lines were new to the project and were selected by the industrial partners (Nijinsky and Charger).

In several instances we also introduced the susceptible allele into the novel genetic background to assess the possibility that the original QTL effect was due to a negative allele from one of the parents rather than to a beneficial allele. This would be the case if the most common allele was functional and a mutant allele decreased performance. In this case the “resistant” allele would be common, but the knowledge of the negative mutant allele would be important so that breeders could select against it when using the susceptible line in crossing pedigrees. For some crosses we were not able to identify polymorphic markers during the first years of the project and hence they were not developed (especially in the Nijinsky background). However, with recent advances in our genomic understanding we have been able to generate new markers and transferred these to the industrial partners. A summary of the alleles introduced into the different common recurrent parents is shown in Figure 20.

Common Recurrent Parents				
QTL Parents	Avalon	Cadenza	Nijinsky	Charger
Avalon (R)			---	YES
Cadenza (R)			YES	YES
Haven	YES	YES	---	---
Soleil (R)	YES	YES	---	YES
Savannah (R)	---	YES	---	YES
Rialto	YES	YES	YES	---

Figure 20: Summary of crossing used to generate BC₃ NILs with different allelic combinations for the target QTL. NILs which were successfully developed are indicated in green, whereas those NILs which were not generated are shown with a dashed line.

Given the complexity of the multiple interactions and analyses, we will present each QTL in turn and evaluate its performance in the different genetic backgrounds. Lines were sown in 2013 and 2014 in different locations and evaluated for HFN, sprouting, yield, height, heading and grain morphometric parameters.

1A QTL: We introduced both the resistant (Soleil) and susceptible (Haven) haplotypes into Avalon and Cadenza, whereas only the resistant haplotype was introduced into Charger. The exact number of NILs carrying alternative alleles are presented in Figure 21.

Common Recurrent Parents

QTL Parents	Avalon	Cadenza	Charger
Haven	2 Hav / 2 Ava	5 Hav / 4 Cad	---
Soleil (R)	2 Sol / 2 Ava	5 Sol / 5 Cad	4 Sol / 4 Cha

Figure 21: BC₃ NILs developed for the 1A QTL. The number of NILs carrying each allele is indicated in the relevant position. For example: we have 2 BC₃ NILs which carry the Soleil resistance allele on 1A and 2 sister NILs which carry the Avalon allele on 1A.

We first analysed the effects of the Haven (S) and Soleil (R) haplotypes into the Avalon background. We present the complete summary of data in Figure 22 and expand on the effects in Table 5.

	Avalon	Soleil-Res	Soleil-1A effect	% effect	P value		Avalon	Haven-Sus	Haven-1A effect	% effect	P value	
2014-HFN_JIC	342	380	37.2	11%	0.01		2014-HFN_JIC	374	351	-23.1	-6%	0.01
2014-HFN_KWS	406	382	-24.0	-6%	0.08		2014-HFN_KWS	386	377	-8.8	-2%	0.61
2014-HFN-Early_RAGT	319	277	-41.7	-13%	0.34		2014-HFN-Early_RAGT	293	217	-75.6	-26%	0.15
2014-HFN-Late_RAGT	302	297	-4.8	-2%	0.86		2014-HFN-Late_RAGT	286	220	-66.0	-23%	0.03
2014-HFN-Early_SW	359	426	66.3	18%	0.01		2014-HFN-Early_SW	420	368	-52.3	-12%	0.02
2014-HFN-Late_SW	389	406	17.0	4%	0.34		2014-HFN-Late_SW	426	354	-71.5	-17%	0.03
2015-HFN-Early_JIC	382	450	67.4	18%	0.14		2015-HFN-Early_JIC	418	392	-25.5	-6%	0.23
2015-HFN-Late_JIC	366	334	-32.8	-9%	0.21		2015-HFN-Late_JIC	310	268	-41.7	-13%	0.10
Early % Sprouted	17.0	21.1	4.1	24%	0.97		Early % Sprouted	16.8	32.0	15.3	91%	0.11
Late % Sprouted	28.8	16.6	-12.2	-42%	0.02		Late % Sprouted	48.6	53.0	4.4	9%	0.83
AdjYield_Y_JIC_15	5.57	5.54	0.0	-1%	no reps		AdjYield_Y_JIC_15	5.88	6.42	0.5	9%	0.10
TGW(g)_Y_JIC_15	54.80	53.20	-1.6	-3%	no reps		TGW(g)_Y_JIC_15	45.96	45.15	-0.8	-2%	0.63
Øarea_Y_JIC_15	24.30	23.35	-0.9	-4%	no reps		Øarea_Y_JIC_15	21.64	21.29	-0.4	-2%	0.04
Øwidth_Y_JIC_15	3.68	3.66	0.0	-1%	no reps		Øwidth_Y_JIC_15	3.40	3.34	-0.1	-2%	0.14
Ølength_Y_JIC_15	7.27	6.99	-0.3	-4%	no reps		Ølength_Y_JIC_15	6.81	6.72	-0.1	-1%	0.02
TGW(g)	58.42	55.92	-2.5	-4%	0.31		TGW(g)	53.24	48.69	-4.5	-9%	0.05
ØArea	25.42	24.40	-1.0	-4%	0.05		ØArea	23.59	22.66	-0.9	-4%	0.10
ØWidth	3.86	3.78	-0.1	-2%	0.30		ØWidth	3.64	3.53	-0.1	-3%	0.10
ØLength	7.22	7.03	-0.2	-3%	0.00		ØLength	6.98	6.84	-0.1	-2%	0.04
2014-Height_RAGT	83.0	89.5	6.5	8%	0.01		2014-Height_RAGT	84.5	81.5	-3.0	-4%	0.41
2014-Height_SW	66.7	68.3	1.7	2%	0.08		2014-Height_SW	64.2	63.3	-0.8	-1%	0.55
Crop Height_Y_JIC_15	84.0	87.9	3.9	5%	no reps		Crop Height_Y_JIC_15	84.8	88.3	3.5	4%	0.22
2014-EE_RAGT	28.0	26.0	-2.0	-7%	no var		2014-EE_RAGT	28.5	28.5	0.0	0%	1.00
2014-Heading_SW	2.0	1.8	-0.2	-8%	0.35		2014-Heading_SW	2.0	1.8	-0.2	-8%	0.35

Figure 22: Summary of phenotypic effects of the Soleil (R) and Haven (S) introgression into Avalon. Significant effects are shown in red ($P < 0.05$) and blue ($P < 0.10$) font with positive effects in grey and negative effects in yellow highlight.

Table 5: Description of phenotypic effects of the 1A QTL haplotypes into the *Avalon* genetic background. The main conclusions are shown in bold.

<i>Avalon</i>	Soleil-1A Resistant	Haven-1A Susceptible
HFN	There was an overall positive effect of the resistant Soleil allele, but this was not too large given the already high HFN values in 2014 and 2015.	There was a consistent negative effect of the susceptible Haven allele into the Avalon background (average -45 s) in 2014 and 2015.
Sprouting	Overall reduction in sprouting, significant in late sample.	Overall increase in sprouting, although non-significant.
Yield	No effect	Non-significant ($P=0.104$) increase in yield +9 %.
TGW	General decrease in components of between 3 and 4%.	General decrease in components of between 4 and 5%.
Height	Significant increase in height (~4 cm).	No effect
Heading	No effect	No effect

We then analysed the effects of the Haven (S) and Soleil (R) haplotypes into the Cadenza background. We present the summary (Figure 23) and describe the effects in Table 6.

	Cadenza	Soleil-1A-Res	Soleil-1A-Effect	%	P value		Cadenza	Haven-1A-Sus	Haven-1A-Sus effect	%	P value
2014-HFN_JIC	369.0	390.8	21.8	6%	0.060		392.7	380.5	-12.2	-3%	0.209
2014-HFN_KWS	355.3	380.1	24.7	7%	0.116		366.7	392.4	25.7	7%	0.132
2014-HFN-Early_RAGT	270.8	284.6	13.9	5%	0.602		284.0	323.6	39.6	14%	0.201
2014-HFN-Late_RAGT	301.3	307.2	5.9	2%	0.827		297.0	326.4	29.4	10%	0.204
2014-HFN-Early_SW	367.8	371.7	3.9	1%	0.684		396.8	372.0	-24.8	-6%	0.223
2014-HFN-Late_SW	337.8	329.8	-7.9	-2%	0.253		381.0	378.4	-2.6	-1%	0.948
2014-Y-HFN_LM	334.5	324.1	-10.4	-3%	0.256		335.8	357.7	21.9	7%	0.071
2015-HFN-Early_JIC	361.3	357.3	-4.0	-1%	0.847		371.2	356.2	-15.0	-4%	0.522
2015-HFN-Late_JIC	307.6	269.1	-38.5	-13%	0.011		309.2	295.4	-13.8	-4%	0.501
2015-Early % Sprouted_JIC	3.8	5.5	1.7	43%	0.319		3.0	3.9	0.8	27%	0.529
2015-Early % Sprouted_JIC_Arc	10.4	12.5	2.1	20%	0.306		9.7	10.4	0.6	6%	0.737
2015-Late % Sprouted_JIC	18.3	24.9	6.6	36%	0.221		24.6	17.6	-7.0	-29%	0.096
2015-Late % Sprouted_JIC_Arc	24.6	29.6	5.0	20%	0.189		29.4	24.2	-5.2	-18%	0.085
2014-Y-Yield (t/ha,15%M)_KWS	12.0	12.5	0.5	4%	<.001		11.6	12.1	0.5	4%	0.011
2014-Yield (t/ha)_RAGT	7.4	7.3	-0.1	-1%	0.875		7.5	7.6	0.1	1%	0.65
2014-Y-Yield (t/ha)_SW	9.3	9.7	0.4	4%	0.012		9.5	9.7	0.1	2%	0.666
2014-Y-Yield (kg)_LM	7.3	7.3	0.1	1%	0.556		7.4	7.3	-0.1	-2%	0.303
AdjYield_Y_JIC_15	10.2	10.6	0.4	4%	0.013		10.4	10.5	0.2	2%	0.651
2014-Y-TGW(g)_LM	56.2	58.3	2.1	4%	0.002		53.8	57.2	3.4	6%	<.001
2014-Y-Øarea_LM	19.9	20.2	0.4	2%	0.005		19.6	20.1	0.5	2%	0.007
2014-Y-Øwidth_LM	3.7	3.7	0.1	2%	0.011		3.7	3.8	0.1	3%	<.001
2014-Y-Ølength_LM	6.8	6.8	0.0	0%	0.894		6.6	6.6	0.0	0%	0.496
2014-Y-Weight (g)_LM	24.9	25.0	0.1	0%	0.635		24.9	25.3	0.4	1%	0.009
2014-Y-SpW_LM	81.0	81.1	0.2	0%	0.635		81.0	82.2	1.2	1%	0.009
TGW(g)_Y_JIC_15	47.9	49.6	1.7	4%	0.012		48.5	51.5	3.0	6%	<.001
Øarea_Y_JIC_15	22.6	22.9	0.3	1%	0.022		22.5	23.0	0.5	2%	0.002
Øwidth_Y_JIC_15	3.5	3.6	0.0	1%	0.079		3.5	3.6	0.1	3%	<.001
Ølength_Y_JIC_15	7.0	7.0	0.0	0%	0.816		6.9	6.9	0.0	0%	0.696
2014-Height_RAGT	98.3	102.0	3.8	4%	0.104		94.8	99.3	4.6	5%	0.847
2014-Height_SW	76.3	76.0	-0.3	0%	0.799		72.9	76.0	3.1	4%	0.353
Crop Height_Y_JIC_15	86.7	90.8	4.1	5%	<.001		86.6	94.7	8.1	9%	0.001
2014-Heading_RAGT	23.0	19.6	-3.4	-15%	0.027		20.8	20.2	-0.6	-3%	0.639
2014-Heading (0=early, 3=late)_SW	1.9	1.5	-0.5	-23%	0.010		1.3	0.9	-0.5	-35%	0.004

Figure 23: Summary of phenotypic effects of the Soleil (R) and Haven (S) introgression into *Cadenza*. Significant effects are shown in red ($P < 0.05$) and blue ($P < 0.10$) font with positive effects in grey and negative effects in yellow highlight.

Table 6: Description of phenotypic effects of the 1A QTL haplotypes into the *Cadenza* genetic background. The main conclusions are shown in bold.

<i>Cadenza</i>	Soleil-1A Resistant	Haven-1A Susceptible
HFN	No effect from the resistant Soleil allele.	Overall no significant effect.
Sprouting	No effect	Reduction in late but non-significant.
Yield	The resistant haplotype confers a 4.2 % yield increase with respect to Cadenza and is significant in 3 of 5 locations.	No significant effect, although generally positive
TGW	Significant positive effect on components in line with yield effect.	Significant positive effect on components.

Height	Significant increase in height (~4 cm)	Increase in height (~5 cm)
Heading	Earlier heading with resistant haplotype.	Slightly earlier heading

Finally, we analysed the effects of the Soleil (R) haplotype into the Charger background and present the summary (Figure 24) and describe the effects in Table 7. Note that two comparisons were made for Charger. We compared first against the 1A sibling NILs (n=4) and then compared to all Charger NILs (n=16) given that there was some variation in phenotype between the isogenic lines. While this changes slightly the conclusions, it does so in magnitude rather than in the direction of the effect.

	Charger 1A	Soleil 1A-Res				vs ALL_Charger		
			Soleil 1A effect	%	P value	Soleil 1A effect	%	P value
2015-HFN-Early_JIC	332	343	11	3%	0.514	41	14%	0.037
2015-HFN-Late_JIC	322	345	23	7%	0.158	52	18%	<.001
2015-Y-HFN-Early_RAGT	312	317	5	2%	0.671	55	21%	0.004
2015-Y-HFN-Late_RAGT	221	208	-13	-6%	0.533	12	6%	0.531
2015-Y-HFN-Early_LM	271	277	6	2%	0.490	41	17%	<.001
2015-Y-HFN-Late_LM	265	268	3	1%	0.769	40	18%	<.001
2015-Y-HFN-Early_KWS	349	343	-6	-2%	0.470	36	12%	0.043
2015-Y-HFN-Late_KWS	154	204	49	32%	0.029	55	37%	0.002
2015-Early % Sprouted_JIC	5.8	7.5	1.6	28%	0.389	-0.1	-2%	0.934
2015-Late % Sprouted_JIC	36.3	50.7	14.4	40%	0.057	12.6	33%	0.019
2015-TGW(g)	47.4	47.8	0.4	1%	0.617	-0.2	0%	0.748
2015-ØArea	22.2	22.2	0.0	0%	0.967	-0.2	-1%	0.340
2015-ØWidth	3.6	3.6	0.0	0%	0.886	0.0	0%	0.499
2015-ØLength	6.6	6.6	0.0	0%	0.872	0.0	0%	0.317
2015-Y-Height_KWS	75.1	74.8	-0.3	0%	0.708	-1.1	-1%	0.212
2015-EE_RAGT	26.9	27.1	0.2	1%	0.698	0.6	2%	0.258
2015-Y-EE (May/June)_KWS	2.2	2.1	-0.1	-4%	0.703	-0.7	-25%	0.581

Figure 24: Summary of phenotypic effects of the Soleil (R) introgression into Charger. Significant effects are shown in red ($P < 0.05$) and blue ($P < 0.10$) font with positive effects in grey and negative effects in yellow highlight. Both comparisons to the 1A sibling NILs (n=4) and all Charger NILs (n=16) is shown.

Table 7: Description of phenotypic effects of the 1A Soleil resistant haplotype into the *Charger* genetic background. The main conclusions are shown in bold.

<i>Charger</i>	Soleil-1A Resistant
HFN	Very strong positive effect of the Soleil allele on HFN across all NILs (41 s), whereas the effect is lower (10 s) in the sibling NILs.
Sprouting	The Soleil resistance allele increases late sprouting compared to both sibling and all NILs.
Yield	Not evaluated.
TGW	No effect
Height	No effect
Heading	No effect

General conclusions of 1A QTL replacement:

- Neither Avalon nor Cadenza improved with the 1A Soleil Resistant allele. In addition we did not identify a QTL in the Avalon x Cadenza DH population for 1A. This could suggest that both these lines already carry the resistant allele. This would be consistent with the negative effect of the Haven susceptible allele in the Avalon background. This would suggest that breeders should be mindful of the 1A region when using Haven derived germplasm in their crossing schemes.
- The Soleil 1A allele has positive effects compared to the Charger 1A allele. Although not that clear in sibling NILs, the effect was very significant in all NILs and also compared to the Charger variety samples.
- There is a ~4 cm increase in height conferred by the Soleil resistant haplotype in both Avalon and Cadenza. This is consistent with a non-significant positive effect of the Soleil haplotype in the 1A NILs which also increased height by ~2.2 cm (Figure 13). No height effect was seen in the Charger background.

2D QTL: We introduced the resistant (Cadenza) haplotype into Charger and Nijinsky. The exact number of NILs carrying alternative alleles are presented in Figure 25.

QTL Parents	Common Recurrent Parents	
	Nijinsky	Charger
Cadenza (R) 2D	3 Cad / 3 Nij	5 Cad / 5 Cha

Figure 25: BC₃ NILs developed for the 2D QTL. The number of NILs carrying each allele is indicated in the relevant position.

We first analysed the effects of the Cadenza 2D (R) haplotype into the Charger background and present the summary (Figure 26) and describe the effects in Table 8. As mentioned for the 1A QTL, for Charger we compared to both sibling and all Charger NILs.

	Charger (2D-3A)	Cadenza 2D-Res	Cadenza 2D effect	%	P value	vs ALL_Charger		
						Cadenza 2D effect	%	P value
2015-HFN-Early_JIC	274.3	302.7	28.4	10%	0.206	0.6	0%	0.965
2015-HFN-Late_JIC	280.8	296.1	15.3	5%	0.427	3.0	1%	0.827
2015-Y-HFN-Early_RAGT	223.7	260.6	36.9	16%	0.051	-1.4	-1%	0.929
2015-Y-HFN-Late_RAGT	194.0	149.7	-44.3	-23%	0.045	-46.1	-24%	0.013
2015-Y-HFN-Early_LM	215.1	240.6	25.5	12%	0.015	4.7	2%	0.610
2015-Y-HFN-Late_LM	206.9	224.8	17.9	9%	0.096	-3.2	-1%	0.726
2015-Y-HFN-Early_KWS	275.1	305.6	30.5	11%	0.136	-1.7	-1%	0.908
2015-Y-HFN-Late_KWS	138.4	115.1	-23.3	-17%	0.107	-34.0	-23%	0.022
2015-Early % Sprouted_JIC	9.3	7.8	-1.5	-16%	0.308	0.2	3%	0.868
2015-Late % Sprouted_JIC	38.2	34.3	-3.8	-10%	0.534	-3.8	-10%	0.372
AdjYield_Y_JIC_15	5.76	5.79	0.03	0%	0.836	-0.11	-2%	0.539
TGW(g)_Y_JIC_15	44.3	43.4	-0.9	-2%	0.259	0.1	0%	0.912
Øarea_Y_JIC_15	21.2	20.9	-0.3	-1%	0.085	-0.2	-1%	0.244
Øwidth_Y_JIC_15	3.5	3.5	0.0	1%	0.132	0.1	2%	0.015
Ølength_Y_JIC_15	6.6	6.4	-0.2	-3%	<.001	-0.2	-2%	<.001
2015-TGW(g)	49.1	50.0	0.8	2%	0.222	1.9	4%	0.004
2015-ØArea	22.4	22.6	0.3	1%	0.114	0.3	1%	0.098
2015-ØWidth	3.6	3.7	0.1	3%	<.001	0.1	3%	<.001
2015-ØLength	6.6	6.6	-0.1	-1%	0.053	-0.1	-1%	0.009
Crop Height_Y_JIC_15	76.4	71.2	-5.2	-7%	0.013	-2.8	-4%	0.074
2015-Y-Height_KWS	79.4	74.4	-5.0	-6%	0.003	-1.5	-2%	0.114
2015-EE_RAGT	25.5	27.1	1.5	6%	0.002	0.5	2%	0.234
2015-Y-EE (May/June)_KWS	3.9	2.5	-1.4	-36%	0.484	-0.3	-11%	0.785

Figure 26: Summary of phenotypic effects of the Cadenza 2D (R) introgression into Charger. Significant effects are shown in red ($P < 0.05$) and blue ($P < 0.10$) font with positive effects in grey and negative effects in yellow highlight. Both comparisons to the 2D sibling NILs ($n=5$) and all Charger NILs ($n=16$) is shown.

Table 8: Description of phenotypic effects of the 2D Cadenza resistant haplotype into the *Charger* genetic background. The main conclusions are shown in bold.

<i>Charger</i>	Cadenza-2D Resistant
HFN	Overall a positive and significant effect of ~25 s. There are two negative effects but in both cases the HFN values are extremely low.
Sprouting	No effect
Yield	No effect
TGW	There is a slight decrease in length and increase in width, but overall not significant.
Height	Significant reduction in height (5 cm)
Heading	Variable effect.

Overall, we did not see any significant agronomic effects when replacing the Nijinsky 2D interval with the Cadenza 2D resistance haplotype. The only effect was for early sprouting at JIC where the positive NILs have on average 44% less sprouting with respect to the Nijinsky NILs.

General conclusions of 2D QTL replacement:

- The Cadenza resistant allele had an overall significant positive effect when replacing the *Charger* haplotype for HFN. It also significantly reduced height most likely due to a change in the *Rht8* allele.

3A AxC QTL: We introduced the resistant (Cadenza) haplotype into Charger and Nijinsky. The exact number of NILs carrying alternative alleles are presented in Figure 27.

QTL Parents	Common Recurrent Parents	
	Nijinsky	Charger
Cadenza (R) 3A	2 Cad/ 4 Nij	7 Cad / 5 Cha

Figure 27: BC₃ NILs developed for the 3A QTL. The number of NILs carrying each allele is indicated in the relevant position.

We first analysed the effects of the Cadenza 3A (R) haplotype into the Charger background and present the summary (Figure 28) and describe the effects in Table 9. As mentioned previously, for Charger we compared to both sibling and all Charger NILs.

	Charger (2D-3A)	Cadenza 3A-Res	Cadenza 3A effect	%	P value	vs ALL_Charger		
						Cadenza 3A effect	%	P value
2015-HFN-Early_JIC	274	266	-8	-3%	0.725	-36	-12%	0.029
2015-HFN-Late_JIC	281	267	-14	-5%	0.497	-26	-9%	0.053
2015-Y-HFN-Early_RAGT	224	231	7	3%	0.748	-31	-12%	0.069
2015-Y-HFN-Late_RAGT	194	164	-30	-16%	0.018	-32	-16%	0.029
2015-Y-HFN-Early_LM	215	221	6	3%	0.899	-14	-6%	0.036
2015-Y-HFN-Late_LM	207	214	7	3%	0.637	-14	-6%	0.041
2015-Y-HFN-Early_KWS	275	279	4	1%	0.875	-29	-9%	0.069
2015-Y-HFN-Late_KWS	138	158	19	14%	0.234	9	6%	0.533
2015-Early % Sprouted_JIC	9.3	8.3	-1.0	-11%	0.544	0.7	10%	0.564
2015-Late % Sprouted_JIC	38.2	30.5	-7.6	-20%	0.230	-7.6	-20%	0.06
AdjYield_Y_JIC_15	5.76	5.81	0.1	1%	0.746	-0.1	-2%	0.529
TGW(g)_Y_JIC_15	44.3	44.2	-0.2	0%	0.822	0.8	2%	0.300
Øarea_Y_JIC_15	21.2	21.2	0.1	0%	0.709	0.1	1%	0.379
Øwidth_Y_JIC_15	3.5	3.5	0.0	0%	0.658	0.0	0%	0.662
Ølength_Y_JIC_15	6.6	6.6	0.0	0%	0.355	0.0	0%	0.399
2015-TGW(g)	49.1	49.5	0.4	1%	0.583	1.4	3%	0.014
2015-ØArea	22.4	22.7	0.3	1%	0.037	0.3	1%	0.036
2015-ØWidth	3.6	3.7	0.0	0%	0.571	0.0	0%	0.402
2015-ØLength	6.6	6.7	0.1	1%	0.019	0.1	1%	0.024
Crop Height_Y_JIC_15	76.4	78.6	2.2	3%	0.353	4.6	6%	0.01
2015-Y-Height_KWS	79.4	82.4	3.0	4%	0.693	6.5	9%	0.02
2015-EE_RAGT	25.5	25.4	-0.1	0%	0.880	-1.1	-4%	0.027
2015-Y-EE (May/June)_KWS	3.9	3.3	-0.6	-15%	0.807	0.5	19%	0.695

Figure 28: Summary of phenotypic effects of the Cadenza 3A (R) introgression into Charger. Significant effects are shown in red ($P < 0.05$) and blue ($P < 0.10$) font with positive effects in grey and negative effects in yellow highlight. Both comparisons to the 3A sibling NILs (n=5) and all Charger NILs (n=16) is shown.

Table 9: Description of phenotypic effects of the 3A Cadenza resistant haplotype into the *Charger* genetic background. The main conclusions are shown in bold.

<i>Charger</i>	Cadenza-3A Resistant
HFN	Overall there is a negative effect with the Cadenza 3A resistant haplotype leading to lower HFN values. This is particularly the case when comparing to all the Charger NILs.
Sprouting	Relatively small decrease in sprouting.
Yield	No effect.
TGW	No effect in one trial and a modest increase in grain parameters in second trial.
Height	Significant increase in height (+2.6 cm sibling NILs / +5.6 cm All NILs).
Heading	No effect.

Similarly to the 2D Cadenza replacement, we did not see any significant agronomic effects when replacing the Nijinsky 3A interval with the Cadenza 3A resistance haplotype. The only effect was for early sprouting at JIC where the positive NILs have on average 39% less sprouting with respect to the Nijinsky NILs.

General conclusions of 3A QTL replacement:

- Changing the 3A Charger haplotype for 3A leads to negative effects on HFN and should therefore be avoided. This could be due to a stronger beneficial allele in Charger compared to Cadenza or other linked genes which we replaced. The effect on height will be discussed separately.

3A SxR QTL: A series of different combinations were achieved for the 3A SxR QTL replacement. We introduced both the resistant (Savannah) and susceptible (Rialto) haplotypes into Cadenza, we introduced the resistant Savannah haplotype into Charger and we introduced the susceptible Rialto haplotype into Avalon. The exact number of NILs carrying alternative alleles are presented in Figure 29.

QTL Parents	Common Recurrent Parents			
	Avalon	Cadenza	Nijinsky	Charger
Savannah (R)	---	3 Sav / 3 Cad	---	6 Sav / 4 Cha
Rialto	3 Ria / 3 Ava	6 Ria / 6 Cad	2 Ria / 4 Nij	---

Figure 29: BC₃ NILs developed for the 3A SxR QTL. The number of NILs carrying each allele is indicated in the relevant position.

We first analysed the effects of the Rialto 3A (S) haplotype into the Avalon background and present the summary (Figure 30) and describe the effects in Table 10.

	Avalon	Rialto-Sus	Rialto-3A effect	% effect	<i>P value</i>
2014-HFN_JIC	376	380	3.2	1%	0.585
2014-HFN_KWS	382	407	24.9	7%	0.141
2014-HFN-Early_RAGT	334	328	-5.9	-2%	0.604
2014-HFN-Late_RAGT	280	302	22.2	8%	0.383
2014-HFN-Early_SW	398	403	4.5	1%	0.767
2014-HFN-Late_SW	426	425	-0.3	0%	0.986
2015-HFN-Early_JIC	422	359	-62.7	-15%	0.297
2015-HFN-Late_JIC	351	356	5.3	2%	0.682
Early % Sprouted	17.2	11.6	-5.6	-33%	0.181
Late % Sprouted	28.8	22.8	-6.0	-21%	0.477
AdjYield_Y_JIC_15	5.63	5.88	0.2	4%	0.105
TGW(g)_Y_JIC_15	50.46	51.40	0.9	2%	0.217
Øarea_Y_JIC_15	23.01	23.20	0.2	1%	0.373
Øwidth_Y_JIC_15	3.57	3.59	0.0	0%	0.581
Ølength_Y_JIC_15	7.00	7.02	0.0	0%	0.529
2014-Height_RAGT	86.0	91.3	5.3	6%	0.033
2014-Height_SW	67.2	72.8	5.6	8%	<.001
Crop Height_Y_JIC_15	88.8	97.1	8.4	9%	<.001
2014-EE_RAGT	26.3	26.0	-0.3	-1%	0.374
2014-Heading_SW	1.8	1.0	-0.8	-44%	<.001

Figure 30: Summary of phenotypic effects of the Rialto 3A (S) introgression into *Avalon*. Significant effects are shown in red ($P < 0.05$) and blue ($P < 0.10$) font.

Table 10: Description of phenotypic effects of the 3A Rialto susceptible haplotype into the *Avalon* genetic background. The main conclusions are shown in bold.

<i>Avalon</i>	Rialto-3A Susceptible
HFN	No effect.
Sprouting	No effect.
Yield	Non-significant 4% increase.
TGW	Tendency to increase, but non-significant.
Height	Significant increase in height (6.4 cm).
Heading	Half day earlier heading.

We then analysed the effects of the Rialto (S) and Savannah (R) haplotypes into the Cadenza background. We summarize (Figure 31) and describe the effects in Table 11. Note that two comparisons were made for Cadenza. We compared first against the 3A sibling NILs (n=3/6) and then compared to all Cadenza NILs (n=23) given that there was some variation in phenotype between the isogenic lines. While this changes slightly the conclusions, it does so in magnitude rather than in the direction of the effect.

	Cadenza	vs ALL Cadenza							Cadenza	vs ALL Cadenza						
		Rialto-3A-Sus	Rialto-3A-Sus effe	%	P value	Rialto-3A-Sus effe	%	P value		Sav-3A-Res	Sav-3A-Effect	%	P value	Sav-3A-Effect	%	P value
2014-HFN_JIC	398	390	-8	-2%	0.236	-0.6	0%	0.966	395	409	14	4%	0.116	17.8	5%	0.013
2014-HFN_KWS	347	373	25	7%	0.147	4.2	1%	0.724	412	377	-35	-9%	0.006	8.3	2%	0.525
2014-HFN-Early_RAGT	306	271	-35	-11%	0.416	-8.5	-3%	0.744	287	281	-6	-2%	0.853	1.0	0%	0.972
2014-HFN-Late_RAGT	310	277	-33	-11%	0.340	-26.1	-9%	0.227	337	324	-13	-4%	0.484	21.3	7%	0.382
2014-HFN-Early_SW	374	353	-20	-5%	0.390	-21.5	-6%	0.135	373	373	0	0%	0.994	-1.8	0%	0.911
2014-HFN-Late_SW	345	292	-53	-15%	0.508	-52.6	-15%	0.180	344	346	2	0%	0.952	1.4	0%	0.957
2014-Y-HFN_LM	338	324	-14	-4%	0.089	-14.6	-4%	0.043	350	324	-26	-7%	0.037	-14.4	-4%	0.100
2015-HFN-Early_JIC	324	327	4	1%	0.861	-8.8	-3%	0.596	310	353	42	14%	0.190	16.6	5%	0.427
2015-HFN-Late_JIC	283	292	9	3%	0.653	-2.4	-1%	0.871	301	335	34	11%	0.102	40.3	14%	0.026
2015-Early % Sprouted_JIC	4.0	8.3	4.3	106%	0.060	4.5	120%	<0.001	4.4	4.4	0.0	1%	0.982	0.6	16%	0.570
2015-Early % Sprouted_JIC_Arc	10.8	15.4	4.6	42%	0.058	5.0	48%	0.001	10.3	11.0	0.6	6%	0.833	0.6	6%	0.713
2015-Late % Sprouted_JIC	17.8	31.8	14.0	79%	0.007	12.3	63%	<0.001	15.4	13.0	-2.4	-16%	0.599	-6.5	-33%	0.074
2015-Late % Sprouted_JIC_Arc	24.5	33.5	9.0	37%	0.014	7.9	31%	0.001	21.8	20.6	-1.2	-6%	0.720	-5.0	-20%	0.068
2014-Y-Yield (t/ha,15%M)_KWS	12.1	11.4	-0.7	-6%	0.008	-0.7	-6%	<0.001	12.4	11.4	-1.0	-8%	<0.001	-0.6	-5%	0.001
2014-Yield (t/ha)_RAGT	7.9	7.3	-0.6	-7%	0.022	-0.4	-5%	0.040	7.7	7.4	-0.3	-3%	0.159	-0.3	-4%	0.257
2014-Y-Yield (t/ha)_SW	9.3	8.9	-0.4	-5%	0.006	-0.6	-7%	<0.001	10.0	9.8	-0.2	-2%	0.518	0.3	3%	0.187
2014-Y-Yield (kg)_LM	7.3	7.2	-0.1	-2%	0.220	-0.2	-2%	0.046	7.4	7.2	-0.2	-3%	0.060	-0.1	-2%	0.209
AdjYield_Y_JIC_15	10.2	9.7	-0.5	-5%	0.007	-0.7	-7%	<0.001	10.9	10.7	-0.2	-2%	0.528	0.3	3%	0.162
2014-Y-TGW(g)_LM	55.9	57.1	1.2	2%	0.142	1.0	2%	0.103	58.1	56.2	-2.0	-3%	0.011	0.1	0%	0.930
2014-Y-Øarea_LM	19.6	19.9	0.3	1%	0.297	0.1	0%	0.758	20.2	19.8	-0.4	-2%	0.029	-0.1	0%	0.736
2014-Y-Øwidth_LM	3.7	3.7	0.0	0%	1.000	0.0	0%	0.611	3.7	3.7	0.0	0%	1.000	0.0	1%	0.542
2014-Y-Ølength_LM	6.6	6.6	0.1	1%	0.262	0.0	0%	0.929	6.7	6.6	-0.1	-2%	0.009	0.0	-1%	0.385
2014-Y-Weight (g)_LM	25.3	25.3	0.0	0%	0.934	0.2	1%	0.076	25.3	25.2	-0.1	0%	0.419	0.0	0%	0.755
2014-Y-SpW_LM	82.3	82.2	0.0	0%	0.934	0.6	1%	0.076	82.1	81.8	-0.3	0%	0.419	0.1	0%	0.755
TGW(g)_Y_JIC_15	50.5	53.3	2.8	6%	0.011	3.7	7%	<0.001	50.0	50.1	0.1	0%	0.919	0.5	1%	0.560
Øarea_Y_JIC_15	22.6	23.4	0.8	3%	0.030	0.8	3%	<0.001	22.8	22.8	0.0	0%	0.963	0.2	1%	0.350
Øwidth_Y_JIC_15	3.6	3.7	0.1	2%	0.003	0.1	3%	<0.001	3.6	3.6	0.1	2%	0.050	0.0	1%	0.160
Ølength_Y_JIC_15	6.8	6.9	0.1	2%	0.205	0.0	1%	0.356	6.9	6.9	-0.1	-1%	0.154	0.0	0%	0.776
2014-Height_RAGT	100.6	96.8	-3.8	-4%	0.386	-2.9	-3%	0.385	104.7	91.0	-13.7	-13%	0.022	-8.7	-9%	0.057
2014-Height_SW	76.7	78.0	1.3	2%	0.476	1.3	2%	0.427	82.2	73.9	-8.3	-10%	<0.001	-2.8	-4%	0.206
Crop Height_Y_JIC_15	91.2	89.3	-1.8	-2%	0.274	-1.0	-1%	0.470	95.6	85.8	-9.8	-10%	0.011	-4.5	-5%	0.035
2014-Heading_RAGT	22.6	19.8	-2.8	-12%	0.254	-2.1	-10%	0.119	21.3	22.7	1.3	6%	0.519	0.8	3%	0.662
2014-Heading (0=early, 3=late)_SW	1.1	0.5	-0.6	-53%	0.005	-0.9	-63%	<0.001	1.4	1.8	0.3	23%	0.082	0.3	23%	0.064

Figure 31: Summary of phenotypic effects of the Rialto (S) and Savannah (R) introgression into Cadenza. Significant effects are shown in red ($P < 0.05$) and blue ($P < 0.10$) font with positive effects in grey and negative effects in yellow highlight.

Table 11: Description of phenotypic effects of the 3A QTL haplotypes into the *Cadenza* genetic background. The main conclusions are shown in bold.

<i>Cadenza</i>	Rialto-3A Susceptible	Savannah-3A Resistant
HFN	Overall a 15s decrease in HFN, but not significant.	Overall no effect, but unexpected significant decrease in HFN in two trials.
Sprouting	Significantly increased sprouting.	No effect.
Yield	Significant 5% reduction in yield.	Significant 4% reduction in yield.
TGW	Non-consistent effect.	Non-consistent effect.
Height	Slight decrease in height, but non-significant.	Significant decrease in height of 10.6 cm associated with the resistant haplotype.
Heading	Earlier heading.	Slight delay in heading.

We evaluated the replacement of the 3A Rialto susceptible allele into Nijinsky. Overall we did not see significant agronomic effects from this replacement. The susceptible allele did decrease HFN by 50 s at JIC but there were no additional locations to validate this.

We then analysed the effect of introducing the 3A resistant Savannah haplotype into Charger (Figure 32; Table 12). As mentioned previously, for Charger we compared to both sibling and all Charger NILs.

	Charger 3A	Savannah 3A-Res	Savannah 3A effect	%	P value	vs ALL_Charger		
						Savannah 3A effect	%	P value
2015-HFN-Early_JIC	286	285	-1	0%	0.942	-17	-6%	0.272
2015-HFN-Late_JIC	279	305	26	9%	0.027	12	4%	0.320
2015-Y-HFN-Early_RAGT	250	244	-6	-2%	0.604	-18	-7%	0.233
2015-Y-HFN-Late_RAGT	210	205	-5	-3%	0.757	9	4%	0.577
2015-Y-HFN-Early_LM	216	215	-1	-1%	0.857	-21	-9%	0.017
2015-Y-HFN-Late_LM	212	220	8	4%	0.135	-8	-4%	0.288
2015-Y-HFN-Early_KWS	285	278	-7	-2%	0.626	-29	-9%	0.042
2015-Y-HFN-Late_KWS	162	150	-12	-7%	0.550	1	0%	0.954
2015-Early % Sprouted_JIC	6.4	5.7	-0.7	-11%	0.683	-1.9	-25%	0.157
2015-Late % Sprouted_JIC	37.2	30.0	-7.3	-20%	0.210	-8.2	-21%	0.063
AdjYield_Y_JIC_15	5.93	5.83	-0.1	-2%	0.569	-0.1	-1%	0.636
TGW(g)_Y_JIC_15	42.5	42.5	-0.1	0%	0.949	-0.9	-2%	0.280
∅area_Y_JIC_15	21.0	21.1	0.1	1%	0.660	0.0	0%	0.824
∅width_Y_JIC_15	3.4	3.4	0.0	0%	0.600	0.0	0%	0.593
∅length_Y_JIC_15	6.6	6.6	0.0	0%	0.647	0.0	0%	0.382
2015-TGW(g)	48.0	47.1	-0.8	-2%	0.465	-0.9	-2%	0.180
2015-∅Area	22.6	22.4	-0.2	-1%	0.439	0.0	0%	0.996
2015-∅Width	3.6	3.6	0.0	-1%	0.533	0.0	0%	0.364
2015-∅Length	6.7	6.7	0.0	-1%	0.343	0.0	0%	0.569
Crop Height_Y_JIC_15	70.8	66.1	-4.7	-7%	<.001	-7.9	-11%	<.001
2015-Y-Height_KWS	72.8	70.1	-2.7	-4%	0.018	-5.8	-8%	<.001
2015-EE_RAGT	27.6	27.8	0.3	1%	0.648	1.3	5%	0.003
2015-Y-EE (May/June)_KWS	2.3	2.7	0.4	17%	0.140	0.0	-2%	0.962

Figure 32: Summary of phenotypic effects of the Savannah (R) introgression into *Charger*. Significant effects are shown in red ($P < 0.05$) and blue ($P < 0.10$) font with positive effects in grey and negative effects in yellow highlight.

Table 12: Description of phenotypic effects of the 3A resistant QTL into the *Charger* genetic background. The main conclusions are shown in bold.

<i>Charger</i>	Savannah-3A Resistant
HFN	Overall no effect.
Sprouting	No effect.
Yield	No effect.
TGW	No effect.
Height	Significant reduction in height (4-7 cm).
Heading	No effect.

General conclusions of 3A SxR QTL replacement:

- We did not observe major differences when introducing either Savannah resistant or Rialto susceptible haplotypes on HFN or sprouting, apart from a significant increase in sprouting and non-significant decrease in HFN when replacing Rialto into Cadenza. This would suggest that we substituted the 3A Cadenza resistance with the 3A susceptible Rialto allele.
- Charger seems to carry a resistance allele on 3A since neither the Savannah 3A nor the Cadenza 3A (Table 9) resistance alleles improved HFN or sprouting scores.
- The resistant Savannah haplotype is associated with a significant reduction in height. This is seen in both the Charger and Cadenza background.

3A height effect: We found a series of effects when replacing the 3A QTL region across different genetic backgrounds. The increases in height are not necessarily associated with improved HFN scores as the Savannah resistance allele is associated with a significant reduction in height in different genetic backgrounds. We used the different results to generate a relative scale of the effect of the 3A QTL region with respect to the Avalon allele (Figure 33). We found that the Cadenza resistance was associated with the largest increase in height with an average effect of 5.5 cm. On the opposite spectrum, the resistance haplotype in Savannah was associated with a 3 cm reduced height with respect to Avalon. This suggests that the height effect is located within the QTL interval, but is not functionally associated with the resistance mechanism. Intermediate height effects were identified for Charger and Rialto.

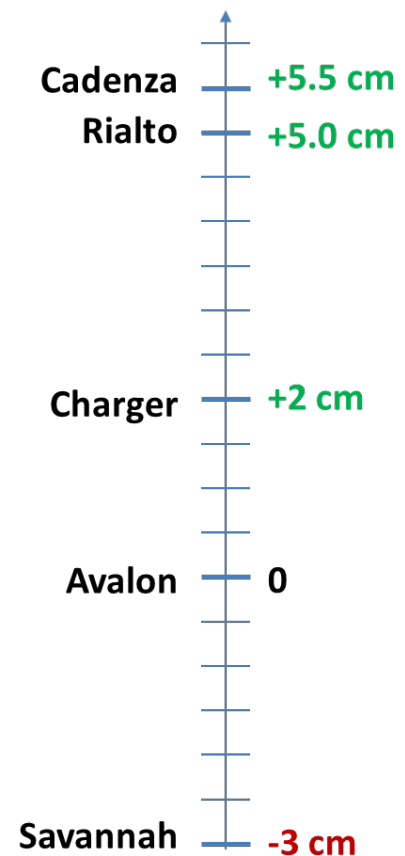


Figure 33: Relative effect of the different 3A haplotypes on plant height with respect to Avalon.

7B AxC QTL: We introduced the resistant (Avalon) 7B haplotype into Charger and extracted 7 Avalon NILS and 3 Charger sibling NILs and evaluated the effects (Figure 34; Table 13).

	Charger	Avalon 7B-Res	Avalon 7B effect	%	P value	vs ALL_Charger		
						Avalon 7B effect	%	P value
2015-HFN-Early_JIC	332	333	1	0%	0.954	31	10%	0.043
2015-HFN-Late_JIC	300	347	47	16%	0.003	54	18%	<.001
2015-Y-HFN-Early_RAGT	275	340	65	23%	<.001	78	30%	<.001
2015-Y-HFN-Late_RAGT	146	189	43	29%	0.129	-6	-3%	0.673
2015-Y-HFN-Early_LM	250	296	46	18%	<.001	60	26%	<.001
2015-Y-HFN-Late_LM	235	276	41	17%	<.001	48	21%	<.001
2015-Y-HFN-Early_KWS	331	352	21	6%	0.076	44	14%	0.003
2015-Y-HFN-Late_KWS	142	146	3	2%	0.900	-4	-2%	0.831
2015-Early % Sprouted_JIC	8.7	9.4	0.7	8%	0.725	1.8	24%	0.162
2015-Late % Sprouted_JIC	41.3	30.4	-10.9	-26%	0.033	-7.7	-20%	0.06
AdjYield_Y_JIC_15	6.18	6.01	-0.2	-3%	0.440	0.1	2%	0.516
TGW(g)_Y_JIC_15	42.5	44.3	1.8	4%	0.013	0.9	2%	0.163
Øarea_Y_JIC_15	21.0	21.3	0.3	1%	0.133	0.2	1%	0.221
Øwidth_Y_JIC_15	3.4	3.5	0.0	1%	0.099	0.0	1%	0.095
Ølength_Y_JIC_15	6.6	6.6	0.0	0%	0.666	0.0	0%	0.907
2015-TGW(g)	47.3	48.8	1.5	3%	0.090	0.7	1%	0.252
2015-ØArea	22.3	22.6	0.3	1%	0.242	0.2	1%	0.105
2015-ØWidth	3.7	3.7	0.0	1%	0.338	0.0	1%	0.019
2015-ØLength	6.6	6.6	0.0	0%	0.489	0.0	0%	0.916
Crop Height_Y_JIC_15	74.3	74.9	0.6	1%	0.565	0.9	1%	0.457
2015-Y-Height_KWS	76.8	75.3	-1.4	-2%	0.129	-0.6	-1%	0.205
2015-EE_RAGT	26.2	26.5	0.3	1%	0.552	0.0	0%	0.994
2015-Y-EE (May/June)_KWS	2.3	2.4	0.1	2%	0.833	-0.4	-14%	0.708
2015-Habit_RAGT	6.1	6.0	-0.1	-1%	0.335	0.0	0%	0.766

Figure 34: Summary of phenotypic effects of the Avalon (R) introgression into *Charger*. Significant effects are shown in red ($P < 0.05$) and blue ($P < 0.10$) font.

Table 13: Description of phenotypic effects of the 7B resistant QTL into the *Charger* genetic background. The main conclusions are shown in bold.

<i>Charger</i>	Avalon-7B Resistant
HFN	We identified a significant increase in HFN when replacing Charger with the Avalon 7B effect (30-38 s). This was significant and consistent across all locations.
Sprouting	We found a significant reduction in sprouting, which was not expected given that the major effect of the 7B QTL is PMA.
Yield	No effect.
TGW	Consistent increase in TGW.
Height	No effect.
Heading	No effect.

General conclusions of 7B AxC QTL replacement:

- The Avalon 7B allele has a major effect on HFN in Cadenza and in the Charger genetic background. This confirms 7B as a major target for further characterisation.

Objective 3: Physiological characterization to understand the mechanism of gene action

Objective 3.1. Establish benchmark for after-ripening germination kinetics for each QTL

Susceptibility to PHS is negatively correlated with the depth of dormancy in grains (Gerjets et al., 2010, Gubler et al., 2005) with grains showing high dormancy being less susceptible to PHS. Given this relationship, the dynamics of dormancy loss was examined in F₃ and BC₃ lines carrying alternate alleles of the 1A, 2D, 3A AxC, 3A SxR, 4A and 7B QTL. These lines are hereafter referred to as susceptible or resistant F₃ lines or NILs. This was done at different developmental stages including Physiological Maturity (PM, 40 % grain moisture content or peduncle senescence), Harvest Maturity (HM, ~20 % moisture content) and Post-harvest Maturity (PH, ~14 days after HM). By examining the germination potential of seeds at these different stages, it was possible to study the nature of the QTL effects, as well as the timing of the QTL effects (i.e. when does the expression of the QTL effect begin).

The rate of dormancy loss in these lines was assessed using the germination index test (GI) as described by Walker-Simmons (1987). The GI test is a weighted score which gives decreasing weights to the number of seeds that germinate in each consecutive day of a 7-day incubation period. The GI test is preferred to the germination percentage test because it not only estimates the proportion of seeds that germinate, but also the rate at which they germinate.

F₃ lines: As shown below in Figure 35, the rate of germination increased rapidly from physiological maturity through to post-harvest maturity in all the lines (parents, F₃ lines with resistant or susceptible alleles) and for all the QTL tested. However, differences were observed in the expression of the QTL effects across the various stages tested. These differences are described below for each QTL.

The 1A QTL did not show any effect on the rate of seed germination at PM, but at HM there was a significant GI difference ($P < 0.05$) between the susceptible F₃ line and the resistant F₃ line, with the susceptible line showing the greater GI (Figure 35a). Although both F₃ lines showed increased germination potential at PH, the GI difference between these lines was further increased at PH ($P < 0.01$).

The 2D QTL, in contrast to the 1A QTL, showed an earlier effect, with significant GI differences between F₃ lines seen as early as PM (Figure 35b). The GI of the susceptible F₃ line was almost twice ($P < 0.01$) the GI displayed by the resistant F₃ line at PM. Although this GI difference was reduced, it was still significant at HM. At PH, there were no significant differences between the F₃ lines

The 3A SxR QTL did not show any effect at PM and HM. However, at PH, a marked GI difference ($P = 0.001$) was observed between the F₃ lines with the susceptible F₃ line having a GI of 0.836 while the resistant F₃ line showed a lower GI of 0.448 (Figure 35c). This difference in GI was mainly caused by a sharp increase in the germination potential of the susceptible F₃ line from HM to PM.

For the 7B QTL, no effect on the rate of germination was observed at any of the stages tested, in contrast to all of the QTL described above (Figure 35d). The susceptible and the resistant F₃ lines showed similar GI profiles.

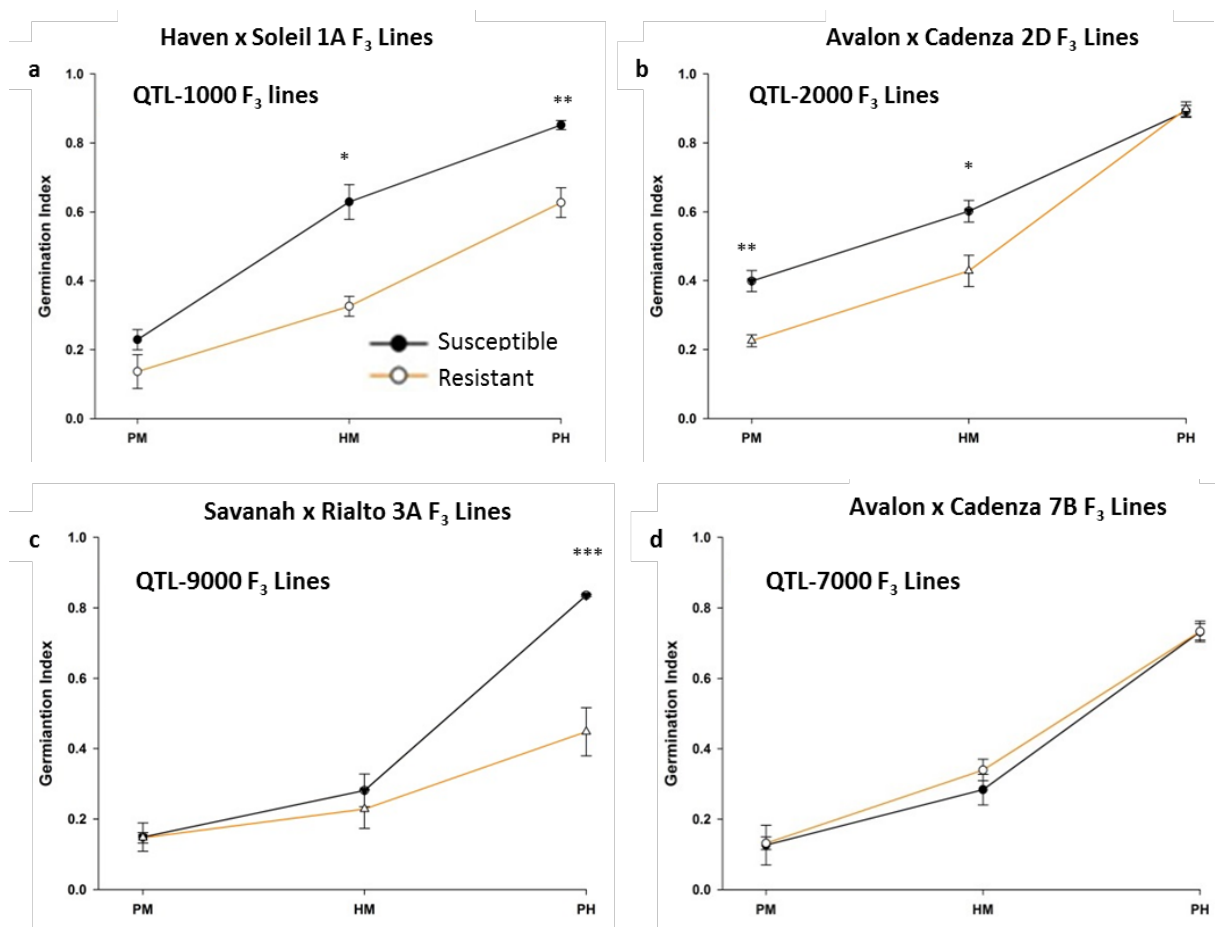


Figure 35: The germination index of seeds harvested from F₃ lines for the 1A (a), 2D (b), 3A SxR (c) and 7B (d) QTL. Seeds were tested at Physiological Maturity (PM), Harvest Maturity (HM) and Post-Harvest Maturity (PH) and germinated at 17°C. Error bars represent SEM of 3 biological replications for each time point. Significant differences at $P < 0.05$ (*), < 0.01 (**), < 0.001 (***) are indicated.

BC₃ NILs: Three independent resistant and susceptible BC₃ NILs for the 1A, 2D, 3A AxC, 3A SxR and 7B QTL were tested for the effects of the QTL on the rate of germination. For the

4A QTL, one resistant and one susceptible BC₃ NIL was used. The dormancy status of these seeds was assessed through the germination index test at four different time points including PM, HM, Post-harvest Maturity (PH, 14 days after HM) and another PH time point at 28 DPH. The results obtained for each QTL are described below.

1A QTL: GI difference was observed between some susceptible and resistant BC₃ NILs for the 1A QTL at the first PH stage of grain maturation (Figure 36a), just as was observed with the F₃ lines (Figure 35a). However, this difference was masked by the non-homogeneity in the phenotypes of sister BC₃ NILs harbouring similar alleles. That is, one of the three NILs with the susceptibility allele behaved like the resistant NILs. Similarly, one of the three NILs with the resistant allele showed similar phenotype as the susceptible NILs.

2D QTL: Unlike the F₃ lines, the resistant and susceptible BC₃ 2D NILs did not show any difference at the physiological or harvest maturity stages (Figure 36b). The only difference observed was at the PH time point, where the susceptible NILs generally showed lower GI to the resistant NILs. Also, just as was observed for the 1A QTL, this GI difference between NILs was masked by the non-homogeneity in the phenotype of sister NILs. This was because one of the three susceptible 2D NILs showed similar phenotype to the resistant NILs.

3A AxC and 3A SxR QTL: The 3A AxC BC₃ NILs did not show any observable GI difference (Figure 36c), while the alleles groups of the 3A SxR QTL only showed a minor but significant difference at PM (Figure 36d). Also, both the susceptible and resistant 3A SxR BC₃ NILs showed high depth of dormancy that persisted to the later post-harvest time points. This is in contrast to what was earlier observed in the F₃ lines.

4A QTL: The 4A QTL showed a significant effect between the susceptible and resistant BC₃ NILs tested (Figure 36e). The effect was distinct at PH after a 14 days after-ripening. At the peak of this effect (first PH time point), the susceptible NIL and parent showed approximately three times the GI of the resistant NIL. At 28 DPH, there was an observable difference between the NIL, however, this difference was not significant ($P = 0.06$).

7B QTL: Like was observed in the F₃ lines, there was no observable GI difference between NILs of the 7B QTL except at the last post-harvest time point (Figure 36f). However, this QTL showed a major effect in the HFN tests suggesting that its effect is not on germination but on PMA induction.

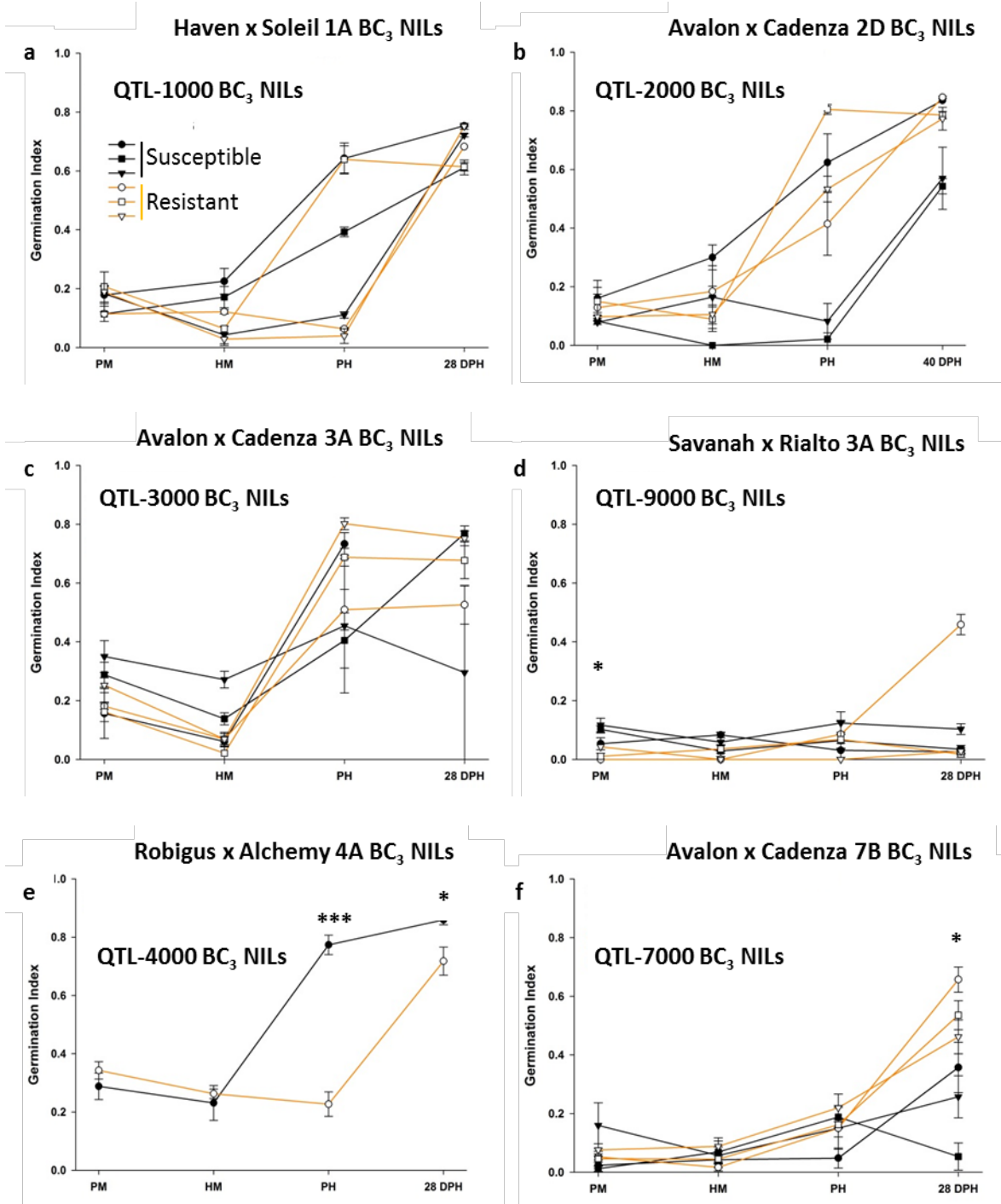


Figure 36: The germination index of seeds harvested from BC₃ NILs with susceptible (black lines) and resistant (orange lines) parental alleles for the 1A (a), 2D (b), 3A AxC (c), 3A SxR (d), 4A (e), and 7B (f) QTL. Seeds were tested at Physiological Maturity (PM), Harvest Maturity (HM) and two Post-Harvest time points (PH) and germinated at 16°C. Error bars represent SEM of 3 biological replications for each time point. Significant differences based on comparison between allele mean at $P < 0.05$ (*), and < 0.001 (***) are indicated.

For the 1A and 2D QTL, NILs which were expected to have similar phenotypes based on the marker-assisted selection showed heterogeneous behaviour (Figure 36a, b). A reason for this phenotypic heterogeneity in the sister NILs could be that they are not as isogenic as expected. The contrasting phenotype of the sister NILs could therefore be caused by residual segregating loci in the background.

Given that two out of the three NILs used in this experiment had been genotyped with the iSelect SNP array we tested this hypothesis. An analysis of residual polymorphisms present between sister NILs (NILs with the same QTL allele) was carried out. For the 1A QTL, the hypothesised resistant line with the unexpected susceptible GI phenotype was compared with its sister line (which shows the expected resistance). For the 2D QTL, the BC₃ NIL which showed the unexpected susceptible phenotype was compared with a sister NIL with the expected resistance phenotype.

For the 1A sister NILs, a large proportion of the polymorphism between the sister NILs also maps to the 1A chromosome (Figure 37a). By comparing the genetic position of these SNPs as published by Wang et al. (2014), it was discovered that the genetic interval of the mapped SNPs between these NILs partly overlaps with the genetic interval of the mapped SNPs found between the allele (resistant and susceptible) groups. This implies that there are residual polymorphisms within or close to the 1A QTL interval between these sister NILs and this might be the reason for the heterogeneous phenotype. In addition there are many additional segregating SNPs across multiple alternative chromosomes which could alter or condition the effect of the 1A QTL. Although the 2DS chromosome arm of the 2D sister NILs appeared isogenic, more than 20% of the polymorphic SNPs between these NILs map to the 5BL chromosome arm (Figure 37b). This is the same chromosome arm harbouring the majority of the polymorphic SNP between the resistant and susceptible 2D allele groups (Figure 11).

These findings (residual polymorphisms) provide an explanation for the heterogeneous behaviour of some of the sister NILs. However, a more detailed characterisation of these lines will be required to confirm this possibility.

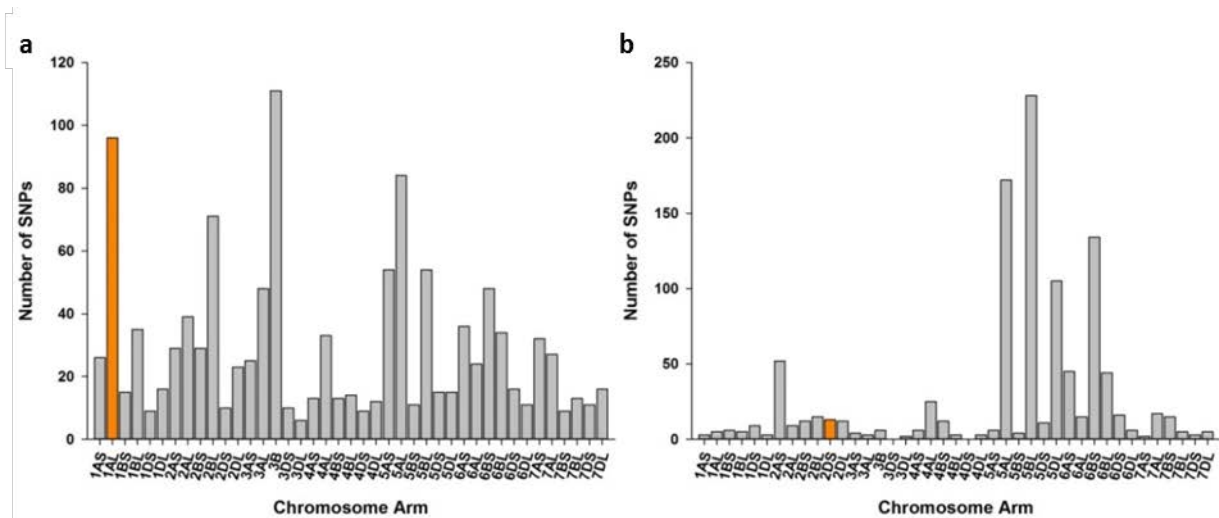


Figure 37: The distribution of residual polymorphisms between heterogeneous sister NILs for the 1A (a) and 2D (b) QTL. The chromosome arm where the QTL is located is represented by the orange bars while other chromosomes are represented in grey.

Objective 3.2. Characterize after-ripening sprouting kinetics for each QTL

Previous studies have shown that there is an inverse relationship between germination temperature and the germination index of grains of different wheat varieties (Reddy et al., 1985, Nyachiro et al., 2002), with increases in germination temperature resulting in decreases in germination index. Also, dormancy is broken in most wheat varieties when germinated at low temperature. However for most of the PHS QTL reported to date, the effect of germination temperature on the expression of these QTL effects has not been studied. Therefore, in addition to germinating the F₃ grains at 17°C described previously, we also germinated seeds at 10°C and 22°C to assess the effect of germination/incubation temperature on the expression of the QTL effects.

The result of this experiment (Figure 38) confirmed a consistent inverse relationship between germination temperature and germination potential of seeds. At almost all stages of grain development tested, GI decreased as the germination temperature was increased from 10°C to 22°C. These results correlate well with the previous reports on the effect of incubation temperature on germination (Nyachiro et al, 2002). The only exception was at PH for the 1A and 3A SxR QTL where the GI of the susceptible parent and F₃ lines were greater at 22°C than at 10°C.

Furthermore, at 10°C the susceptible and resistant F₃ lines of all the QTL showed no significant GI difference. The only exception to this was the small but significant GI difference

between the 7B F₃ lines, and this was only observed at harvest maturity. The absence of the QTL effects at 10°C is probably due to the breaking of dormancy in all the lines.

In addition, at 22°C, the QTL effects were expressed in a very similar pattern to what was observed at 17°C. The 3A SxR QTL parents, Savannah and Rialto, showed GI difference in the opposite direction to the difference observed between the F₃ lines at 22°C. This was consistent with the results at 17°C (data not shown) and further confirms the phenotype discrepancy between parental and F₃ lines for this QTL. In addition, when the GI of lines were compared at 17°C and 22°C, the effects of late expressing QTL (1A and 3A SxR) were found to be greater at 22°C than at 17°C. This was mainly due to increases in the dormancy of the resistant lines for the QTL. Taken together, our results show an influence of temperature on the expression of our target QTL effects.

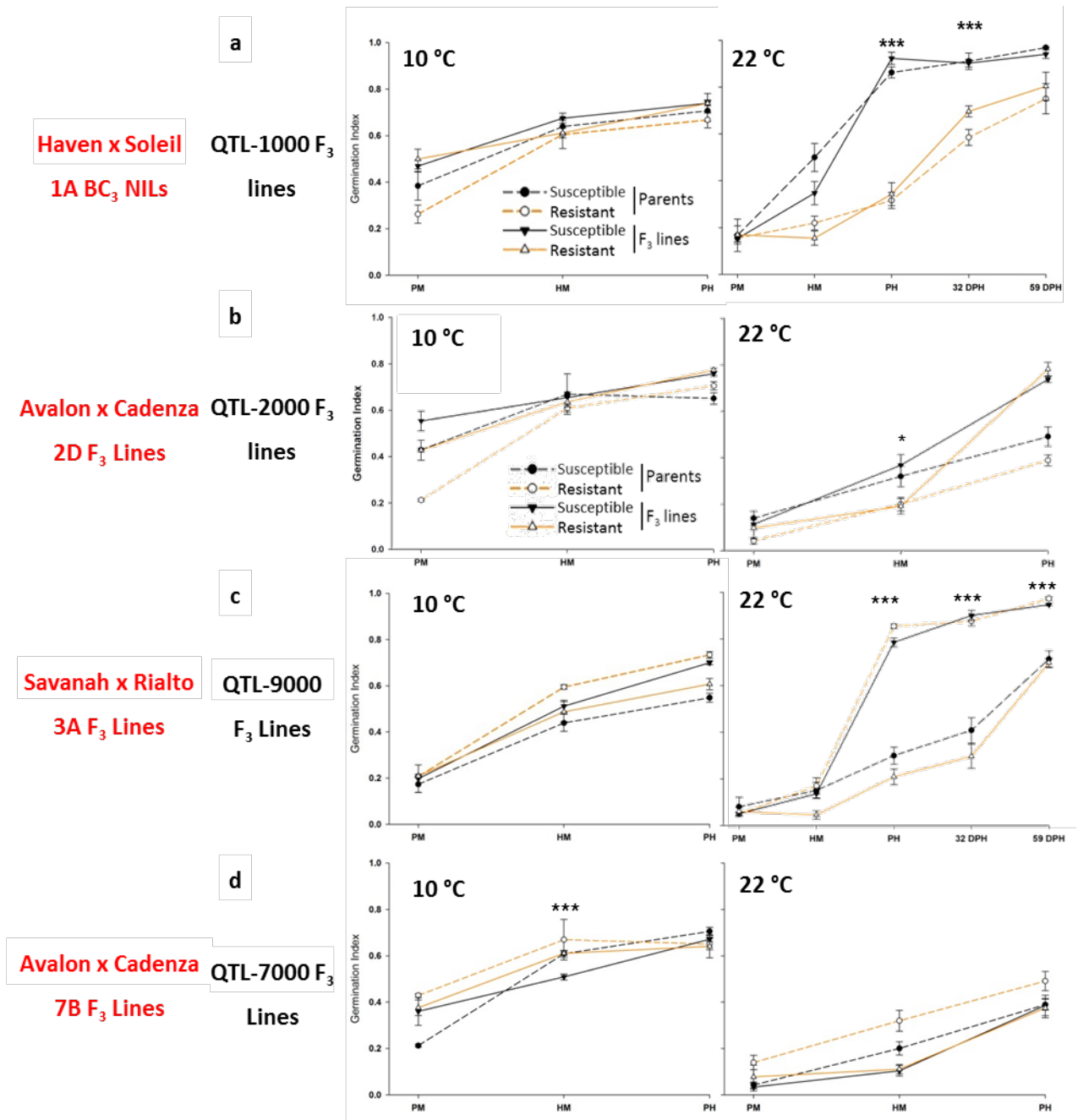


Figure 38: The effect of germination temperature on the expression of QTL effect. Seeds from parents (dashed lines) and F₃ seeds (solid lines) carrying the susceptible (black) or resistant (orange) QTL 1A (a), 2D (b), 3A SxR (c) and 7B (d) QTL alleles were harvested at Physiological Maturity (PM), Harvest Maturity (HM) and Post-Harvest Maturity (PH) and germinated at 10°C and 22°C. For the 1A and 3A SxR lines, two more post-harvest experiments were done at 32 Days post-harvest (DPH) and 59 DPH. Error bars represent SEM of 3 biological replications for each time point. Significant differences between F₃ lines at $P < 0.05$ (*), and < 0.001 (***) are indicated.

To further investigate the late QTL effect expressed by the 1A and 3A SxR QTL, more post-harvest GI test were done at 32 days post-harvest (DPH) and 59 DPH. These were germinated at 22°C since the highest GI difference was observed at this temperature. This showed that the significant GI difference observed for these QTL persisted until 32 DPH for the 1A QTL and 59 DPH for the 3A SxR QTL, even though the resistant lines showed a rapid increase in germination potential at these late time points (Figure 38a,c).

Temperature effect during grain development: Some studies have shown that temperature during grain developmental plays a role in setting the depth of dormancy displayed by wheat seeds during maturation (Buraas and Skinnes, 1985, Reddy et al., 1985). In a similar manner, the temperature at the onset of grain development can also influence the expression of PHS resistance QTL at the later stages of grain maturation and after-ripening. In a recent study, where a PHS susceptible line and a PHS resistant line were grown at 13°C and 25°C, difference in germination percentage was found between the lines only when grown at 13°C and not at 25°C (Nakamura et al., 2011). These results point to an effect of grain developmental temperature in the control of PHS QTL.

To investigate the effect of temperature during grain development on the level of dormancy and possibly the expression of the QTL effect, the BC₃ NILs used in the previous physiological characterisation experiment were also grown at 13°C from anthesis onwards. The rate of germination in these lines was assessed using the germination index test. Using thermal time calculations, samples were harvested at similar stages as the samples used in the previous physiological experiment (Figure 38).

Plants of NILs grown at 13°C from anthesis were expectedly delayed in their overall development and maturation due to the lower growth temperature compared to NILs grown at 20°C. Also, NILs grown at 13°C displayed a higher depth of dormancy when compared with NILs grown at 20°C at a similar thermal duration post anthesis (Figure 39). This increase in dormancy, however, varied between QTL. For instance, while NILs for the 1A and 4A QTL showed a moderate increase in dormancy depth when grown at 13°C from anthesis, dormancy in NILs for the 2D, 3A AxC and 3A SxR was markedly increased when grown at 13°C.

Due to this increase in dormancy, most of the QTL did not show any effect on germination rate. The only exception was the 4A QTL which caused GI difference between the NILs at PH ($P=0.02$) with the susceptible NIL having a higher germination rate than the resistant NIL. This GI difference was still observed at 35 DPH ($P=0.02$) suggesting that this QTL effect is

expressed during the after-ripening period. This 4A QTL effect was similar to that observed in plants grown at 20°C (Figure 39e).

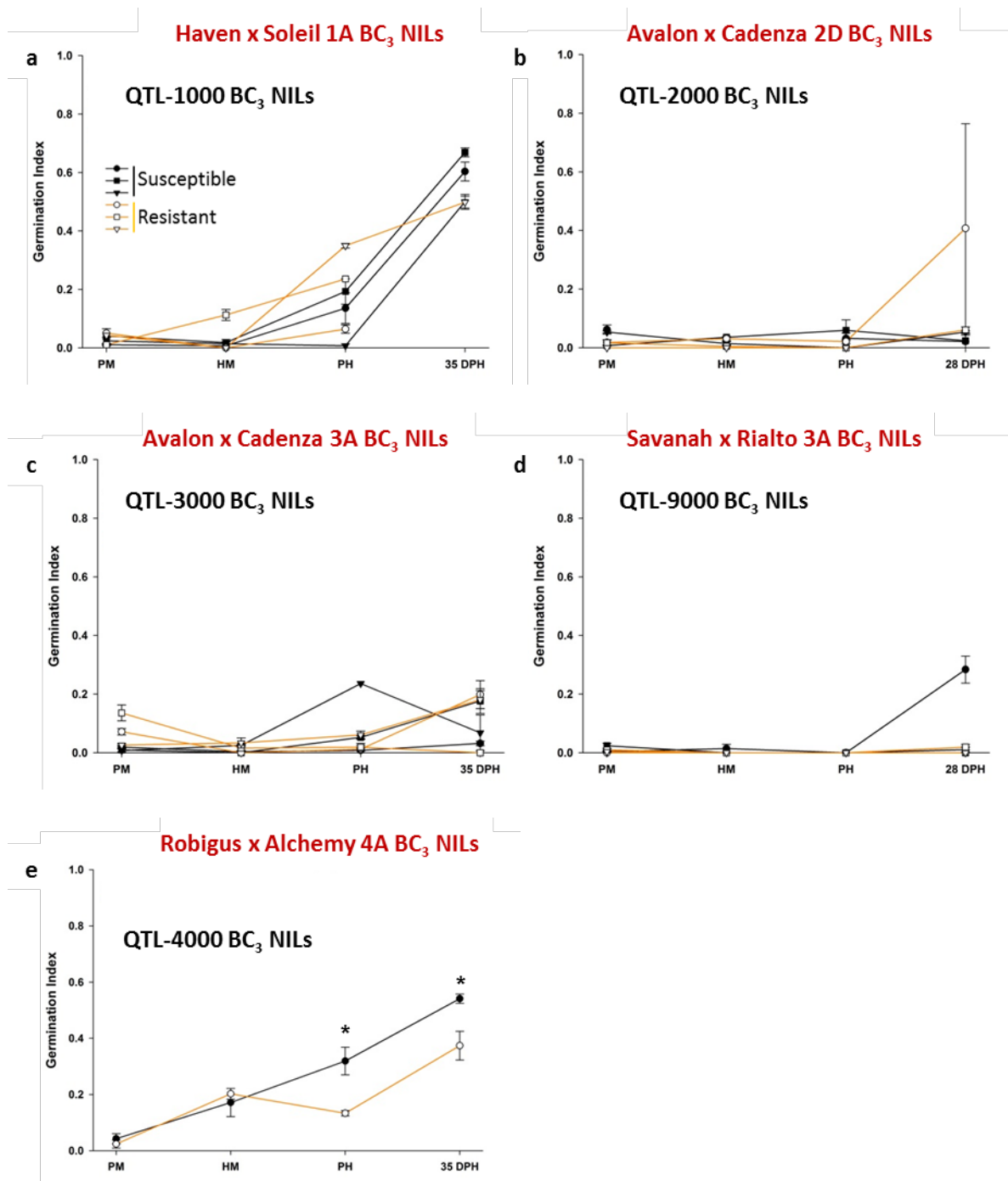


Figure 39: Low grain developmental temperature increases the depth of dormancy in wheat NILs. The GI of seeds harvested from NILs with susceptible (black lines) and resistant (orange lines) parent alleles for the 1A (a), 2D (b), 3A AxR (c), 3A SxR (d) and 4A (e) QTL grown at 13°C from anthesis. Seeds were tested at Physiological Maturity (PM), Harvest Maturity (HM) and two Post-Harvest time points (PH) and germinated at 16°C. Error bars represent SEM of

3 biological replications for each time point. Significant differences based on comparison between allele mean at $P < 0.05$ (*) is indicated.

Cold inducible PMA: In the F_3 and BC_3 GI experiments, the 7B QTL did not show any observable effect on the germination potential of grains. This might relate to the fact that the 7B QTL is mainly a PMA QTL, which is a trait that is independent of the PHS phenotype and hence the dormancy status of seeds. In view of this, the effect of the 7B QTL on PMA induction was tested in two independent F_3 lines per allele and three independent BC_3 NILs per allele. This was done by measuring the α -amylase activity of grains using the Megazyme (UK) Ceralpha α -amylase test kit.

The average α -amylase activity of the susceptible F_3 lines was higher than those of the resistant lines, however, this difference was not statistically significant ($P = 0.06$, Figure 40a). Similarly, difference in α -amylase activity was observed between the susceptible and resistant BC_3 NILs of the 7B QTL. The NILs harbouring the susceptibility allele showed more amylase activity than the resistant NILs (Figure 40b). However, the observed difference was not statistically significant. These results were most likely due to high variability in the induction of PMA in individual seeds (Mares and Mrva, 2008). The tests, however, show a potential resistance effect of the 7B QTL on PMA induction.

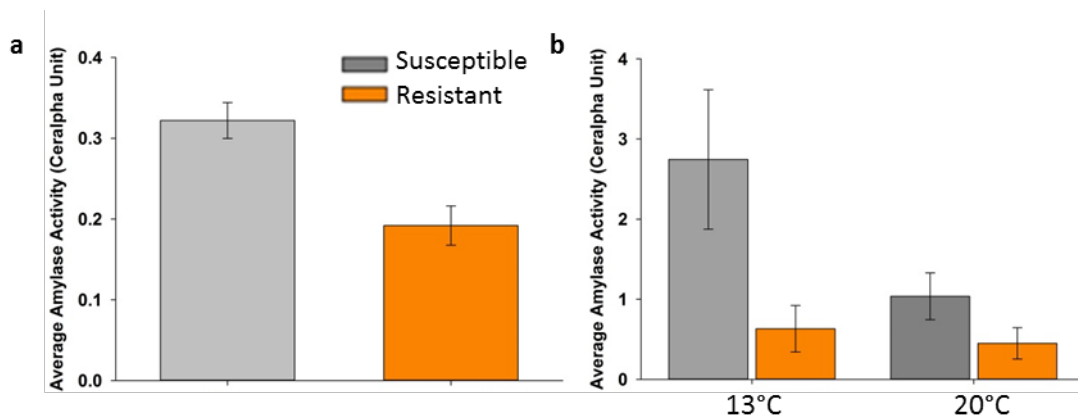


Figure 40: Potential effect of the 7B QTL on PMA induction. Average α -amylase activity of grains harvested from 7B resistant and susceptible F_3 lines (a) and BC_3 NILs (b). Error bars represent SEM of amylase activity of the 2 independent lines in (a) or 3 independent lines in (b).

In addition, the 13°C cold temperature treatment during grain development also had a marked effect on PMA induction, especially in the susceptible 7B NIL. There was more than a two-fold increase in α -amylase activity in grains of the susceptible NILs when grown at 13°C compared with plants grown at 20°C. This result is consistent with the reports by Mrva et al. (2006) which showed a strong PMA induction in susceptible lines when plants were transferred to the cold between 25 to 35 days post anthesis. This increase in PMA induction in the cold was not however observed in plants of the resistant NILs.

Objective 4: QTL haplotype analysis using next-generation sequencing to facilitate breeder deployment.

Fine mapping and cloning of the 4A RxA QTL

We have developed tightly linked markers which were described under Objective 1. For one of the QTL we took a more in depth approach and cloned the underlying gene. Here we describe the fine mapping, cloning and haplotype analysis of the 4A QTL.

The 4A QTL is known to segregate in UK wheat varieties and was identified in DH populations derived from crosses between Alchemy x Robigus and Option x Claire (Alchemy and Option providing the resistance allele). The QTL is flanked by markers *barc170* and *wmc491* in the Alchemy x Robigus population (Figure 41) and as such collocated with the major *Phs-A1* QTL identified across multiple studies (Barrero et al., 2015; Flintham et al., 2002; Imtiaz et al., 2008; Torada et al., 2008).

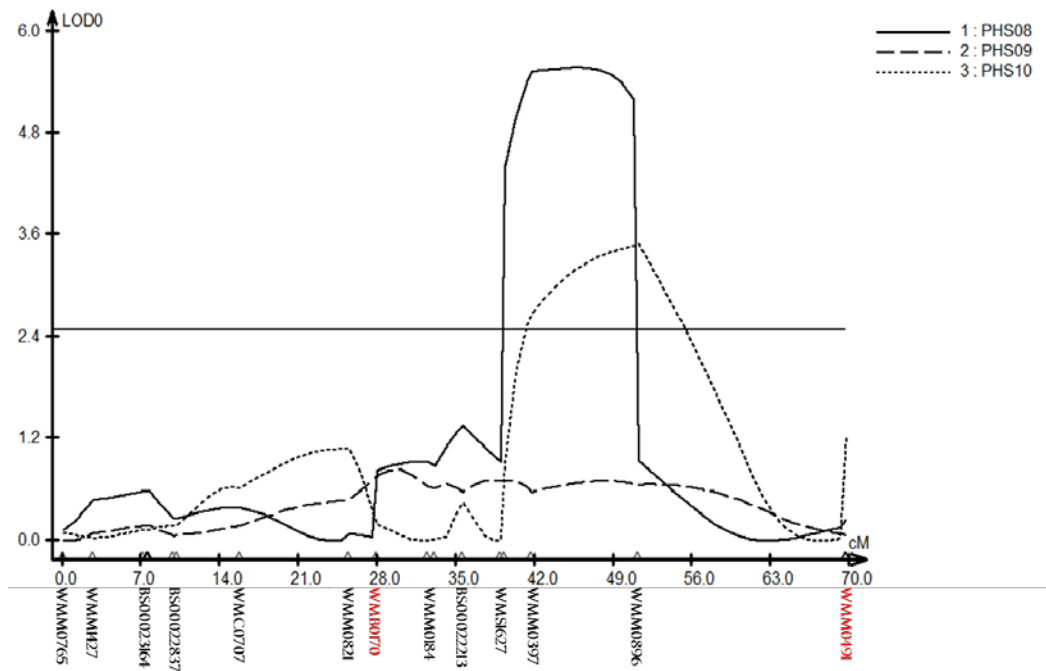


Figure 41: PHS resistance QTL on chromosome arm 4AL in the Alchemy x Robigus DH population. A QTL for PHS resistance was identified from composite interval mapping of the arcsin transformed sprouting percentage of DH lines phenotyped across three years of field trial (2008, 2009 and 2010). QTL was detected in 2008 and 2010 but not in 2009. The flanking markers used for selecting the QTL are highlighted in red. Figure from Shorinola et al 2016.

To independently validate the effect of 4A QTL, we developed NILs from the Alchemy x Robigus cross through marker-assisted backcrossing. Five markers distributed across the 4A chromosome arm were used for NIL development, including *barc170* and *wmc420* (1 cM

proximal to the *wmc491* flanking marker) as well as *wmc707*, *wmc760* and *wmc313* which are distal to *barc170* (Figure 42a). Seven overlapping recombination haplotypes (designated as NIL Groups 1 - 7) were developed (Figure 42b) with only Group 3 NILs containing the Alchemy resistant haplotype across the complete QTL interval.

We assessed the seed dormancy and PHS resistance phenotype of these NILs through a GI test on threshed seeds (GI experiment-1) and an artificial sprouting test on whole spikes (sprouting experiment-1). In the GI test, highly significant differences were observed between the Robigus and Alchemy parental controls ($P < 0.001$; Figure 42c). NILs were classified as either resistant or susceptible based on a Dunnett's test to the parental controls. NILs with higher or non-significant GI difference to Robigus were classified as susceptible, while NILs with lower or non-significant GI difference to Alchemy were classified as resistant. NIL Groups 1, 5 and 7 with the Robigus haplotype across the QTL interval, and NIL Groups 2 and 4 with recombinant haplotypes within the QTL interval, all showed the susceptible GI phenotype (Figure 42c). Group 3 NILs showed significantly lower GI to Robigus ($P < 0.001$) but also significantly higher GI than Alchemy ($P < 0.001$). Likewise, Group 6 NILs also showed significant difference to both parents but the GI was only slightly lower to the susceptible Robigus parent.

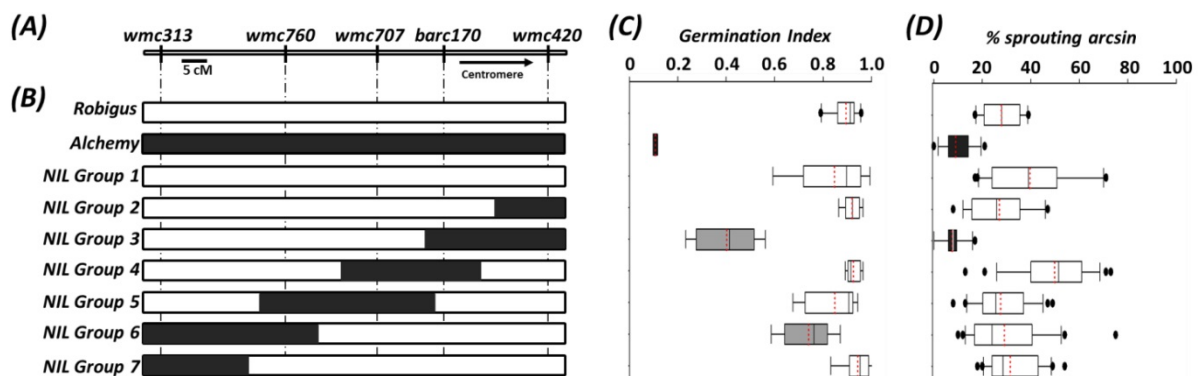


Figure 42: (A) Genetic map of SSR markers across the 4AL chromosome arm used to develop the NILs. (B) Graphical genotypes of Alchemy x Robigus NILs. The NILs are grouped based on their recombination haplotype across the marker intervals, with each group comprised of two independent NILs. The black filled portion in the graphical genotype represents the Alchemy alleles, whereas the white sections represent the Robigus alleles. (C) Mean germination index of each NIL group in GI experiment-1. (D) Sprouting phenotype of each NIL group in sprouting experiment-1. Figure from Shorinola et al 2016.

In the sprouting test, all the NIL groups (except Group 3) were significantly different to Alchemy, but not to Robigus and were therefore classified as being susceptible to sprouting

(sprouting experiment-1; Figure 42d). Group 3 NILs showed comparable sprouting levels to the resistant variety Alchemy, and were significantly different to Robigus ($P < 0.001$), consistent with the GI results. Taken together, the GI and sprouting results validate the resistance effect of the 4A QTL in NILs with the Alchemy haplotype across the complete *barc170-wmc420* interval. NILs from Group 2 and 4 which have the Alchemy allele at either one or the other, but not both, flanking markers were susceptible, suggesting that the 4A QTL resistance is delimited by, but not linked to these markers.

Previously, Torada et al. (2008) mapped *Phs-A1* to a 2.6 cM interval between *barc170* and *xhbe03*. We therefore used *barc170*, *xhbe03*, and another marker - *wms894* - in the same physical bin (4AL_13-0.59-0.66), to characterise Option x Claire F₄ RILs (Figure 43a,b). We selected 27 homozygous recombinants across the interval, grouped these according to their haplotypes (Figure 43b), and assessed the sprouting phenotype using the artificial sprouting test (sprouting experiment-2). Two significantly different sets were identified in this experiment: one was made up of RIL Group 2 and Option Control RILs with between 3 and 5 % sprouting, whereas the second set contained RIL groups 1, 3, 4 and the Claire Control RILs with average sprouting between 15 and 22 % (Figure 43c). RIL Group 2 and the Option Control RILs were similar to the resistant Option parent and had the Option haplotype between *wms894* and *xhbe03*. RIL Groups 1, 3, 4 and the Claire Control RILs were similar to the susceptible Claire parent and carried a homozygous Claire or recombinant haplotype across the *wms894 - xhbe03* interval. This suggests that the *Phs-A1* resistance is only observed when RILs have the Option haplotype across the 0.5 cM *wms894-xhbe03* interval.

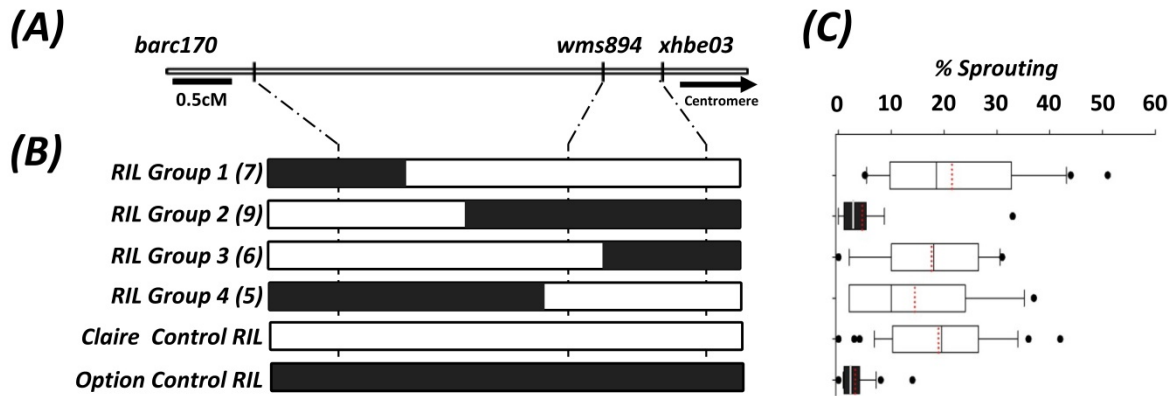


Figure 43: Interval mapping of *Phs-A1* in the Option x Claire RIL population. (A) Genetic map of the SSR markers flanking *Phs-A1*. (B) Graphical genotypes of RILs and controls are presented with the Option and Claire alleles represented in black and white, respectively. The RILs are grouped according to their fixed genotype across the *Phs-A1* interval and the number of lines in each RIL group is indicated in parenthesis. (C) Sprouting phenotype of RIL groups and controls in sprouting experiment-3. Boxes with the same colour are similar to each other based on pairwise comparisons. Figure from Shorinola et al 2016.

Synteny reveals the putative gene content of the *Phs-A1* locus: Given the small genetic interval to which *Phs-A1* mapped, we evaluated the gene content across this locus. We first identified genes containing the flanking markers (*xhbe03* and *wms894*) in wheat: *xhbe03* is designed from the 3' UTR sequence of *PM19-A2* (Traes_4AL_F99FCB25F) while the sequence of *wms894* is located in the promoter region of an OTU Cysteine Protease gene (Traes_4AL_F00707FAF). We next examined the collinear region in *Brachypodium*: reciprocal BLASTs against the *Brachypodium* genome identified *Bradi1g00600* and *Bradi1g00720* as orthologues of *PM19-A2* and OTU Cysteine Protease, respectively. This defined the collinear *Phs-A1* interval in *Brachypodium* to a 75 kb region which contains 11 genes (*Bradi1g00607* to *Bradi1g00710*).

The *Brachypodium* genes were used to search the wheat chromosome arm assemblies of the hexaploid wheat cultivar, Chinese Spring (IWGSC, 2014). Orthologous contigs and gene models to *Bradi1g00600* - *Bradi1g00620* and *Bradi1g00670* - *Bradi1g00720* were identified on chromosome arm 4AL. These included *PM19-A2* and its paralogue *PM19-A1*, as well as additional genes (Figure 44). No wheat orthologues were identified for *Bradi1g00630* to *Bradi1g00660*. Within the wheat IWGSC contigs, a non-collinear gene encoding for an *Aminocyclopropane Carboxylate Oxidase 1-Like* protein (*ACC Oxidase-1*; Traes_4AL_65DF744B71) was also identified. All these genes/contigs were mapped within or linked to the critical *wms894-xhbe03* interval using SNP-based KASP assays, except for

Traes_4AL_C56125840 which we did not map due to the lack of a genetic marker. This confirmed the collinear gene order between wheat and *Brachypodium* and suggests possible candidate genes for *Phs-A1*.

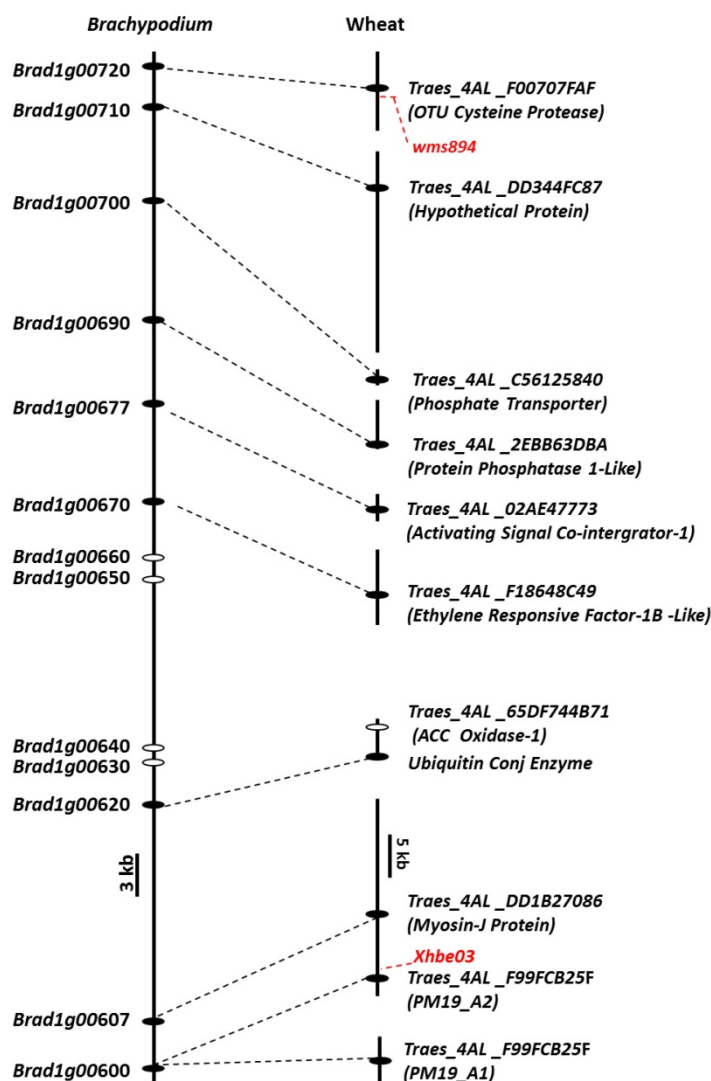


Figure 44: Sequences of genes containing the *Phs-A1* flanking markers (*wms894* and *xhbe03*; in red) were used to obtain genes in the orthologous *Brachypodium* interval (*Brad1g00600* - *Brad1g00720*). Collinear genes are represented by black ovals while non-collinear genes are represented by the white ovals. Orthologous wheat contigs (black lines) and genes models are connected to their corresponding *Brachypodium* genes. All the wheat gene were genetically mapped within or linked to the *wms894-xhbe03* interval except for *Traes_4AL_C56125840*. Figure from Shorinola et al 2016.

Phs-A1 maps distal to the *PM19* genes in two UK fine-mapping populations: Barrero et al. (2015) identified *PM19-A1* and *PM19-A2*, as the main candidates for a seed dormancy QTL on wheat 4AL chromosome arm in a multi-parental mapping population. To determine if these genes determined the allelic variation observed in the UK populations we further fine-mapped

Phs-A1 in the Option x Claire F₄ RILs with homozygous recombinant and non-recombinant haplotypes in the *Phs-A1* interval. We first defined the linkage between the gene-based KASP assays previously used to map the syntenic genes (Figure 45a). The two *PM19* genes were completely linked and so too were the *PP1-like*, *ERF-1B-like* and *ASC1* genes. There were however recombination events between *PP1-Like/ ERF-1B-Like/ ASC1* and *OTU Cysteine Protease* and between *ACC Oxidase-1* and *PM19-A2/PM19-A1*. Given the genetic linkage between some of these markers, four SNP markers including *OTU Cysteine Protease*, *PP1-Like*, *ACC Oxidase-1* and *PM19-A2* were used to define five distinct recombinant haplotypes (RIL Group 11 - 15; Figure 45b).

A subset of lines from each RIL group, in addition to the parental cultivars and non-recombinant Claire and Option control RILs were phenotyped using the artificial sprouting test (sprouting experiment-3; Figure 45b). Variation in sprouting percentage was observed defining a bimodal distribution. To unequivocally assign sprouting phenotypes to these lines, the mean sprouting percentages of each RIL group (Figure 45c) as well as the individual sprouting percentages of each RIL were compared against those of Claire and Option using the Dunnett's test. This showed that the sprouting phenotype is completely associated to the *PP1-Like/ERF-1B-Like/ASC1* linkage in all the lines tested. Five independent recombination events (Group 12 and 13) map *Phs-A1* proximal to the *OTU Cysteine Protease (wms894)* marker. Similarly, the six lines from RIL Groups 11, 14 and 15, map *Phs-A1* distal to both the *ACC Oxidase-1* and the *PM19* genes. This was unexpected given the reported association of the *PM19* genes with sprouting resistance. We confirmed this result in an independent sprouting experiment (sprouting experiment-4) using the critical Group 12 - 14 RILs. Although a higher level of sprouting was observed in this experiment, *Phs-A1* still conferred a moderately level of resistance which was associated with the *PP1-Like/ERF-1B-Like/ASC1* linkage.

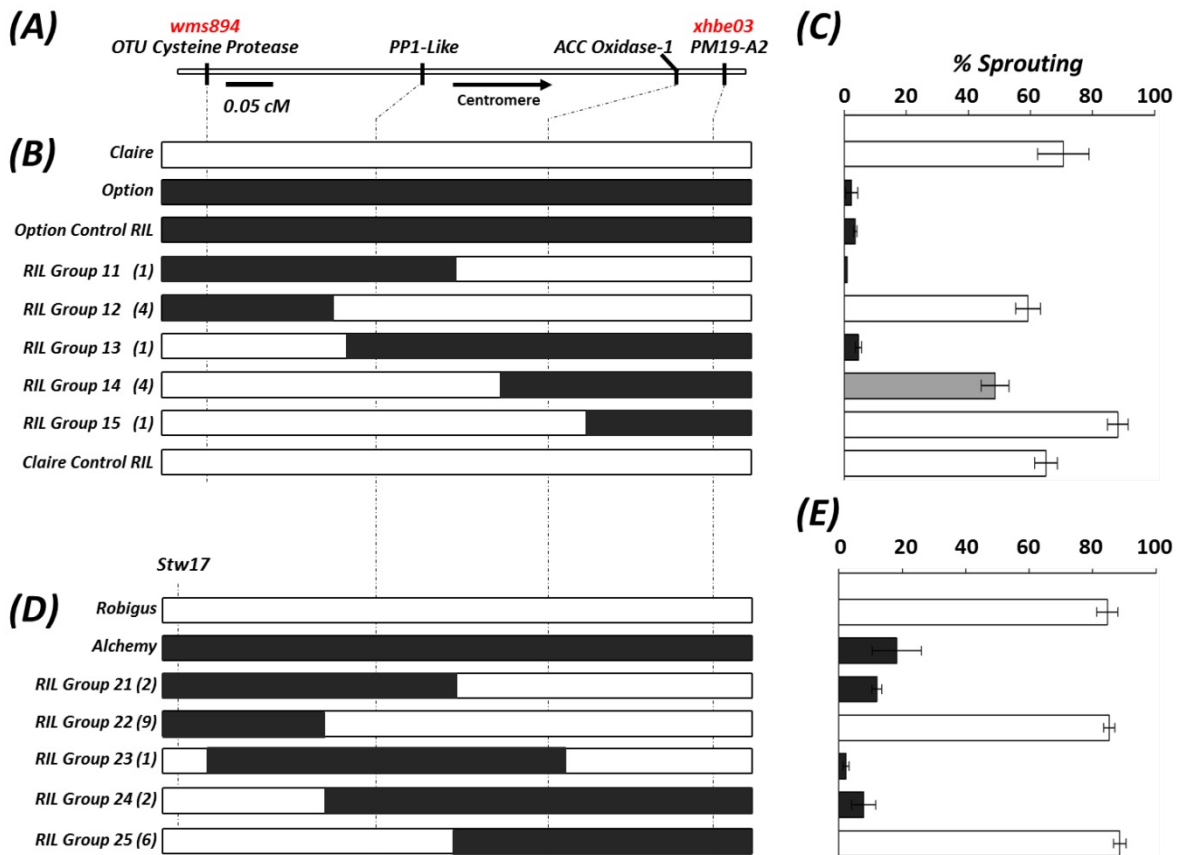


Figure 45: (A) Linkage map of SNP (black) and SSR (red) markers across the *Phs-A1* interval. The graphical genotype of Option x Claire RILs (B) and Alchemy x Robigus RILs (D) are aligned against their sprouting phenotype (C and E, respectively). RILs are grouped based on their recombination haplotype across the marker interval and the number of lines in each group is indicated in parenthesis. Resistant parent alleles (Option and Alchemy) are represented in black, whereas the susceptible parent alleles (Claire and Robigus) are shown in white. Marker *stw17* (2 cM distal to *wms894*) was used in the Robigus x Alchemy population as *wms894* and *OTU Cysteine Protease* are monomorphic. The sprouting phenotype of each RIL group is designated as susceptible (white), moderate (grey) or resistant (black) based on statistical comparison with the parental controls. Error bars represents SEM. Figure from Shorinola et al 2016.

We also independently fine-mapped *Phs-A1* in an Alchemy x Robigus RIL population which contained similar recombination haplotypes (RIL Groups 21 - 25; Figure 45d) as in the Option x Claire population. However, marker *stw17* was used in place of the *OTU Cysteine Protease* marker as this was not polymorphic in the Alchemy x Robigus cross. We assessed the sprouting phenotype of these lines using the artificial sprouting test (sprouting experiment-5). Similar to the previous results, the mean sprouting percentages of each RIL group (Figure 45e) confirmed the complete linkage of *Phs-A1* to *PP1-Like*, *ERF-1B-Like* and *ASC1* genes. Eleven independent recombination events in RIL Group 22 and 24 map *Phs-A1* proximal to *stw17*, whereas nine independent RILs map *Phs-A1* distal to the *ACC Oxidase-1* and *PM19* genes (RIL Groups 21, 23 and 25). This provides strong genetic evidence that in the two UK mapping populations *Phs-A1* maps distal to the *PM19* genes.

TaMKK3 as a candidate gene: During the project Torada et al. (2016) identified the *mitogen-activated protein Kinase Kinase 3* gene (*TaMKK3-A*), as a candidate gene for *Phs-A1*. The *TaMKK3-A* gene was identified through a traditional positional cloning strategy using biparental mapping populations. It is unclear whether the sprouting variation associated with *Phs-A1* across diverse germplasm is due to allelic variation at *PM19* or *TaMKK3-A* alone, or if it's due to a combination of both genes.

We constructed an extended physical map across the *Phs-A1* interval to investigate the physical proximity between the *TaMKK3-A* and *PM19* candidate genes. Using *PM19-A1* and *TaMKK3-A* sequences as queries, we screened *in silico* a Bacterial Artificial Chromosome (BAC) library of flow sorted 4AL chromosome arm of the bread wheat cultivar Chinese Spring (CS). *PM19-A2* and *TaMKK3-A* were found on two independent non-overlapping BAC clone clusters which were anchored on chromosome 4A. Cluster 16421 (*PM19*) MTP as comprised of eleven BAC clones whereas Cluster 285 (*TaMKK3-A*) MTP included four BAC clones (Figure 46a).

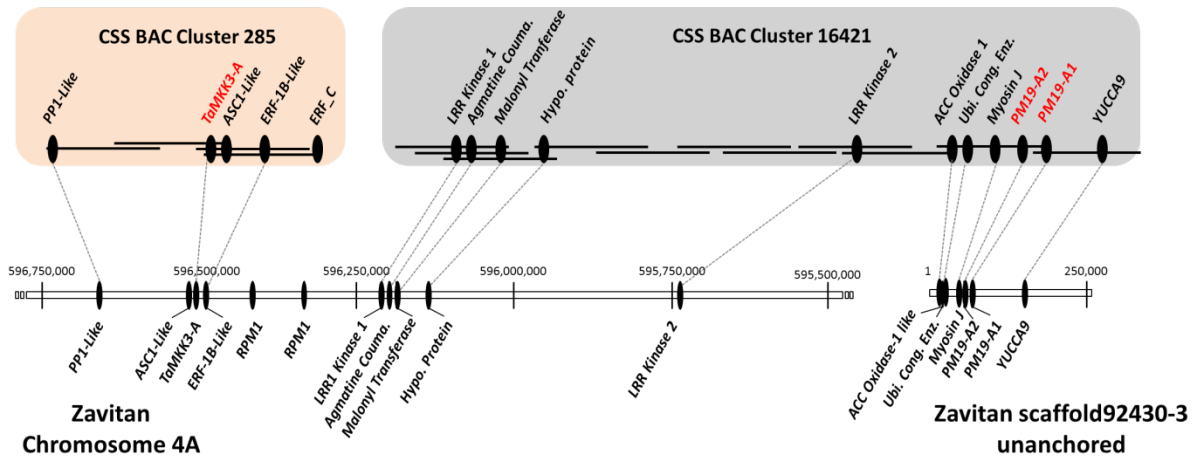


Figure 46: Physical map of the *Phs1-A1* interval in bread wheat (CSS) and wild emmer (Zavitan). (a) *Phs1-A1* interval in CSS is covered by two non-overlapping BAC clusters: Cluster 285 (4 BACs) and Cluster 16421 (11 BACs). BACs are represented by solid lines while genes found on the BAC are represented by filled ovals. The proposed candidate genes for *Phs-A1* are highlighted in red font. (b) Whole genome assembly of Zavitan, wild emmer with the *Phs1-A1* interval represented across two scaffolds. Genes present in both assemblies are joined by dotted lines.

Individual BACs were sequenced, assembled and annotated for repeat sequences and coding sequences using the IWGSC gene models (Meyer et al 2014). Cluster 16421 included nine high confidence genes in addition to the *PM19-A1* and *PM19-A2* genes. In addition to *TaMKK3-A*, Cluster 285 contained four additional genes. Together, this suggests the presence of at least 16 protein coding genes across the *Phs-A1* interval in hexaploid bread wheat. We also characterised the interval in the recently constructed NRGene assembly of a wild emmer wheat accession Zavitan (Figure 46b). Fifteen of the 16 genes found in the CSS physical map were located on two Zavitan scaffolds. Nine genes were positioned across a 0.93 Mb interval on the Zavitan 4A pseudomolecule. These included 4 genes from BAC Cluster 285 and five genes from BAC Cluster 16421 (Figure 46). The remaining six genes spanned a 0.13 Mb interval on an unanchored scaffold. Combining the CSS and Zavitan physical map information, the physical region between *TaMKK3-A* and the *PM19* genes was covered and estimated to be approximately 1.2 Mb.

Torada et al. (2016) reported an A>C mutation in position 660 of the *TaMKK3-A* coding sequence (A660C) as being causative of the *Phs-A1* effect. Using alignments of the three

wheat genomes we developed a genome-specific and co-dominant KASP assay for this SNP designated as TaMKK3-A-snp1. We used this assay to genotype an association panel comprised of the parents of six bi-parental mapping populations and a MAGIC population in which *Phs-A1* had previously been reported (Mares et al. 2005; Ogbonnaya et al. 2007; Flintham 2000; Lohwasser et al. 2013). TaMKK3-A-snp1 was polymorphic and perfectly diagnostic for *Phs-A1* in this diverse panel (Table 14). All the non-dormant sprouting-susceptible parents shared the “A” *TaMKK3-A* allele while all the dormant sprouting-resistant parents shared the TaMKK3-A-snp1 “C” allele (Figure 47a), consistent with Torada et al. (2016). The TaMKK3-A-snp1 assay is co-dominant as it distinguished between heterozygotes and homozygotes F₂ progenies in the Alchemy x Robigus population.

Table 14: *TaMKK3* and *PM19-A1* functional polymorphisms in parental lines of published mapping populations segregating for *Phs-A1*.

Population	Variety	Origin	Status	<i>TaMKK3-A</i> Allele	<i>PM19-A1</i> promoter del	Reference
Alchemy x Robigus	Alchemy	UK	Dormant	C	-	Shorinola et al (2016)
	Robigus	UK	Non-dormant	A	+	
Option x Claire	Option	UK	Dormant	C	-	Shorinola et al (2016)
	Claire	UK	Non-dormant	A	+	
MAGIC Pop.	Yitpi	AUS	Dormant	C	-	Barrero et al (2015)
	Baxter	AUS	Non-dormant	A	+	
	Chara	AUS	Non-dormant	A	+	
	Westonia	AUS	Non-dormant	A	+	
Janz x AUS1408	Aus1408	AUS, SA	Dormant	C	-	Mares et al (2005); Ogbonnaya et al (2007)
	Janz	AUS	Non-dormant	A	+	
Cranbrook x Halberd	Halberd		Dormant	C	-	Mares et al (2005); Zhang et al (2008)
	Cranbrook	AUS	Non-dormant	A	+	
Boxer x Soleil	Soleil	UK	Dormant	C	-	Flintham (2000)
	Boxer	UK	Non-dormant	A	+	
Opata x W7984	W7984	MEX	Dormant	C	-	Lohwasser et al, (2013)
	Opata	MEX	Non-dormant	A	+	
SW95-50213 x Cunningham	SW95-50213	CHN	Dormant	C	+	Mares et al (2005)
	Cunningham	AUS	Non-dormant	A	+	

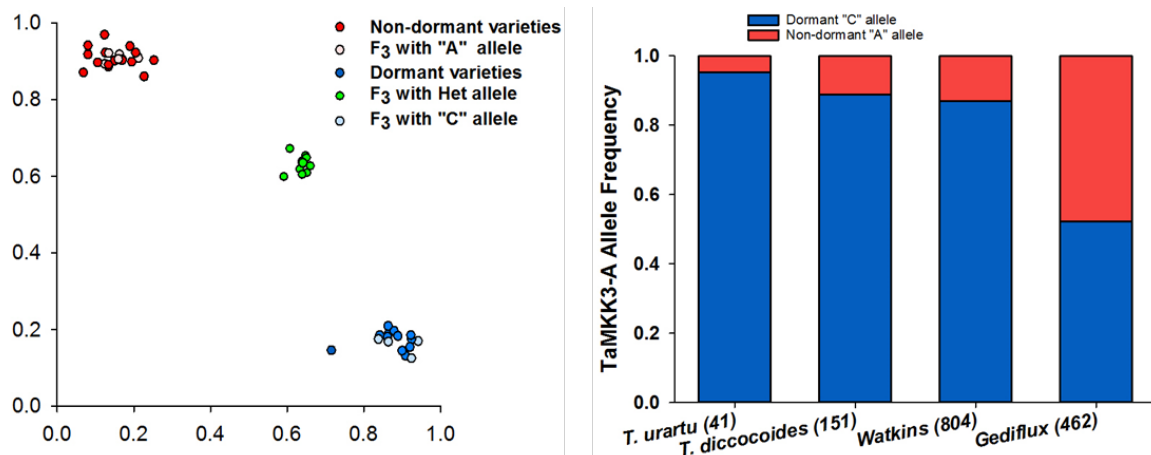


Figure 47: Marker development and allele distribution of *MKK3* in ancestral and historic germplasm. Genotype plot of varieties and F₃ population segregating for *Phs-A1* using newly developed *MKK3* KASP assay. Right panel shows the allele frequency of the causal A/C SNP in *T. urartu* and *T. turgidum* ssp. *diccoccoides* accessions as well as the Watkins and Gediflux collection. The number of genotyped lines is indicated at the base of the bars.

To examine the origin, distribution and allele frequencies of the causative *TaMKK3-A* A660C SNP, we genotyped a diverse set of *Triticum urartu* (2x) and *T. turgidum* ssp. *diccoccoides* (4x) accessions. These represent the diploid and tetraploid donors of modern bread wheat A genome on which *Phs-A1* is located. Torada et al previously suggested that the non-dormant "A" allele was the mutant form since the dormant "C" SNP was conserved across different species. Across 41 *T. urartu* accession, the dormant "C" allele was predominant (39 accessions; 95% allele frequency) while the non-dormant "A" allele was present in only two accessions. Similarly, across 151 *T. diccoccoides* accessions, the dormant "C" allele frequency was 89% while the non-dormant allele was found in 17 accessions (Figure 47). Our results are consistent with Torada et al in that the non-dormant "A" allele is derived from the wild type "C" allele. In addition, the presence of the A allele across both progenitor species suggests that the mutation predates the hybridization and domestication events that gave rise to modern bread wheat.

We also genotyped the Watkins Collection representing a set of global bread wheat landraces collected in the 1920 and 1930s (Wingen et al. 2014), as well as the Gediflux collection comprised of modern European bread wheat varieties released between 1945 and 2000 (Reeves et al. 2004). The allele frequency of the non-dormant "A" allele was 13% in the Watkins landrace collection (Figure 47), comparable to that in the wild emmer *T. diccoccoides* (11%). The non-dormant "A" allele frequency in the Gediflux collection was 48% across 462 varieties (Figure 47). This represented a marked increase in the susceptibility allele in this

more modern Europe collection when compared to the 14% “A” allele frequency of European sub-population within the Watkins collection. This could be due to selective pressure by breeders for the non-dormant C allele in European environments.

We examined the allelic diversity of the *TaMKK3-A* locus with the aim of elucidating the haplotype structure across the extended *Phs-A1* interval. For this, we used the SNP Haplotype Map (HapMap) dataset obtained from whole exome capture sequence of 62 diverse germplasm (Jordan et al. 2015). From this SNP dataset, we were able to obtain data for eight of the sixteen genes found in the *Phs-A1* interval corresponding to 51 SNPs. To improve the accuracy of the haplotype analysis, we selected SNP loci with more than 80 % homozygous calls across the dataset and more than a 5 % minimum allele frequency. This yielded 39 SNPs across the eight genes in 58 accessions.

Across *Phs-A1* interval from *PM19-A1* to *PP1-like*, 14 distinct haplogroups were identified (Haplogroup 1 – 14; Figure 48). Each haplogroup comprised a mix of cultivars, landrace, breeding lines and synthetic population, in varying proportions (Figure 48b). Haplogroup 1 represented the major haplotype with 33 % of lines having this haplotype. Also, we observed haplotype linkage from the *TaMKK3-A* to *LRR Kinase 2* in 76 % of the lines highlighting possible evidence for limited recombination in this 780 kb interval in global germplasm. Similarly, there was linkage in the haplotype observed at the tandem *PM19* loci in all but one of the 58 lines.

Five of the selected SNPs were found in *TaMKK3-A* including the causal A660C SNP in the third exon of *TaMKK3-A*. The other four SNP were found in introns of *TaMKK3-A*. Only Four distinct haplotypes (*TaMKK3A_Haplotype1-4*; Fig 3c) were defined across these 5 *TaMKK3-A* SNP loci in this diverse germplasm with only one of these having the susceptible “A” allele at the causal A660C loci (*TaMKK3A_Haplotype1*). As was observed in the modern Gediflux collection, the non-dormant *TaMKK3-A* “A” allele frequency was 0.5 in the HapMap population, suggesting that a significant proportion of global germplasm might be predisposed to the problem of PHS.

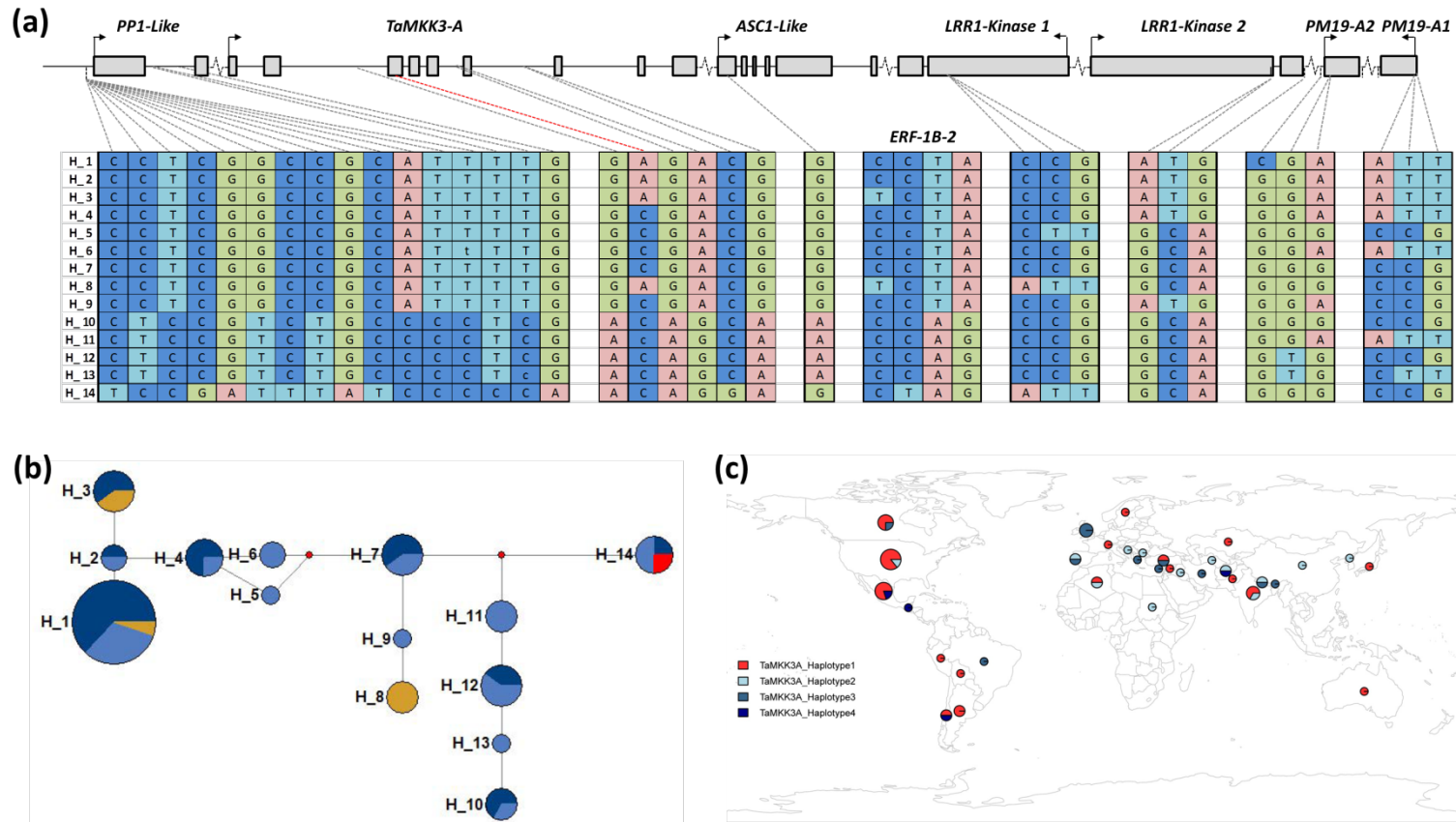


Figure 48: *Phs-A1* haplotype analysis (a) Structure of 14 distinct haplotype group identified in HapMap population across 39 SNP loci in the *Phs-A1* interval. (b) Haplotype Network of the 14 distinct haplogroups. Each circle corresponds to the number of lines in each haplogroup. The blue, light blue, amber and red pie represents the proportion of cultivars, landraces, breeding and synthetic line in each haplogroup (c) Geographical distribution of the four distinct *TaMKK3-A* haplotypes.

We next examined a larger set of UK varieties for the *TaMKK3* genotype (157 varieties) and the broader *Phs-A1* haplotype (115 varieties) shown in Figure 48. This included current, recent and older UK varieties from the RL list and from different market classes. We found a balance between the susceptible and resistant allele at *TaMKK3* across the UK varieties, with 70 carrying the susceptible allele (45%) and 87 lines carrying the resistant allele (55%; Fig 49). A broader look across the haplotypes of 50 susceptible lines showed three distinct haplotypes (1-3) with the majority carrying either Haplotype 1 (60%) or Haplotype 3 (32%). This includes RL varieties such as Oakley, JB_Diego, Robigus, Nijinsky, Claire (Haplotype 1) and Kielder (Haplotype 3). We also looked at 65 resistant lines and identified four haplotypes (Haplotypes 4-7) across the *Phs-A1* region. Here, Haplotype 5 dominated with 83% of resistant lines carrying the same haplotype across the region and 11% of lines carrying Haplotype 4. Lines carrying Haplotype 5 include Alchemy, Santiago, Skyfall, Hereward, Consort, Solstice, whereas lines with Haplotype 4 include Xi19, Panorama, Cubanita.

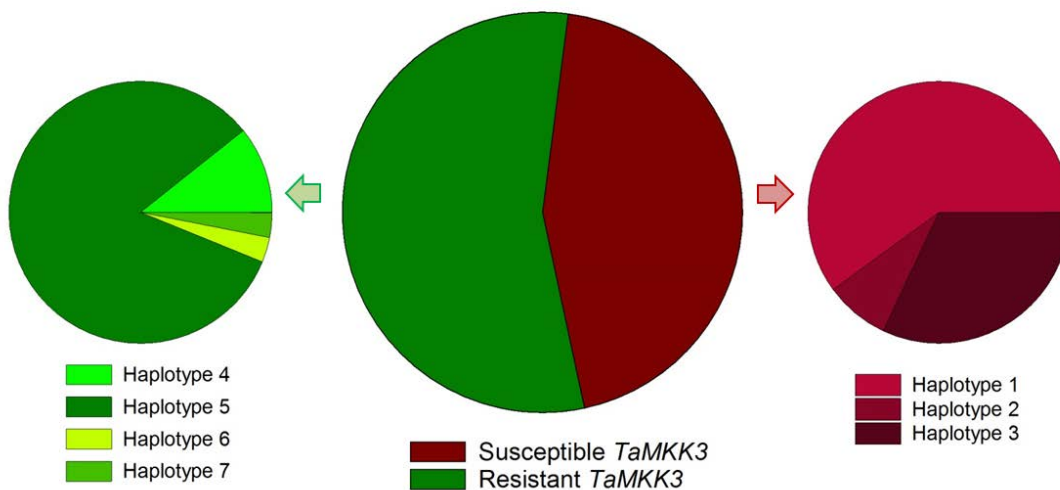


Figure 49: Allelic variation at *TaMKK3* and extended *Phs-A1* haplotype (Figure 48) of UK varieties. Centre chart shows the *TaMKK3* information for 157 varieties and the smaller side charts show the breakdown of Haplotype groups within each category (50 susceptible and 65 resistant). Green colours are associated with the resistant allele/haplotype; red colours with the susceptible allele/haplotype.

We used the published nabim Group 1-4 classifications to determine the relative frequency of the susceptible and resistant *TaMKK3* allele across the different end-use groups. Overall, we found a consistent pattern where nabim group 1 varieties only carried the resistant *TaMKK3* allele, whereas the frequency of this allele decreased towards group 4 varieties (Figure 50; Table 15).

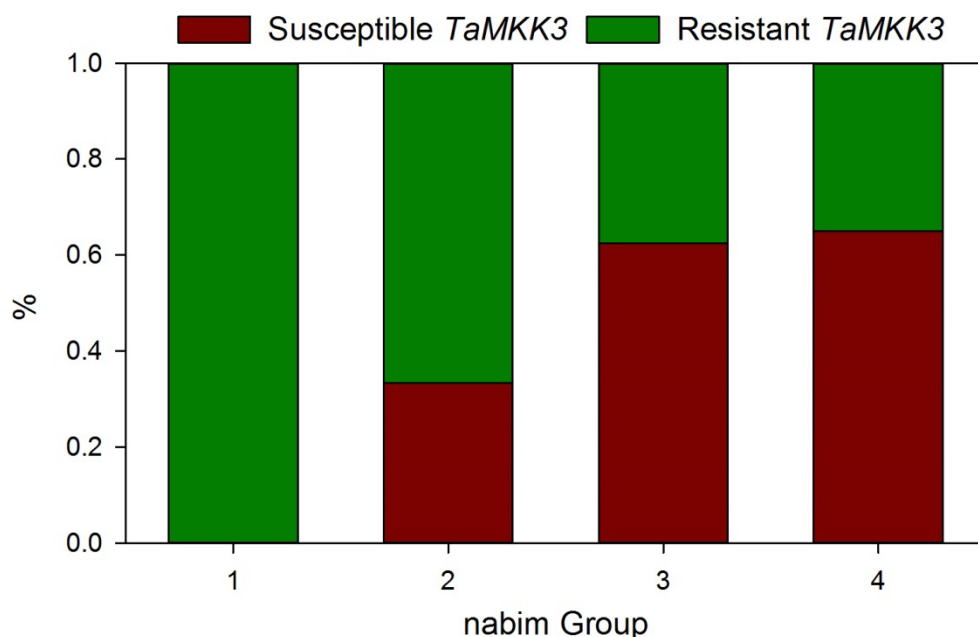


Figure 50: Frequency of the two allelic variants at *TaMKK3* for 41 RL varieties classified according to their nabim Group. Green bars represent the resistant *TaMKK3* allele whereas red bars the susceptible allele. Details of the varieties are shown in Table 15.

Table 15: Details of *TaMKK3* allele in RL varieties arranged based on their nabim Group.

nabim Group	Susceptible <i>TaMKK3</i>	Resistant <i>TaMKK3</i>
1	---	Crusoe, Gallant, Xi19, Hereward, Malacca, Skyfall, Solstice
2	Charger, Sterling	Cubanita, Panorama, Cordiale, Ketchum
3	Claire, Invicta, Nijinsky, Robigus, Scout	Consort, Deben, Wizard
4	Access, Cougar, Dickens, Icebreaker, JB Diego, Myriad, Oakley, Savannah, Relay, KWS_Kielder, Brompton, Gladiator, Welford	Alchemy, Equinox, Napier, Riband, Santiago, Stigg, Tanker

We next explored the possible origins of the different resistant sources and haplotypes in UK wheat. We generated a pedigree of the UK and European varieties for which we had *TaMKK3* allelic and haplotype data. This generated a large scale pedigree where particular pedigrees could be explored in greater detail. Figure 51 shows the general pedigree view using the Helium visualisation developed at James Hutton Institute (Shaw et al 2014).

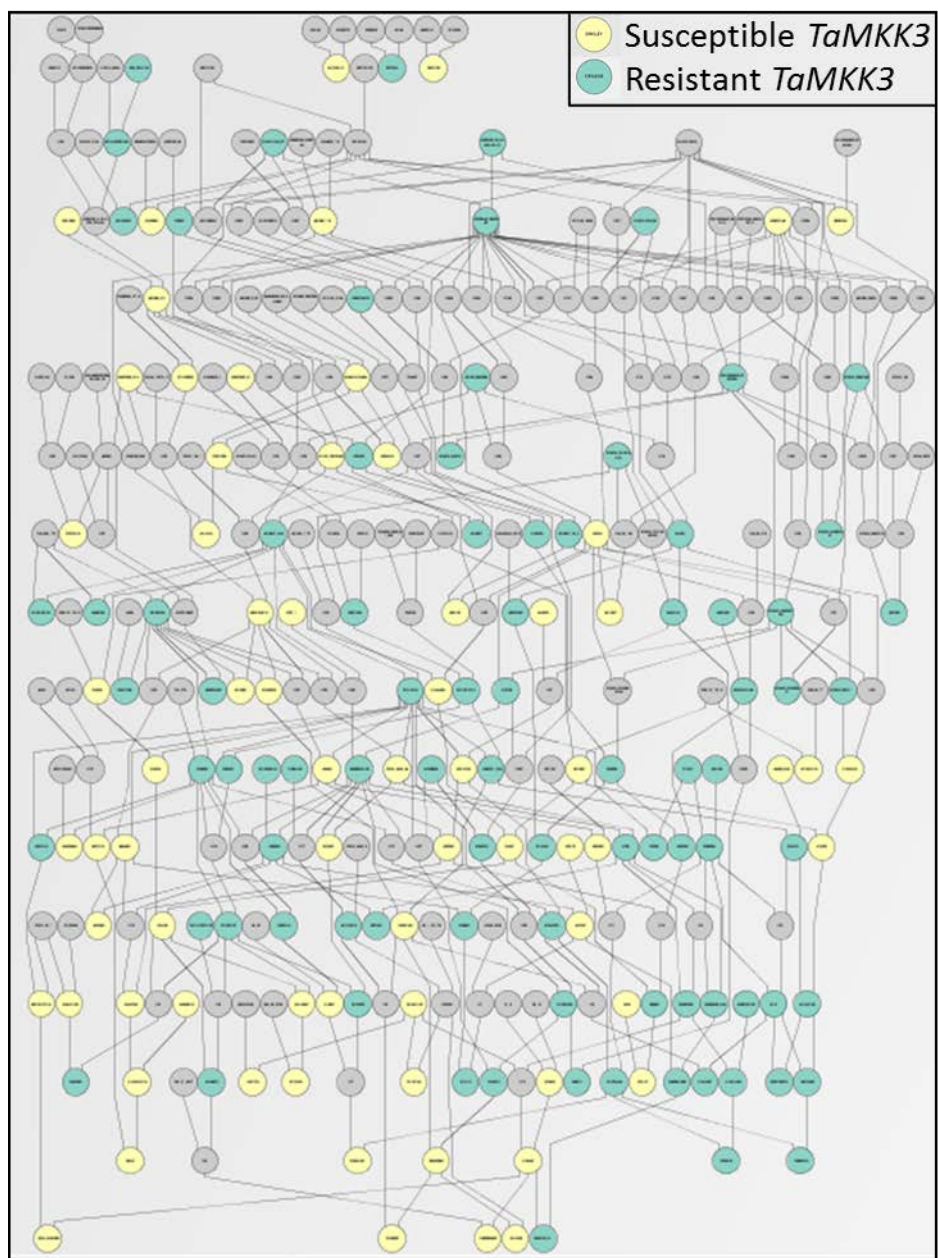


Figure 51: Pedigree of UK and European varieties with the corresponding *TaMKK3* allelic status. Each circle represents a variety and the lines correspond to the parents that were crossed to generate them. Yellow circles correspond to susceptible *TaMKK3* alleles, teal circles represent resistant *TaMKK3* alleles.

As an example we looked at the pedigree of Group 1 variety Gallant to determine the origin of its haplotype. Looking at the single *TaMKK3* SNP the pedigree of Gallant includes two resistant parents Malacca and Xi19 (teal; Figure 52a), and the susceptible parent Charger (yellow). This suggests that the resistance in Gallant originates from either Malacca or Xi19. Looking at the haplotypes this relationship becomes clearer (Figure 52b); Malacca carries the

resistant Haplotype 5 (blue), whereas Xi19 carries the resistant Haplotype 4 (red terra cotta). This suggests that Haplotype 4 was selected by breeders at the *Phs-A1* locus for Gallant. Following a similar logic, the Xi19 haplotype originates from Cadenza since the other Xi19 parent Rialto carries resistant Haplotype 4.

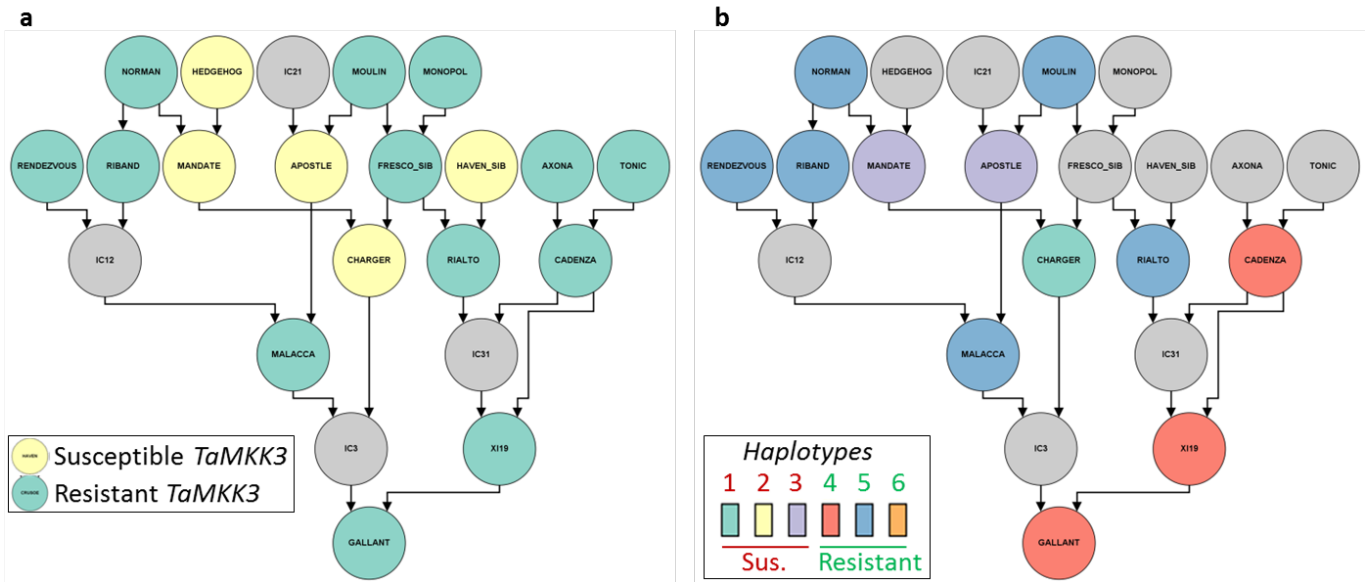


Figure 52: Pedigree analysis of Group 1 variety Gallant based on the *TaMKK3* allele (a) and the *Phs-A1* haplotype (b). In cases where three-way crosses have been used to develop a variety, an intermediate cross (IC) needs to be introduced in the pedigree visualisation. Hence Gallant’s immediate parents are shown as ‘IC3’ x ‘Xi19’, but IC3 corresponds to Malacca x Charger; thus the true pedigree (Malacca x Charger) x Xi19 is maintained. Note that IC’s in the tree are not assigned a haplotype or *TaMKK3* allele and are thus coloured in grey (unknown).

The importance of the Cadenza haplotype across the *Phs-A1* region in Group 1 varieties is evident when analysing the pedigree from the point of view of the Cadenza descendants (Figure 53). Performing a similar analysis as above, many Cadenza derived varieties which have been selected for Haplotype 4 (red terra cotta) have been classified as Group 1 or 2 varieties (Xi19, Panorama, Gallant, Cubanita, Crusoe).

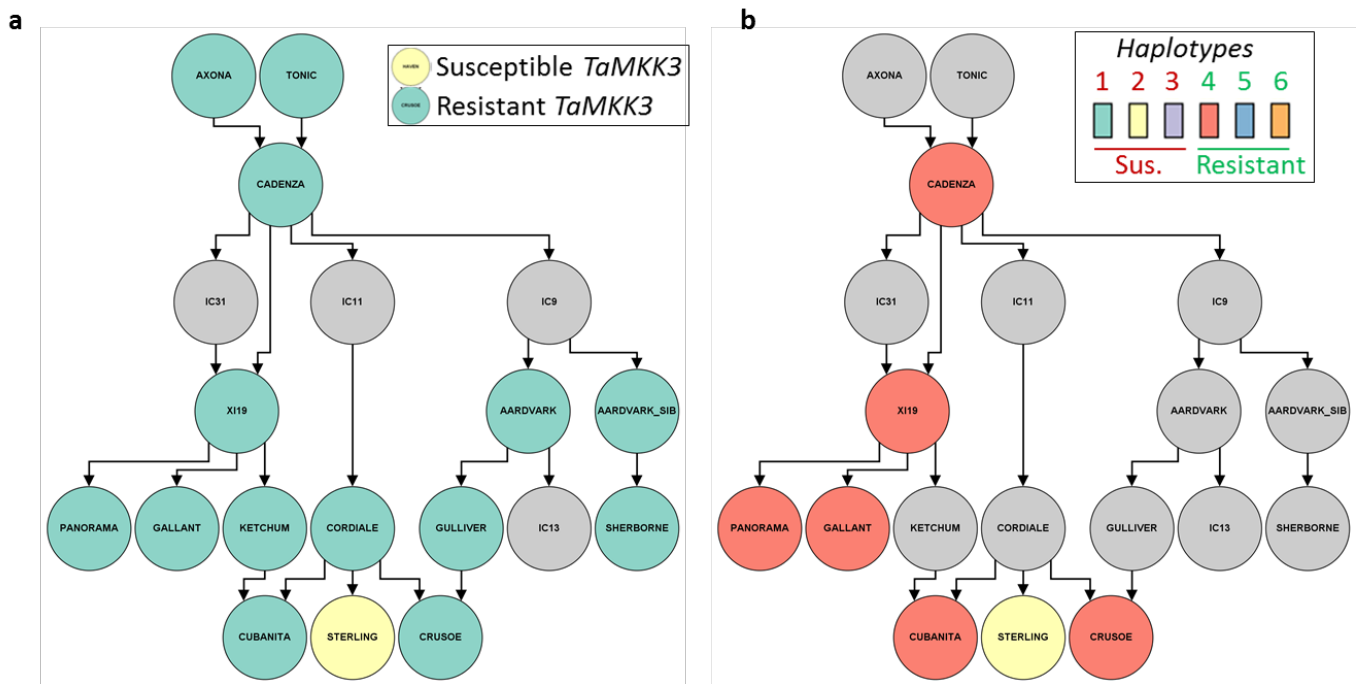


Figure 53: Pedigree of Cadenza derived varieties for *TaMKK3* (a) and the *Phs-A1* haplotype (b). Legend details are the same as for Figure 52.

We have shown the value of the pedigree and haplotype analysis through these static examples, but much of the value of these analyses comes from interactive queries and examination of the haplotypes. We foresee that with the new genomic resources these types of analyses will become more common place and in many ways this project has been a good example and test-case for the use of defined SNP and haplotype analyses.

General Discussion

Our goal was to develop a ‘breeders’ tool kit’ to allow high-throughput marker assisted selection for improved Hagberg Falling Number in UK wheat. We set out an ambitious goal by targeting six distinct QTL which had previously been shown to be good candidates to further characterise. These QTL differed in their effect on HFN, some affecting sprouting and other affecting PMA.

Our first goal was to validate the six QTL and to develop more precise genetic maps and markers to allow their deployment into UK varieties. We conducted tests using different germplasm and were able to validate the majority of the QTL for their improved HFN scores or sprouting resistance. The 1A, 2D, 4A and 7B QTL stood out given their consistency across locations. In the case of the 1A, 2D and 7B QTL we observed significant improvements in HFN scores which averaged 25, 21 and 32 s, respectively, across all trials (Figure 19). These four QTL had subtle pleiotropic effects on agronomic traits (apart from the height effect of 2D; Objective 2) and did not affect yield. Using a variety of germplasm, the 3A QTL in AxC and SxR had more subtle effects on HFN across locations and were therefore more difficult to fine map and define. Although these were not left behind, as a group we made the decision to prioritise the 1A, 2D, 4A and 7B QTL during the later stages of the project.

We defined different modes of action for the four prioritised QTL. The 7B QTL has no effect in different sprouting or germination assays and is a major gene affecting PMA and HFN scores. This is distinct from the 4A QTL which confers protection to late induction of sprouting as the gene affects the rate in which seeds lose dormancy. Hence the protective allele provides a delay in the loss of dormancy at the end of grain development. This means that seeds will not germinate in cases where late rains disrupt or delay the harvest of wheat crops. However, this protection is sufficiently short lived given that there is no effect in seed germination for commercial sowings a few months or even weeks later. The 1A and 2D QTL provide similar types of protection as the 4A QTL, although their effect seems to be manifested earlier than 4A. This suggests that the “1A/2D + 4A + 7B” combination could provide robust protection to low HFN values for UK wheat.

The fact that these four QTL affect HFN through different modes of action is very relevant. Low HFN can be brought about due to premature sprouting or high PMA; these two factors vary in their relative importance year on year and hence it is difficult to predict *a priori* which of the two effects will predominate. Likewise, this could vary geographically within the UK. Hence providing breeders with the tools to deploy alternative modes of action to protect against low HFN is a critical outcome of the project. Breeding varieties which incorporate the different resistance mechanisms would equate to an insurance policy for farmers as the

variety would be protected against several different types of low HFN inducing conditions. In some years or locations with a year the 4A gene could be providing protection whereas in other years or locations the 7B gene could be the dominant protective effect.

We focused on these four QTL for fine mapping and marker development. In the case of the 4A QTL we were able to fine map and clone the gene responsible for this QTL. This was done alongside other groups working on this same gene in Australia and Japan. While we were not first to publish the positional cloning of the 4A gene, our work allowed us to rapidly interpret the results in a UK context and make breeders aware that the first gene cloned and proposed as the underlying gene was not relevant for UK varieties and was a red-herring in many regards. Breeders had access to the closely linked markers in late 2014 and in 2016 we published a different position for the gene. The Japanese group then showed within months the specific *MKK3* genes as the underlying gene. We quickly developed a breeder friendly KASP assay for the functional *MKK3* polymorphism and performed a detailed haplotype analysis of this gene and the overall region in UK varieties.

For the 1A, 2D and 7B QTL we were able to advance to different degrees. The 2D QTL is within a complex region which seems to have been involved in a translocation with the 5BL chromosome arm. This makes the fine mapping of the gene very difficult as recombination is affected. Despite this, we were able to confirm tight linkage with a major height effect gene, *Rht8*, in the region and identified lines with recombination between the two effects suggesting that the sprouting resistance is independent of the *Rht8* height effect. For 1A we narrowed down the genetic interval significantly and defined the gene to a 4 cM interval between KASP markers, and identified an additional 27 markers in the region. This constitutes a very robust set of markers for breeders to be able to deploy this resistance in UK varieties.

We also showed that the 1A Soleil resistance allele was able to significantly improve HFN values in the novel background of Charger. This provides an important proof of concept that the resistance allele should be relevant in different genetic backgrounds. For the 7B QTL, we were able to define the gene to an 8 cM interval flanked by KASP markers. Here, we observed some rearrangements between our genetic map and the physical map available from the new wheat genome. Hence, the development of more closely linked markers was made difficult. The QTL effect was mapped to the end of the chromosome arm and previously breeders did not have markers flanking the trait, hence deployment was hindered. Now, we have been able to map the gene more precisely and provide the KASP flanking markers which are critical to allow the use of the gene in marker assisted selected strategies.

Conclusions

- We have cloned a major gene affecting pre-harvest sprouting in UK wheat (4A QTL). We translated this knowledge into a breeders' toolkit by developing a high-throughput perfect SNP marker which allows breeders to tag the functional polymorphism which confers resistance to pre-harvest sprouting. We screened and categorised UK germplasm based on this SNP marker and have identified different versions of the chromosome region (haplotypes). This information is now being implemented by breeding partners to deliver varieties with enhanced sprouting resistance to UK growers.
- We have further prioritised two additional genes which confer resistance to sprouting (1A) and PMA (7B). Both genes were validated across multiple independent datasets. We show that these genes do not affect yield in a series of trials which is a critical consideration when evaluating their deployment into elite varieties. Across experiments these genes provide an increase in HFN of 25 and 32 s, respectively. Importantly, these genes have distinct mechanisms of action. This suggests that combining both genes could lead to average increases in HFN of over 50 s in UK wheat. Similarly, combining both genes could provide alternative resistance mechanism that could be triggered independently depending on weather events for the particular year. Both genes have been mapped to relatively small genetic intervals and breeder-friendly markers have been developed and transferred to industrial partners. This will enable rapid targeted deployment into UK elite varieties.
- We have developed a new tool (PolyMarker) to improve the speed of transfer of SNP from fixed platforms (such as the iSelect 90k chip) into functional assays that can be routinely implemented in a high-throughput manner in breeders' molecular laboratories. This accelerates the rate in which new genomic information can be deployed for the benefit of UK growers. This tool is open source and is being used to generate markers for many additional traits within the breeding community.
- This project, alongside advances by others in the field, has now made marker-assisted selection for high HFN a reality in UK wheat breeding programmes.

Knowledge and Technology Transfer

Press articles

Farmer's Weekly:

- <http://www.fwi.co.uk/community/blogs/farmingfutures/archive/2013/02/17/what-future-yield-can-i-expect.aspx>
- <http://www.fwi.co.uk/Articles/13/06/2012/133378/Cereals-2012-Wheat-breeding-on-the-verge-of-DNA-revolution.htm%E2%80%A9>

Crop Production Magazine

- Breeding route to better bread (Sept 2013)
<https://cereals.ahdb.org.uk/media/330023/T2F-September-2013-Breeding.pdf>

Scientific papers

- Ramirez-Gonzalez R, Uauy C, Caccamo M (2015) PolyMarker: A fast polyploid primer design pipeline. *Bioinformatics*. 31 (12): 2038-2039.
- Shorinola O, Bird N, Simmonds J, Berry S, Henriksson T, Jack P, Werner P, Gerjets T, Scholefield D, Balcárková B, Valárik M, Holdsworth MJ, Flintham J, Uauy C (2016) The wheat *Phs-A1* pre-harvest sprouting resistance locus delays the rate of seed dormancy loss and maps 0.3 cM distal to the *PM19* genes in UK germplasm. *Journal of Experimental Botany*. 67 (14): 4169-4178.

Conference presentations / paper / posters

- Association of Applied Biologists: Reading, UK
- UK-Brazil workshop on wheat improvement: Londrina, Brazil.
- UK-Brazil workshop
- FIA-PIPRA Workshop
- EMBRAPA Trigo-UK Wheat workshop

Interaction with policy and decision makers

Speaker at event

- Cereals Event: 2011 HGCA stand; 2012-2015 JIC stand
- UK House of Lords: 100 years of separating wheat from chaff. London, UK 2010
- Royal Agricultural Society of England (RASE): Breeding and Genetic Modification. London, UK 2010
- Friends of JIC field walk 2011
- Velcourt Agronomist Technical Workshop: Future wheat yields and breeding techniques. UK 2011
- BBSRC Food Security and Biotechnology Seminar: How will future developments in biotechnology impact on the food supply chain? London, UK 2011.
- Leverhulme Centre for Integrative Research in Agriculture and Health (LCIRAH): Translating fundamental plant research for the needs of the community. London, UK 2011
- Guest speaker Strutt & Parker Cereals Event 2012 breakfast
- NIAB Innovation Farm: How the sequencing revolution is changing the wheat improvement landscape. Cambridge, UK 2012
- BBSRC-IGD workshop: Plant breeding for food chain sustainability. London, UK 2012
- Oxford Farming Conference at Cereals: Can we break the wheat yield plateau? Boothby Graffoe, UK 2013
- NIAB Outlook Conference: Applied molecular genetics for improved crop yields. Scotch Corner, UK 2013
- Big Food Group: Applied molecular genetics for sustainable crop production. London, UK 2013
- CropTec: Emerging trends and technologies in crop science. Peterborough, UK 2014
- Technical Seminar at Cereals: 20:20 Wheat - a reality or a pipe dream? Boothby Graffoe, UK 2014
- NRP event at Cereals: Collaborating to revolutionise UK wheat. Boothby Graffoe, UK 2014
- Farming Futures: Emerging trends and technologies in crop science. Meriden, UK 2014

Speaker and small group discussions

- NIAB Trust
- BBSRC Institute Directors

- John Innes Foundation
- Peter Kendall and Dr Helen Ferrier (NFU) and Jock Willmott (Strutt & Parker)
- Sir John Beddington (Government Chief Scientific Adviser)
- Uzbekistan Ambassador
- Frontier Agronomists
- Jim Paice MP
- Dominic Dyer (Crop Protection Association)
- Lord Cameron
- Melanie Welham (BBSRC Director of Science)
- Tim Benton (UK Champion for Global Food Security)
- Soil Association
- Rob Horsch (Deputy Director of R&D in Ag Development at BMGF)

Glossary

ANOVA	Analysis of variance
BAC	Bacterial Artificial Chromosome
BC _x	Back cross x (x= number of times the lines has crossed to the recurrent parent)
BLAST	Basic local alignment search tool
CER	Controlled Environment Room
CS	Chinese Spring
CSS	Chinese Spring Chromosome arm survey sequence
DH	Doubled haploid
DPH	Days post-harvest
GH	Glasshouse
GI	Germination Index
HapMap	wheat SNP Haplotype Map
HFN	Hagberg Falling Number
HM	Harvest maturity
IWGSC	International Wheat Genome Sequencing Consortium
KASP	Kompetitive Allelic Specific PCR
<i>MKK3</i>	mitogen-activated protein kinase kinase 3 gene
MTP	Minimum Tilling Path
NABIM	National Association of British and Irish Millers
NILs	Near isogenic lines
PCR	Polymerase chain reaction
PH	Post-harvest maturity
PHS	Pre-harvest sprouting
PM	Physiological maturity
<i>PM19</i>	Plasma membrane 19 gene
PMA	Pre-maturity amylase
POPSEQ	Population Sequencing

QTL	Quantitative Trait Loci
RILs	Recombinant inbred lines
SEM	Standard error of the mean
SNP	Single nucleotide polymorphism
SSR	Simple sequence repeat
TGW	Thousand gran weight
TREP	Triticeae Repeat Database

References

- AHDB (2014) AHDB Cereals & Oilseeds Quality Calculator. <http://cereals-data.ahdb.org.uk/calculator/>
- AHDB (2015a) AHDB Cereals & Oilseeds Variety Survey. <http://cereals.ahdb.org.uk/markets/survey-results.aspx>
- AHDB (2015b) Market Data Centre, Corn Returns Ex-farm Regional Spot & Forward Prices - Weekly Prices
- Barrero JM, Cavanagh C, Verbyla KL, Tibbits JF, Verbyla AP, Huang BE, Rosewarne GM, Stephen S, Wang P, Whan A, Rigault P, Hayden MJ, Gubler F (2015) Transcriptomic analysis of wheat near-isogenic lines identifies *PM19-A1* and *A2* as candidates for a major dormancy QTL. *Genome Biology*, 16, 93.
- Borrill P, Fahy B, Smith AM, Uauy C (2015) Wheat Grain Filling Is Limited by Grain Filling Capacity rather than the Duration of Flag Leaf Photosynthesis: A Case Study Using *NAM* RNAi Plants. *PLoS One*, 10, e0134947.
- Buraas T, Skinnes H (1985) Development of Seed Dormancy in Barley, Wheat and Triticale under Controlled Conditions. *Acta Agriculturae Scandinavica*, 35, 233-244.
- DEFRA (2014) Farming Statistics – 2014 wheat and barley production, UK. <https://www.gov.uk/government/statistics/farming-statistics-final-crop-areas-yields-livestock-populations-and-agricultural-workforce-at-1-june-2014-uk>
- DEFRA (2015) Farming Statistics Final crop area and cattle, sheep and pig populations. <https://www.gov.uk/government/statistics/farming-statistics-final-crop-areas-and-cattle-sheep-and-pig-populations-as-at-1-june-2015-england>
- Flintham JE (2000) Different genetic components control coat-imposed and embryo-imposed dormancy in wheat. *Seed Science Research*, 10, 43-50.
- Flintham J, Adlam R, Bassoi M, Holdsworth M, Gale MD (2002) Mapping genes for resistance to sprouting damage in wheat. *Euphytica*, 126, 39-45.
- Flintham JE, Holdsworth MJ, Jack P, Kettlewell PS, Phillips AL (2011) An integrated approach to stabilising HFN in wheat: screens, genes and understanding. *_HGCA PROJECT REPORT 480*.
- Gasperini D, Greenland A, Hedden P, Dreos R, Harwood W, Griffiths S (2012) Genetic and physiological analysis of *Rht8* in bread wheat: an alternative source of semi-dwarfism with a reduced sensitivity to brassinosteroids. *Journal of Experimental Botany*. 63, 4419-36
- Gerjets T, Scholefield D, Foulkes MJ, Lenton JR, Holdsworth MJ (2010) An analysis of dormancy, ABA responsiveness, after-ripening and pre-harvest sprouting in

hexaploid wheat (*Triticum aestivum* L.) caryopses. *Journal of Experimental Botany*, 61, 597-607.

- Gubler F, Millar AA, Jacobsen JV (2005) Dormancy release, ABA and pre-harvest sprouting. *Current Opinion in Plant Biology*, 8, 183-187.
- IBGSC (2012) A physical, genetic and functional sequence assembly of the barley genome. *Nature*, 491, 711-716.
- Imtiaz M, Ogbonnaya FC, Oman J, Van Ginkel M (2008) Characterization of quantitative trait loci controlling genetic variation for preharvest sprouting in synthetic backcross-derived wheat lines. *Genetics*, 178, 1725-36.
- Jordan KW, Wang S, Lun Y, Gardiner LJ, Maclachlan R, Hucl P, Wiebe K, Wong D, Forrest KL, Sharpe AG, Sidebottom CH, Hall N, Toomajian C, Close T, Dubcovsky J, Akhunova A, Talbert L, Bansal UK, Bariana HS, Hayden MJ, Pozniak C, Jeddelloh JA, Hall A, Akhunov E (2015) A haplotype map of allohexaploid wheat reveals distinct patterns of selection on homoeologous genomes. *Genome Biology*, 16, 48.
- Krasileva K, Buffalo V, Bailey P, Pearce S, Ayling S, Tabbita F, Soria M, Wang S, IWGSC, Akhunov E, Uauy C, Dubcovsky J (2013) Separating homeologs by phasing in the tetraploid wheat transcriptome. *Genome Biology*, 14, R66.
- Lohwasser U, Rehman Arif MA, Börner A (2013) Discovery of loci determining pre-harvest sprouting and dormancy in wheat and barley applying segregation and association mapping. *Biologia Plantarum*, 57, 663-674.
- Mares D, Mrva K, Cheong J, Williams K, Watson B, Storlie E, Sutherland M, Zou Y (2005) A QTL located on chromosome 4A associated with dormancy in white- and red-grained wheats of diverse origin. *Theoretical and Applied Genetics*, 111, 1357-1364.
- Mares D, Mrva K (2008) Late-maturity α -amylase: Low falling number in wheat in the absence of preharvest sprouting. *Journal of Cereal Science*, 47, 6-17.
- Met Office (2015) Climate Summaries, UK actual and anomaly maps http://www.metoffice.gov.uk/climate/uk/summaries/anomacts_21/09/2015.
- Meyer et al International Wheat Genome Sequencing Consortium (IWGSC) (2014) A chromosome-based draft sequence of the hexaploid bread wheat (*Triticum aestivum*) genome. *Science*. 345
- Mrva K, Wallwork M, Mares DJ (2006) α -Amylase and programmed cell death in aleurone of ripening wheat grains. *Journal of Experimental Botany*, 57, 877-85.
- Nakamura S, Abe F, Kawahigashi H, Nakazono K, Tagiri A, Matsumoto T, Utsugi S, Ogawa T, Handa H, Ishida H, Mori M, Kawaura K, Ogihara Y, Miura H (2011) A wheat

homolog of *MOTHER OF FT AND TFL1* acts in the regulation of germination. *Plant Cell*, 23, 3215-29

- Nyachiro JM, Clarke FR, Depauw RM, Knox RE, Armstrong KC (2002) Temperature effects on seed germination and expression of seed dormancy in wheat. *Euphytica*, 126, 123-127.
- Ogonnaya FC, Imtiaz M, Depauw RM (2007) Haplotype diversity of preharvest sprouting QTLs in wheat. *Genome*, 50, 107-118.
- Pallotta MA, Warner P, Fox RL, Kuchel H, Jefferies SJ, Langridge P (2003) Marker assisted wheat breeding in the southern region of Australia. *In*: Romano M, Pogna, EA, Galterio Z (eds). 10th International Wheat Genetics Symposium Paestum. pp 789–791.
- Pretty JN, Ball AS, Lang T, Morison JIL (2005) Farm costs and food miles: An assessment of the full cost of the UK weekly food basket. *Food Policy*, 30, 1-19.
- Ramirez-Gonzalez R, Uauy C, Caccamo M (2015) PolyMarker: A fast polyploid primer design pipeline. *Bioinformatics*. 31 (12): 2038-2039.
- Reddy LV, Metzger RJ, Ching TM (1985) Effect of Temperature on Seed Dormancy of Wheat. *Crop Science*, 25, 455-458.
- Reeves J, Chiapparino E, Donini P, Ganal M, Guiard J, Hamrit S, Heckenberger M, Huan X, Van Kaauwen M, Kochieva E, Koebner R, Law J, Lea V, LeClerc V, Van der Lee T, Leigh F, Van der Linden G, Malysheva L, Melchinger A, Orford S, Reif J, Röder M, Schulman A, Vosman B, Van der Wiel C, Wolf M, Zhang D (2004) Changes over time in the genetic diversity of four major European crops: a report from the GEDIFLUX Framework 5 Project. *In*: Vollmann J, Grausgruber H, Ruckebauer P (eds) Genetic variation for plant breeding. Proceedings of the 17th EUCARPIA general congress, Tulln, Austria, 8–11 September 2004, pp 3–7.
- Shaw P, Graham M, Kennedy J, Milne I, Marshall D (2014) Helium: visualization of large scale plant pedigrees. *BMC Bioinformatics*. 15:259.
- Shorinola O, Bird N, Simmonds J, Berry S, Henriksson T, Jack P, Werner P, Gerjets T, Scholefield D, Balcárková B, Valárik M, Holdsworth MJ, Flintham J, Uauy C (2016) The wheat *Phs-A1* pre-harvest sprouting resistance locus delays the rate of seed dormancy loss and maps 0.3 cM distal to the *PM19* genes in UK germplasm. *Journal of Experimental Botany*. 67 (14): 4169-4178
- Shorinola O (2015) Understanding the genetic and physiological control of pre-harvest sprouting and pre-maturity amylase in UK wheat. PhD Thesis University of East Anglia

- Solovyev V, Kosarev P, Seledsov I, Vorobyev D (2006) Automatic annotation of eukaryotic genes, pseudogenes and promoters. *Genome Biology*, 7 Suppl 1, S10 1-12.
- Torada A, Koike M, Ikeguchi S, Tsutsui I (2008) Mapping of a major locus controlling seed dormancy using backcrossed progenies in wheat (*Triticum aestivum* L.). *Genome*, 51, 426-432.
- Torada A, Koike M, Ogawa T, Takenouchi Y, Tadamura K, Wu J, Matsumoto T, Kawaura K, Ogihara Y (2016) A Causal Gene for Seed Dormancy on Wheat Chromosome 4A Encodes a MAP Kinase Kinase. *Current Biology*. 26:782
- Walker-Simmons M (1987) ABA Levels and Sensitivity in Developing Wheat Embryos of Sprouting Resistant and Susceptible Cultivars. *Plant Physiology*, 84, 61-66.
- Wang S, Wong D, Forrest K, Allen A, Chao S, Huang BE, Maccaferri M, Salvi S, Milner SG, Cattivelli L, Mastrangelo AM, Whan A, Stephen S, Barker G, Wieseke R, Plieske J, IWGSC, Lillemo M, Mather D, Appels R, Dolferus R, Brown-Guedira G, Korol A, Akhunova AR, Feuillet C, Salse J, Morgante M, Pozniak C, Luo MC, Dvorak J, Morell M, Dubcovsky J, Ganai M, Tuberosa R, Lawley C, Mikoulitch I, Cavanagh C, Edwards KJ, Hayden M, Akhunov E (2014) Characterization of polyploid wheat genomic diversity using a high-density 90000 single nucleotide polymorphism array. *Plant Biotechnology Journal*, 12, 787-796.
- Wingen LU, Orford S, Goram R, Leverington-Waite M, Bilham L, Patsiou TS, Ambrose M, Dicks J, Griffiths S (2014) Establishing the A. E. Watkins landrace cultivar collection as a resource for systematic gene discovery in bread wheat. *Theoretical and Applied Genetics* 127(8):1831-42
- Zhang XQ, Li C, Tay A, Lance R, Mares D, Cheong J, Cakir M, Ma J, Appels R (2008) A new PCR-based marker on chromosome 4AL for resistance to pre-harvest sprouting in wheat (*Triticum aestivum* L.). *Molecular Breeding*, 22, 227-236.